

2016-05-01

Model based Technologies for Enhancing Building Operation

Sen Huang

University of Miami, jhy1987@gmail.com

Follow this and additional works at: https://scholarlyrepository.miami.edu/oa_dissertations

Recommended Citation

Huang, Sen, "Model based Technologies for Enhancing Building Operation" (2016). *Open Access Dissertations*. 1637.
https://scholarlyrepository.miami.edu/oa_dissertations/1637

This Open access is brought to you for free and open access by the Electronic Theses and Dissertations at Scholarly Repository. It has been accepted for inclusion in Open Access Dissertations by an authorized administrator of Scholarly Repository. For more information, please contact repository.library@miami.edu.

UNIVERSITY OF MIAMI

MODEL BASED TECHNOLOGIES FOR ENHANCING BUILDING OPERATION

By

Sen Huang

A DISSERTATION

Submitted to the Faculty
of the University of Miami
in partial fulfillment of the requirements for
the degree of Doctor of Philosophy

Coral Gables, Florida

May 2016

©2016
Sen Huang
All Rights Reserved

UNIVERSITY OF MIAMI

A dissertation submitted in partial fulfillment of
the requirements for the degree of
Doctor of Philosophy

MODEL BASED TECHNOLOGIES FOR ENHANCING BUILDING
OPERATION

Sen Huang

Approved:

Wangda Zuo, Ph.D.
Assistant Professor of Civil,
Architectural, and Environmental
Engineering

Matthew Jacobs Trussoni,
Ph.D., Assistant Professor in
Practice of Civil,
Architectural, and
Environmental Engineering

Gang Wang, Ph.D.
Assistant Professor of Civil,
Architectural, and Environmental
Engineering

Guillermo Prado, Ph.D.
Dean of the Graduate School

Michael D. Sohn, Ph.D.
Staff Scientist
Lawrence Berkeley National Laboratory
Berkeley, California

Abstract of a dissertation at the University of Miami.

Dissertation supervised by Professor Wangda Zuo.

No. of pages in text (140)

In the U.S., the building sector accounts for the largest portion of primary energy consumption and its energy consumption is expected to continuously increase in the coming decades. Many methods have been proposed to enhance building operations. Among these methods, the model predictive control and the regression-model-based-control are promising for large-scale applications. However, the model predictive control is difficult to implement due to the lack of appropriate modeling tools and thermal load prediction methods, while the regression-model-based-control has low accuracy.

In this dissertation, a software environment for implementing the model predictive control is first presented. In this software environment, Modelica is used for system modeling while Python is used to automatize workflow, including state variable resetting. With this software environment, the study focuses on optimizing the design of the model predictive control for the purpose of resetting the condenser water return temperature set point (condenser water set point) and chiller staging. The results show that the speed and accuracy of the condenser water set point optimization can be improved by using the proposed method for selecting the initial point for searching. Results also reveal that the energy savings from the condenser water set point optimization is not sensitive to the reset frequency for the mild climate in which the study was conducted. Regarding the

chiller staging optimization, results show that there is a trade-off among the energy use of chillers, pumps, and cooling towers. If the trade-off is considered in the design of the model predictive control, more energy savings can be achieved.

A Bayesian network model for the cooling load prediction is then proposed. Compared to the existing methods, the Bayesian network model is easier to implement. A case study shows that the Bayesian network model can achieve comparable accuracy to the support vector machine method that has been recommended by previous studies. For both the Bayesian network model and the support vector machine model, the accuracy of the cooling load prediction is not always proportional to the amount of training data and may be significantly affected by the uncertainties in the inputs.

The Bayesian network model is then applied in the regression-model-based-control for resetting the condenser water set point. The case study shows that the linear and polynomial models that were proposed in the previous studies sometimes even increase energy consumption, while the Bayesian network model can achieve nearly optimal energy savings.

Finally, this dissertation demonstrates the preliminary work of implementing a model predictive control for an integrated community energy system that serves a net zero energy community. Suggestions for future work are also provided.

ACKNOWLEDGEMENT

I would like to express my deep gratitude to Dr. Wangda Zuo, who inspired and constantly supported me throughout the completion of this dissertation. Without his encouragement and guidance, I would never have been able to finish it. I would also like to thank him for training me in writing papers and for introducing me to the community.

I am fortunate to know Dr. Michael D. Sohn of the Lawrence Berkeley National Laboratory. His advice was critical when I encountered problems.

I am grateful to Dr. Gang Wang, a member of my dissertation committee. He helped me a great deal in understanding the problems I studied in this work.

I am thankful to Dr. Matthew Jacobs Trussoni, who is also on my committee. His guidance greatly broadened the scope of my research.

This research was supported by the U.S. Department of Defense under the ESTCP program. I wish to thank Dr. Marco Bonvini, Dr. Michael Wetter, Mary Ann Piette, Dr. Jessica Granderson, Oren Schetrit, Rong Lily Hu, and Dr. Guanqing Lin for the support they provided throughout this research process.

I would like to thank all of the former and current students in my group. Among them are Reymundo J. Miranda, Wei Tian, Dan Li, and Dong He. I also extend my sincere

thanks to all of the people in the Department of Civil, Architectural, and Environmental Engineering. I am so proud to be a member of this great family.

I deeply appreciate my parents for their unconditional love, and I am so proud to have had my son, Kelvin, at the end of my studies. He is always my source of happiness.

Finally, I would like to thank my wife, Chao, who has always stayed with me. Without her, I could not have even started this dissertation work.

Table of Contents

LIST OF FIGURES	viii
LIST OF TABLES	x
Chapter 1: Introduction	1
1.1 Problem Statement	1
1.1.1 Building Energy Consumption in the U.S.	1
1.1.2 Challenges in Reducing Building Energy Consumption	3
1.2 Literature Review in Building Operation Optimization	4
1.2.1 Design Optimization	4
1.2.2 Control Optimization	6
1.2.3 Summary	11
1.3 Research Objectives	11
1.4 Dissertation Outline	12
Chapter 2: Model Predictive Control for Condenser Water Loop Operation	15
2.1 Condenser Water Loop Operation Optimization	15
2.2 Model Predictive Control for Optimizing the Condenser Water Set Point	19
2.3 A Software Environment for Implementing the Model Predictive Control	20
2.3.1 Overall Structure	20
2.3.2 Dynamic Optimization Module	21
2.3.3 Pre-processing Module	23
2.3.4 Post-processing Module	24
2.4 Starting Point Selection for the Condenser Water Set Point Optimization	24
2.4.1 Local Minima Problem	25
2.4.2 Current Methods for Selecting Starting Point	27
2.4.3 Approach Temperature Method	28
2.5 Case Study	29
2.5.1 Case Description	29
2.5.2 Plant Models	31
2.5.3 Optimization Settings	36
2.5.4 Evaluation of Starting Point Selection Methods	38
2.5.5 Evaluation of the Optimization Frequency on the Energy Saving	43
2.6 Conclusion	48
Chapter 3: Model Predictive Control for Chiller Staging Control	50
3.1 Cooling Load based Control for Chiller Staging	50
3.2 Chiller Staging Optimization	52
3.3 New Approaches for the CLC Optimization	57

3.3.1 General Assumptions	57
3.3.2 The New Approaches	58
3.3.3 Implementation	61
3.4 Case Study	62
3.4.1 Case Description	62
3.4.2 Results	64
3.5 Conclusion	74
Chapter 4: A Bayesian Network Model for the Cooling Load Prediction in the Model Predictive Control	75
4.1 Cooling Load Prediction Methods	75
4.2 Bayesian Network Model	78
4.2.1 Theory	78
4.2.2 The Procedure for Developing the Bayesian Network Model	81
4.2.3 The Bayesian Network Model for Cooling Load Prediction	82
4.3 Case Study	84
4.3.1 Training and Testing Data	84
4.3.2 Other Regression Models	85
4.3.3 Evaluation Merits	86
4.3.4 The Impact of the Training Data on the Cooling Load Prediction	86
4.3.5 The Impact of the Uncertainties on the Cooling Load Prediction	91
4.4 Conclusion	93
Chapter 5: A Bayesian Network Model for the Optimization of a Chiller Plant's Condenser Water Set Point	95
5.1 Regression-Model-based-Control Methods to Optimize the Condenser Water Set Point	95
5.2 Bayesian Network Model for Condenser Water Set Point Optimization	96
5.3 Case Study	97
5.3.1 The Training Dataset	99
5.3.2 Testing	101
5.3.3 Results	103
5.4 Conclusion	107
Chapter 6: Modeling for a Net Zero Energy Community	109
6.1 The Studied System	109
6.2 The Proposed Research	113
6.3 Data Acquisition	114
6.4 System Modeling	115
6.4.1 The Partitioning Modeling Method	115
6.4.2 The Ground-Coupled Heat Pump Subsystem	117

6.4.3 The Solar PV Subsystem	119
6.5 Preliminary Simulation Results	120
6.6 Conclusion	121
Chapter 7: Conclusion and Future Work	122
7.1 Conclusion	122
7.2 Future Works	124
WORKS CITED	127

LIST OF FIGURES

Figure 1-1 The distribution of energy use in the U.S.	1
Figure 1-2 The change of building energy use in the U.S.	2
Figure 1-3 The existing methods for enhancing the energy efficiency of buildings	4
Figure 2-1 The framework for model predictive control	22
Figure 2-2 Flat ranges in the condenser water set point optimization	26
Figure 2-3 The schematic of the studied chiller plant (the primary loop)	30
Figure 2-4 The state graph for the supervisor controller	31
Figure 2-5 Diagram of the top-level Modelica model for the studied chiller plant	32
Figure 2-6 Diagram of the subsystem model for the Chillers	32
Figure 2-7 Diagram of the subsystem model for the Cooling Towers with Bypass	34
Figure 2-8 Diagram of the subsystem model for the Supervisor Controller	36
Figure 2-9 Input data for the optimization (a) cooling load (b) outdoor wet bulb temperature	38
Figure 2-10 The scenarios when different starting point selection methods fail to find the global minimum	42
Figure 2-11 The energy saving penalty due to the failure in predicting the optimal condenser water set point	43
Figure 2-12 The annual distribution of daily variations in the outdoor wet bulb temperature	45
Figure 2-13 The simulation results for April 20, 2012	47
Figure 2-14 The simulation results for July 20, 2012	48
Figure 3-1 The state graph of a conventional CLC for a chiller plant with three identical chillers	51
Figure 3-2 The relationship between PLRs and the relative COPs for three different chillers calculated according to the chiller dataset provided by EnergyPlus [42]	53
Figure 3-3 The relationship between the temperature of the condenser water entering the chiller and the relative cooling capacity for three different chillers calculated according to the chiller dataset provided by EnergyPlus [42]	55
Figure 3-4 Comparison of the energy savings by different approaches	65
Figure 3-5 Daily energy saving by Approach 1	66
Figure 3-6 Daily energy saving by Approach 2	67
Figure 3-7 Daily energy saving by Approach 3	68
Figure 3-8 Simulated system statuses for a non-summer day	70
Figure 3-9 Simulated energy consumptions for a non-summer day	71
Figure 3-10 Simulated system statuses for a summer day	72
Figure 3-11 Simulated energy consumptions for a summer day	73
Figure 4-1 The structure of a typical Bayesian Network model	79
Figure 4-2 The structure of Bayesian Network model for the cooling load prediction	83
Figure 4-3 The training and testing dataset (blue = testing data; the rest = training data)	85
Figure 4-4 The week indexes of the training data	87
Figure 4-5 The relation between the amount of training data and the RMSD for the cooling load prediction	89
Figure 4-6 The cooling load prediction results (16 weeks training data)	90
Figure 4-7 The uncertainties in the weather forecast (static error is 2°C)	92

Figure 4-8 The cooling load prediction with error in inputs.....	93
Figure 5-1 The structure of the Bayesian Network model for the optimization of the condenser water set point.....	97
Figure 5-2 The procedure for generating a training dataset.....	99
Figure 5-3 The hourly cooling load and outdoor wet bulb temperature data for the mild month in Washington D.C.	101
Figure 5-4 The hourly cooling load and outdoor wet bulb temperature data for the summer month in Washington D.C.	102
Figure 5-5 The cooling load, outdoor wet bulb temperature, predicted condenser water set point, and the total chiller and cooling tower energy consumption of the mild day.....	105
Figure 5-6 The cooling load, outdoor wet bulb temperature, predicted condenser water set point, and the total chiller and cooling tower energy consumption of the summer day .	107
Figure 6-1 Historic Green Village on Anna Maria Island, FL.....	109
Figure 6-2 The schematic of the studied building system	110
Figure 6-3 The schematic of power distribution of HGV.....	111
Figure 6-4 The schematic of HGV Ground Loop.....	112
Figure 6-5 The proposed research for HGV	113
Figure 6-6 the data acquisition mechanism	115
Figure 6-7 The structure for the system model.....	116
Figure 6-8 Diagram of top level model of the heat pump subsystem.....	117
Figure 6-9 Diagram of heat pump module: (a) heat pump; (b) air side; (c) water side ..	118
Figure 6-10 Diagram of top level model of the solar subsystem.....	119
Figure 6-11 Simulated and measured energy production of PVs in building Warehouse in winter (a) and summer (b) of 2014	121

LIST OF TABLES

Table 2-1 Comparison of the accuracy using different starting point selection methods.	39
Table 2-2 Comparison of the computational performance using different starting point selection methods.....	40
Table 2-3 Performance comparison of different optimization frequencies	44
Table 3-1 Settings for each CLC optimization approach.....	64
Table 4-1 The category of days	83
Table 4-2 the groups for the training data.....	88
Table 5-1 The general result for the testing set.....	103
Table 6-1 The specification of circulation pumps	112

Chapter 1

Introduction

1.1 Problem Statement

1.1.1 Building Energy Consumption in the U.S.

As shown in Figure 1-1, the building sector in the U.S. accounted for the largest portion of primary energy consumption in 2010, which is 44% more than that of the transportation sector and 36% more than that of the industrial sector. In addition, the energy consumption by the building sector has increased dramatically. As shown in Figure 1-2, building energy use increased by 51% from 1980 to 2010 and is expected to rise by 67% in 2030.

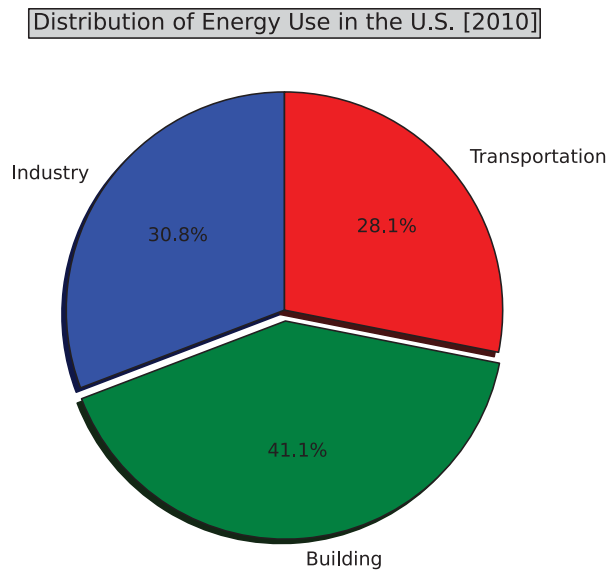


Figure 1-1 The distribution of energy use in the U.S.

Data source: [1]

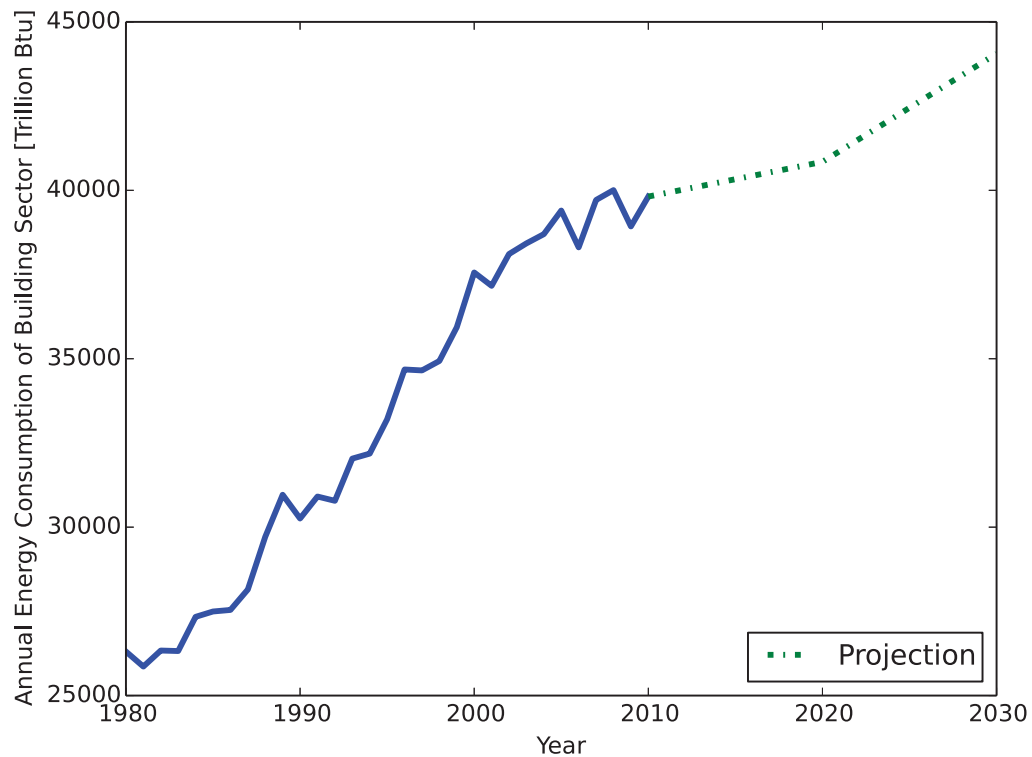


Figure 1-2 The change of building energy use in the U.S.

Data source: [1, 2]

Increased building energy consumption has many negative effects. For example, it leads to higher operational costs for buildings. In addition, since a major portion of energy used by buildings is generated by fossil fuels such as coal [1], the building sector also contributes to fossil-fuel-associated environmental issues, such as global warming and the rising of sea levels. Given these negative effects, it is of great importance to study how to improve the energy efficiency of buildings

1.1.2 Challenges in Reducing Building Energy Consumption

Enhancing building energy efficiency, however, is difficult. The challenges come from two aspects of buildings. First, buildings are complicated and their energy performances require a great deal of effort to understand. Buildings usually consist of multiple systems, such as a heating, ventilation, and air conditioning (HVAC) system, lighting system, electric system, and control system. To understand the behavior of those systems, one needs to have knowledge from different disciplines regarding heat and mass transfer, fluid dynamics, electricity generation and conversion, and control theory. In addition, buildings are becoming increasingly integrated. This integration is achieved not only physically by energy/mass exchange between different systems (e.g., heat recovery from HVAC systems to domestic hot water systems), but also operationally via integrated control of different systems (e.g., hybrid ventilation realized by integrated control of mechanical ventilation and natural ventilation). This integration requires taking into account the interactions between different systems, which may be described in different time domains (continuous and discrete) with time-scales from sub-seconds (such as in control systems) to years (such as in geothermal systems) [3].

Second, constraints in thermal comfort and economy should be considered when designing energy-saving strategies. Enhancing building energy efficiency may have negative impacts on a building's thermal environment and/or its initial cost. For example, by using demand-response strategies (e.g., pre-cooling) to control the HVAC system, one may save energy but also would expect a deviation from the existing level of thermal comfort. Employing a thermal recovery system can lead to increases both in energy

efficiency and initial costs. However, impacts on cost should be minimized or balanced with the achieved building energy savings.

1.2 Literature Review in Building Operation Optimization

To improve building energy efficiency, research was performed and a great number of resulting methods were proposed [4-39]. As shown in Figure 1-3, those methods can be divided into two groups: design optimization methods [4-16] and control optimization methods [17-39].

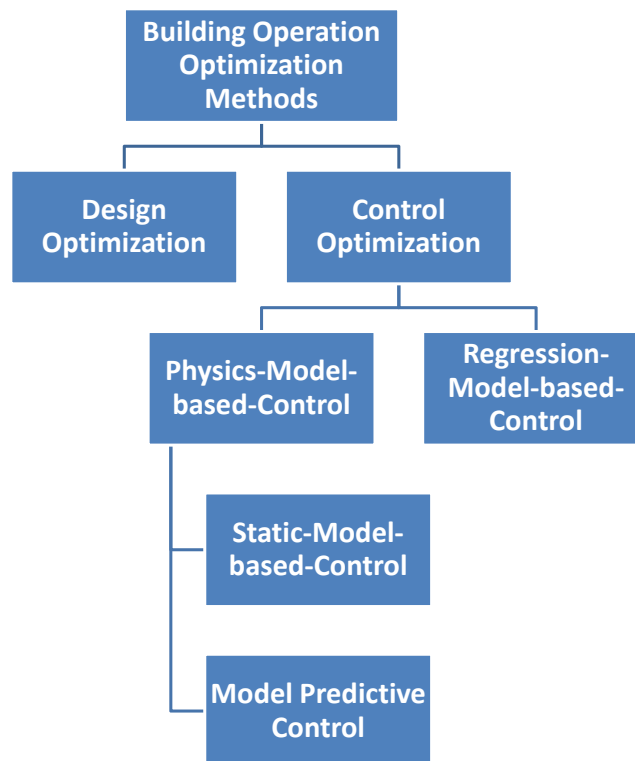


Figure 1-3 The existing methods for enhancing the energy efficiency of buildings

1.2.1 Design Optimization

For the design optimization methods, the basic idea is to adjust the design parameters or system configurations so that higher energy efficiency can be achieved. For example,

Gordon, Ng, et al. [4] proposed a method to reduce the chiller power by varying the condenser water flow rate instead of keeping it as a constant design parameter. Shimoda, Nagota, et al. [8] found that it would be more efficient to employ a centralized cooling system rather than individual cooling systems.

Although they demonstrate energy-saving potential, design optimization methods have one limitation: They may not be suitable for all buildings. Current design optimization methods usually require the modification of the building's physical systems. However, the modification of the physical systems can be impossible for existing buildings, for the following reasons:

a) The cost for the modification can be unacceptably high

The modification usually requires the redesign and/or replacement of existing systems, which may be expensive, especially when the systems are large or complicated. In addition, the building owners also need to invest in the training of operators for the new systems. Those costs may offset the benefits of energy savings.

b) Building systems may be difficult to be modified

Conventionally, building systems are designed in such a way that operators are not expected to change anything but the predefined control parameters. For such systems, modification of the physical systems can be extremely difficult because the systems are enclosed and components may be highly coupled.

1.2.2 Control Optimization

Control optimization methods are designed to optimize the predefined control parameters of building systems according to operating conditions. Compared to the design optimization methods, they do not require the modification of the physical system. Thus, they are suitable for large-scale applications in existing buildings. The operation optimization methods can be further divided into two sub-groups: physics-model-based-control and regression-model-based-control methods. The following sections will elaborate on both methods.

a) Physics-Model-based-Control

In physics-model-based-control methods [17, 18, 22, 24, 25, 28, 29, 34, 37-39], first principles and engineering models (e.g., performance curves) are developed to characterize the behavior of buildings. Those models are then coupled with the optimization algorithms to find the optimal values of the control parameters for a given operating condition and/or system status. Constraints for this optimization can be included in either the models or the optimization algorithms. Depending on whether the dynamics are considered, the physics-model-based control methods can be further divided into two groups: static-model-based-control and predictive control methods.

Static-Model-based-Control

In static-model-based-control methods [17, 18, 22, 24, 25, 29, 38], the objective function is usually the power of the studied system, while the studied system is

assumed to respond to the change of the control parameters instantaneously. For example, Lu, Cai, et al. [17] developed a static-model-based-control method of optimizing cooling tower speeds of chiller plants for measuring outdoor wet bulb temperatures and cooling loads (In this dissertation, the cooling load is the heat handled by the chiller plant. It includes the space cooling load and the fresh air cooling load) so that the total power of the chillers, cooling towers, and pumps could be minimized.

The major problem with static-model-based-control methods is that they may not be suitable for buildings with significant dynamics. The dynamics may significantly affect the building's energy performance. For example, Ulpiani, Borgognoni, et al. [40] found that changing the dynamic pattern of the on-off controller by modulating the dead band width could lead to an approximately 25% increase in energy efficiency of the studied heating system.

Model Predictive Control

Model Predictive control methods [28, 34, 37, 39] solve dynamic optimization problems in which the objective function is usually the energy consumption or cost of the studied building system for a future period. The predicted operating conditions are the inputs for the dynamic optimization problems. For instance, Ma, Borrelli, et al. [28] presented a model predictive control for building cooling systems with thermal energy storage. In their method, the optimization was intended to minimize the electricity bill of the studied cooling system for a future period. The adjusted control

parameters included temperature set points of the chilled water and the condenser water as well as the operating status (on/off) of the studied system.

Model predictive control methods cannot take into account the impact of the dynamics on the building performance. Thus, they can provide more accurate results compared to static-model-based-control methods. However, many existing obstacles prevent predictive control methods from being widely implemented in buildings. These obstacles include:

- Existing building modeling tools are not suitable for model predictive control

The commonly used building energy modeling tools include DOE-2 [41], EnergyPlus [42], TRNSYS [43], and ESP-r [44]. Although these modeling tools are widely used in the design and optimization of building systems [45-49], they are not suitable for model predictive controls for the following reasons:

1. It is difficult to use the above tools to model the control process. DOE-2 [41], EnergyPlus [42], and ESP-r [44] are primarily designed for the long period of assessing building performance, with the aim of supporting building design and policy development. To achieve this goal, those tools tend to idealize the control process in order to accelerate the long simulation period. For TRNSYS [43], the major problem is that it employs a fixed time step length. A fixed time step length forces modelers to select a small time step in TRNSYS [43] to capture the dynamics in the control process. However, the small time step leads to a long computational time to perform the simulation.

2. It is difficult to reset the initial value of state variables with existing building modeling tools. When using the model predictive control, initial values of all state variables of the system model need to be reset prior to evaluating the performance of different control parameter values. However, in existing building modeling tools, resetting the initial value of state variables is difficult if not impossible without making significant code changes.

- Predicting the thermal load is challenging

The predicted thermal load is a critical input for performing the model predictive control. The thermal load is affected by many factors. Also, the relationship between those factors and the thermal load is complicated. The current thermal load prediction methods are problematic. For example, in Corbin, Henze, et al. [34] method, the building modeling tool, EnergyPlus [42], is used to predict the thermal load for a given weather forecast. The problem is that EnergyPlus requires detailed information about the building, such as the thermal characteristic of the envelope and the occupancy schedule, which may not be available for real-world applications.

b) Regression-Model-based-Control

In the regression-model-based-control methods [19-21, 23, 30], simple algebraic equations (e.g., linear equations) are developed to describe the relationships between the operating conditions and the corresponding optimal values of control parameters. The coefficients of those equations can be obtained based on the regression analysis

of the results obtained from simulation and/or experimentation. Those equations are then implemented into the controllers directly to enable an automatic resetting process of the control parameters. For example, Sun and Reddy [19] proposed a linear equation to reset the condenser water return temperature set point (condenser water set point) for chiller plants according to the outdoor wet bulb temperature and cooling load. Compared to the physics-model-based control methods, regression-model-based-control methods are easier to implement because they do not require the solving of complicated optimization problems that usually require substantial computational time and resources.

The main problem with regression-model-based-control methods is that the relationship between the operating conditions and the corresponding optimal values of control parameters may not be described by simple algebraic equations due to the non-linear nature of buildings. For example, Ma, Wang, et al. [22] compared the performance of a physics-model-based control method for optimizing the condenser water set point of chillers with that of the regression-model-based-control method proposed by Sun and Reddy [19]. They found that the annual energy savings of the physics-model-based control method was 183,495 kWh, while that of the regression-model-based-control method was only 130,236 kWh. Thus, the physics-model-based control method can achieve 41% more energy savings than the regression-model-based-control method.

1.2.3 Summary

In summary, design optimization methods can usually achieve better energy savings compared to control optimization methods, because they allow more independent variables to be considered in the optimization. The control optimization methods are more suitable for large-scale applications, since they do not require the modification of physical systems. Among the control optimization methods, the predictive control methods can achieve the best accuracy in predicting the optimal values of the control parameters for two reasons. First, they employ the physics models, which can provide a better representation of the studied systems than other models, such as regression models; second, they take the dynamics of the studied systems into account. However, the predictive control methods are difficult to implement due to the lack of appropriate modeling tools and thermal load prediction methods. The static-model-based-control methods are easier to implement because they employ a static system model, which requires little effort for implementation. The static-model-based-control methods also do not require thermal load prediction. However, the static-model-based-control methods may not be suitable for buildings with significant dynamics. The regression-model-based-control methods require the least effort for implementation, although they have lower accuracy.

1.3 Research Objectives

The objectives of this dissertation are:

- 1) To create a software environment for the model predictive control.

This software environment will not only facilitate the implementation of the model predictive control by addressing the limitations mentioned above, but will also enable studies to support the design of predictive control methods.

- 2) To invent an accurate cooling load prediction method for the model predictive control.

This thermal load prediction method should not require information that is not easily to access, in order to minimize the effort required for implementation. It should also provide reasonably strong accuracy so that no significant uncertainties will be introduced into the model predictive control.

- 3) To develop a new regression-model-based-control method.

The new regression-model-based-control method is expected to be able to effectively manage the complicated relationships in the buildings. It will require little effort in training and will be computationally efficient in predicting the results.

1.4 Dissertation Outline

The rest of the dissertation elaborates on efforts made in this study to develop model-based technologies for enhancing building operation.

Chapter 2 discusses the research on enhancing the design of the model prediction control method for condenser water set point optimization. First, the condenser water set point optimization problem is introduced and a model predictive control method is proposed. Then, a new software environment for implementing the predictive control

method is demonstrated. Based on this software environment, this chapter then evaluates how the selection of the initial point for the search affects the energy savings from the proposed predictive control method through a case study. In this case study, the impact of the optimization frequency on the condenser water set point optimization is also assessed using the software environment previously described.

Chapter 3 presents research on optimizing the model predictive control design for chiller staging. The chapter begins with a review of the chiller staging optimization problem and then proposes three new model predictive control approaches for chiller staging. Next, the software environment proposed in Chapter 2 is employed to implement these three approaches. Finally, an offline simulation is performed to evaluate the three approaches via a case study.

Chapter 4 presents the research on cooling load prediction. First, it introduces the existing methods for cooling load prediction. Next, it proposes a Bayesian network modeling method for cooling load prediction. Then, a case study is presented to evaluate the Bayesian network modeling method for cooling load prediction. In the case study, the performance of the Bayesian network modeling method is compared to that of a support vector machine method, which has been recommended by previous studies. In addition, impacts related to the volume of training data and uncertainties about the inputs in the cooling load prediction results are also evaluated.

Chapter 5 elaborates on the research on the condenser water set point optimization with a regression-model-based-control method. First, it discusses the existing regression-model-based-control methods for the condenser water set point. Then, it demonstrates the procedure of applying the Bayesian network model, proposed in Chapter 4, in the condenser water set point optimization. To evaluate the Bayesian network model for the condenser water set point optimization, a case study is presented that compares the performance of the Bayesian network modeling method with that of existing regression-model-based-control methods.

Chapter 6 discusses the research on modeling an integrated building system that serves a net zero energy community. This research is the initial work for developing a model predictive control for the studied system. This chapter first discusses the studied system and then describes the proposed research on developing the model predictive control for the studied system. Finally, it describes how the current modeling works and reveals preliminary results for the modeling.

Chapter 7 presents the major conclusions found in this study. Plans for future work are also discussed.

Chapter 2

Model Predictive Control for Condenser Water Loop Operation

This chapter discusses the research on enhancing the design of the model prediction control for the condenser water loop operation.

2.1 Condenser Water Loop Operation Optimization

Depending on how chillers reject the waste heat, chiller plants can be categorized as water-cooled or air-cooled. Water-cooled chiller plants with cooling towers are common for large buildings. A typical water-cooled chiller plant consists of two water loops: a chilled water loop and a condenser water loop. The chilled water loop transfers the cooling energy generated by the chiller to the demand side; the condenser water loop rejects the waste heat from the chiller to the ambient environment through the water evaporation occurs in cooling towers [50].

Water-cooled chiller plants are typically controlled by a two-level control structure. The low-level control (local controller) is enabled by a feedback control system. For instance, the temperature of the condenser water leaving the cooling towers is typically controlled by adjusting the speed of the cooling tower fans to meet a predefined set point, which is referred as to the condenser water set point. The upper-level control (supervisor controller) is used to specify set points for the local control and other time-dependent modes of operation [50]. Conventionally, set points are fixed at the nominal values.

One commonly used approach to achieve higher efficient chiller plants is to optimize the operation of cooling towers. This is achieved by adjusting the operation of cooling towers and/or chillers. For example, one can reach lower energy consumption of chillers by making cooling towers at higher fan speeds so that the temperature of the condenser water entering the chillers is lower. However, higher fan speeds mean more energy is used by cooling towers. Thus, the goal of optimizing the cooling tower operation is to achieve the minimum energy consumption of cooling towers and chillers by adjusting fan speeds of cooling towers.

Unsurprisingly, finding optimal cooling tower fan speeds is challenging. The difficulties derive from the nonlinear nature of the chiller plant energy use. For example, the energy performance curves of the chillers and cooling towers are usually non-linear, which means the commonly used system analysis tools, such as linear optimization methods, may not be suitable for this problem. In addition, according to the ASHRAE Handbook [50], optimal fan speeds of cooling towers may be affected by both the cooling load and weather conditions. Therefore, finding optimal cooling tower fan speeds is a multiple-input nonlinear problem, which requires more efforts to be solved.

Various methods have been proposed to find the optimal cooling tower fan speeds [17, 19, 21-23, 28, 30, 31, 51-53] and those methods can be categorized into two groups. In the first group, researchers [21, 51] proposed to replace a two-level control structure by directly controlling the fan speed according to the cooling load. For example, Braun, Klein, et al. [51] proposed a systematic method to control speeds of the variable-speed

cooling tower fans: all the cooling tower fans should operate at the same speed and a linear equation was proposed to determine the optimal fan speed according to the cooling load. This method is easy to be implemented and can make the control of cooling towers more stable.

In the second group, researchers [17, 19, 22, 23, 28, 30, 31, 52, 53] have proposed methods to reset the condenser water set point according to the weather and/or cooling load. Some researchers [19, 23, 30, 52] proposed regression-model-based-control methods in order to reduce the computational time. In the regression-model-based-control methods, regression models are used to describe the relationship between the optimal condenser water set point and the outdoor wet bulb temperature, and/or cooling load conditions. The regression models are usually linear [19, 30] or polynomial regression models [23] to facilitate the implementation in a real controller. Although simple, the regression models may lead to significant deviations from the real optimal condenser water set point temperature [22, 50]. Other researchers [17, 22, 31, 53] developed static-model-based-control methods to increase the optimization accuracy. For example, Lu, Cai, et al. [17] proposed to model the studied chiller plant with an empirical model and optimize the system using a genetic algorithm to find the optimal condenser water set point. They found that they could save approximately 10% of the energy consumption for the studied condenser water loop during high load periods compared to the baseline in which cooling tower fans and condenser water pumps were always at the full speed.

However, above methods are not suitable for legacy chiller plants. The methods in the first group are not often applied in legacy chillers because of the difficulty in changing the control structure of the legacy chiller plants. The control systems of the legacy chiller plants are usually designed to be enclosed and any modification can be difficult and uneconomical. For the methods in the second group, the most promising static-model-based-control methods are usually complicated and computationally intensive. However, for legacy chiller plants, the control systems are usually simple programmable logic controllers with limited computational resource available, which makes the implementation of static-model-based-control methods very challenging.

An additional operational constraint in legacy systems is that the condenser water set point cannot be changed very often since resetting the set points can only be done manually. Therefore, identifying an appropriate resetting frequency for changing the condenser water set point is critical. On one side, reducing the resetting frequency could alleviate associated efforts by the building operators. On the other side, a reduced resetting frequency may reduce the energy savings due to the failure in capitalizing on the system dynamics; in addition, a lower resetting frequency leads to a longer prediction horizon for model inputs. A longer prediction horizon is likely to decrease the prediction accuracy [54] so that more uncertainties will be introduced into the optimization. Thus, it is important to quantitatively assess the impact of the resetting frequency on the energy consumption by chiller plants.

This study attempts to provide a model predictive control to optimize the cooling tower operation for legacy chiller plants. This model predictive control uses the predicted cooling load and outdoor wet bulb temperature as inputs to search the optimal condenser water set points for a future period. The operators can then manually change the set points in the chiller control system, which alleviates the difficulties in the implementation. To improve the optimization accuracy and increase the optimization speed, the author also proposes an approach temperature based method for the selection of optimization starting point. To quantify the impact of set points changing frequency on the energy savings, the author evaluates the energy savings with different optimization frequencies. The proposed model predictive control is then evaluated using a case study on a legacy chiller plant located in Washington D.C.

2.2 Model Predictive Control for Optimizing the Condenser Water Set Point

For the condenser water set point optimization, the author considers a water-cooled chiller plant with multiple chillers and cooling towers. For each cooling tower, there is a variable speed fan controlled by one condenser water set point. The author assumes that all the cooling towers are controlled by the same condenser water set point and there is no other independent variable in the optimization. Thus, the optimization problem can be defined as

$$\min(E|_{t_0}^{t_0+\Delta t}) = \min \left(\int_{t_0}^{t_0+\Delta t} f \left(T_{cw,set}(t_0), \dot{Q}^P(t), T_{wb}^P(t), \vec{S}(t_0) \right) \right), \quad (1)$$

for $t \in [t_0, t_0 + \Delta t)$

$$s.t. \quad T_{cw,set,L} \leq T_{cw,set}(t_0) \leq T_{cw,set,H}, \quad (2)$$

where $E|_{t_0}^{t_0+\Delta t}$ is the total energy consumption of the chillers and cooling towers during the optimization period $[t_0, t_0 + \Delta t)$, $T_{cw,set}$ is the condenser water set point, \dot{Q}^P is the predicted cooling load, T_{wb}^P is the predicted outdoor wet bulb temperature, \vec{S} is the state vector of the system (e.g. equipment operating status, water temperature in chiller condenser and evaporator), $T_{cw,set,L}$ and $T_{cw,set,H}$ are the low and high limit of the condenser water set point during $[t_0, t_0 + \Delta t)$. Using the evaporative cooling, the cooling tower cannot cool the condenser water to a temperature lower than T_{wb} . Thus, the actual $T_{cw,set,L}$ can be determined by

$$T_{cw,set,L} = \text{minimum} \{T_i \in \{T_1, \dots, T_n\} \mid T_i \geq T_{wb,L}^P\}, \quad (3)$$

where $\{T_1, \dots, T_n\}$ is the set of all the possible value for the condenser water set point, $T_{wb,L}^P$ is the lowest T_{wb}^P during $[t_0, t_0 + \Delta t)$. The $T_{cw,set,H}$ is set as

$$T_{cw,set,H} = \text{maximum} \{T_1, \dots, T_n\}. \quad (4)$$

2.3 A Software Environment for Implementing the Model Predictive Control

2.3.1 Overall Structure

To facilitate the implementation of the model predictive control, the author develops a software environment. As show in Figure 2-1, the software environment consists of three modules: Dynamic Optimization, Pre-processing and Post-processing. As the core of the framework, the Dynamic Optimization module is made of an optimization engine and a system model. The raw data is processed in the Pre-processing module that provides clean inputs for the Dynamic Optimization module. The optimization results are then processed in the Post-processing. The following sections introduce the details of each module.

2.3.2 Dynamic Optimization Module

The Dynamic Optimization module is designed to perform the dynamic optimization for the control parameters of the building system. The optimization problem is defined as:

$$\min(OB|_{t_0}^{t_0+\Delta t}) = \min \left(\int_{t_0}^{t_0+\Delta t} f_1(\overline{OP}(t), \overline{IP}(t), \vec{S}(t_0)) \right), \text{ for } t \in [t_0, t_0 + \Delta t), \quad (5)$$

$$s.t. \quad \overline{OP}(t) \in CP_{valid} \quad (6)$$

$$f_2(\overline{OP}(t), \overline{IP}(t), \vec{S}(t_0)) = 0 \quad (7)$$

$$f_3(\overline{OP}(t), \overline{IP}(t), \vec{S}(t_0)) \leq 0 \quad (8)$$

where $OB|_{t_0}^{t_0+\Delta t}$ can be the energy consumption or cost of the studied system during the optimization period $[t_0, t_0 + \Delta t)$, $\overline{OP}(t) = \{OP_1(t), \dots, OP_n(t)\}$ is the set which contains n control parameters to be optimized. \overline{IP} is the vector of the input variables for the optimization, such as the cooling load and the outdoor wet bulb temperature, \vec{S} is the state vector of the studied system, OP_{valid} is the set consists of all valid options for \overline{OP} . $f_2(\overline{OP}(t), \overline{IP}(t), \vec{S}(t_0))$ and $f_3(\overline{OP}(t), \overline{IP}(t), \vec{S}(t_0))$ are the equality and inequality constrains, respectively.

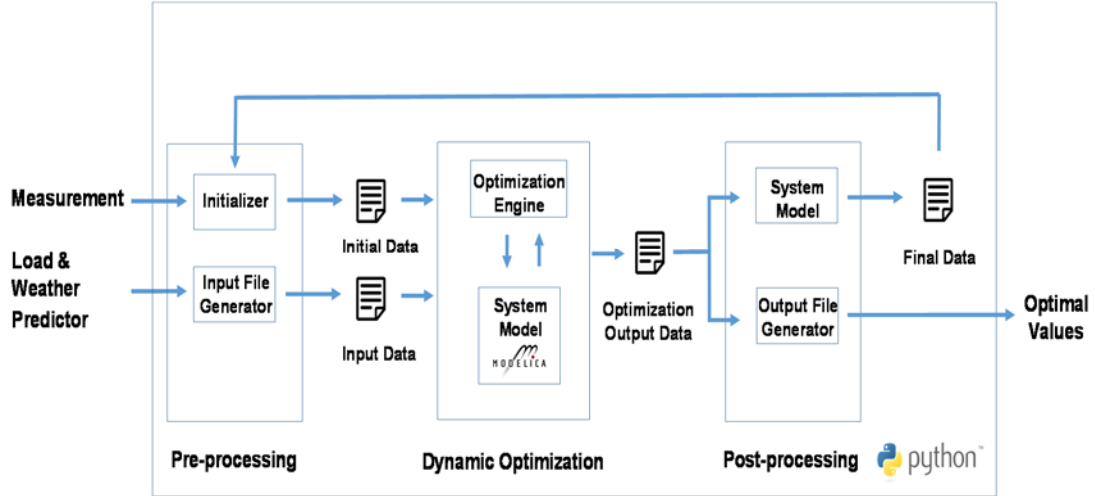


Figure 2-1 The framework for model predictive control

To simplify the optimization, the author assumes that $OP_i(t)$ remains constant within the optimization period,

$$\overline{OP}(t) = \overline{OP}(t_0), \text{ for } t \in [t_0, t_0 + \Delta t). \quad (9)$$

Thus, the optimization problem defined in equation (5) can be simplified as

$$\min \left(\int_{t_0}^{t_0 + \Delta t} f_1(\overline{OP}(t_0), \overline{IP}(t), \vec{S}(t_0)) \right) \text{ for } t \in [t_0, t_0 + \Delta t), \quad (10)$$

$$s.t. \quad \overline{OP}(t_0) \in CP_{valid} \quad (11)$$

$$f_2(\overline{OP}(t_0), \overline{IP}(t), \vec{S}(t_0)) = 0 \quad (12)$$

$$f_3(\overline{OP}(t_0), \overline{IP}(t), \vec{S}(t_0)) \leq 0 \quad (13)$$

In this module, $\overline{IP}(t)$ is from the Input Data, which is the processed raw data. The $\vec{S}(t_0)$ is imported from the Initial Data (Figure 2-1) and it is used to reinitialize the simulation for the optimization period $[t_0, t_0 + \Delta t)$. The system model then evaluates the objective function $\int_{t_0}^{t_0 + \Delta t} f(\overline{OP}(t_0), \overline{IP}(t), \vec{S}(t_0))$. Based on the evaluation, the optimization engine would identify the optimal values for $\overline{OP}(t_0)$. After the optimization is completed, the optimal $\overline{OP}(t_0)$ as well as $\vec{S}(t_0 + \Delta t)$ are exported as the Optimization Output Data.

To build the system model, the author uses Modelica, which is an equation based modeling language. A key difference between Modelica and the conventional building energy modeling tools is that Modelica separates model development and numerical process. The users are responsible for modeling the studied system with mathematical equations. Then the simulation environment will analyze these mathematical equations, design corresponding numerical solutions, and finally translate those equations and the numerical algorithms into executable codes for performing the simulation. The separation of modeling and numerical processes makes it easy to adjust the state variables since the change of the state variables doesn't affect the mathematical equations. In addition, some Modelica simulation environments, such as Dymola [55], store the initial and final values of the state variables in dedicated files, which makes the resetting even more convenient.

Modelica is also suitable for modeling the control process in building systems. Most Modelica simulation environments provide adaptive time step solvers, which can adjust the time step sizes according to how fast the system changes. This mechanism makes a balance between simulation accuracy and computing time demand so that fast dynamics can be caught with minimized computing efforts.

2.3.3 Pre-processing Module

The Pre-processing module contains two components: Initializer and Input File Generator. The Initializer generates the Initial Data based on the Final Data from the previous optimization period. The Input File Generator converts the raw data, such as cooling load and weather data, into the Input Data, which can be directly read by the system model. The raw data can be either predicted data or historical data. For instance,

the prediction model in [56] can be used to provide the predicted cooling load by using the weather prediction obtained from the weather forecast service. A Python package called Pandas [57] is used to process the possible missing or erroneous raw data.

2.3.4 Post-processing Module

In the Post-processing module, the System Model reads the Optimization Output Data and generates the Final Data, which is then used for the next optimization period $[t_0 + \Delta t, t_0 + 2\Delta t)$. The Final Data includes the state vector $\vec{S}(t_0 + \Delta t)$. In addition, a component called Output File Generator processes the raw data in the Optimization Output Data and exports the data for later use, such as plotting the results and generating control signals.

The optimization problem defined in section 2.2 is a special case of a general optimization problem defined in section 2.3.2. Thus, one can directly implement the optimization problem defined in section 2.2 with the proposed software environment.

2.4 Starting Point Selection for the Condenser Water Set Point Optimization

In general, a good starting point of the optimization can significantly increase the success rate of finding the global minimum and reduce the searching time. For the condenser water set point optimization, finding the global minimum can be a critical issue since many local minima exist. The optimization algorithm can potentially be trapped in a local minimum if the starting point is not appropriately selected. In the following sessions, the author will first introduce the local minima problem in the condenser water set point optimization. Then the author will discuss benefits and

limitations of three typical methods for selecting the optimization starting point. Finally, the author proposes an alternative method, which is simple and effective.

2.4.1 Local Minima Problem

As shown in Figure 2-2, it is possible that $E|_{t_0}^{t_0+\Delta t}$ is constant if $T_{cw,set}$ is within a certain range (the author names this range as “flat range”). When \dot{Q} or T_{wb} is high, the flat range will occur when $T_{cw,set}$ is lower (Figure 2-2 a). In this case,

$$T_{cw,low} \geq T_{cw,set,L}, \quad (14)$$

where $T_{cw,low}$ is the lowest possible temperature of the condenser water leaving the cooling tower when the cooling tower fans are running at the full speed. Thus, when $T_{cw,set} \leq T_{cw,low}$, one always has

$$E_{tw}|_{t_0}^{t_0+\Delta t} = \text{constant}, \quad T_{cw,set} \in [T_{cw,set,L}, T_{cw,low}], \quad (15)$$

$$T_{cw,ent} = T_{cw,low}, \quad T_{cw,set} \in [T_{cw,set,L}, T_{cw,low}], \quad (16)$$

where $E_{tw}|_{t_0}^{t_0+\Delta t}$ is the energy used by the cooling towers. With a constant $T_{cw,ent}$, the chiller energy consumption, $E_{ch}|_{t_0}^{t_0+\Delta t}$, will also remain unchanged. Thus, one will also have

$$E|_{t_0}^{t_0+\Delta t} = \text{constant}, \quad T_{cw,set} \in [T_{cw,set,L}, T_{cw,low}]. \quad (17)$$

When \dot{Q} or T_{wb} is low, the flat range may occur when $T_{cw,set}$ is higher (Figure 2-2 b). Under this condition, one will have

$$T_{cw,hig} \leq T_{cw,set,H}, \quad (18)$$

where $T_{cw,hig}$ is the highest possible temperature of the condenser water leaving the cooling tower when the cooling tower fans are off and only natural cooling happens.

Thus, the cooling tower energy is zero:

$$E_{tw}|_{t_0}^{t_0+\Delta t} = 0, \quad T_{cw,set} \in [T_{cw,hig}, T_{cw,set,H}]. \quad (19)$$

And one will also have

$$T_{cw,ent} = T_{cw,hig}, \text{ and } E_{ch}|_{t_0}^{t_0+\Delta t} = \text{constant}, \quad T_{cw,set} \in [T_{cw,hig}, T_{cw,set,H}]. \quad (20)$$

As a result, the total energy consumption of chillers and cooling towers is also constant:

$$E|_{t_0}^{t_0+\Delta t} = \text{constant}, \quad T_{cw,set} \in [T_{cw,hig}, T_{cw,set,H}] \quad (21)$$

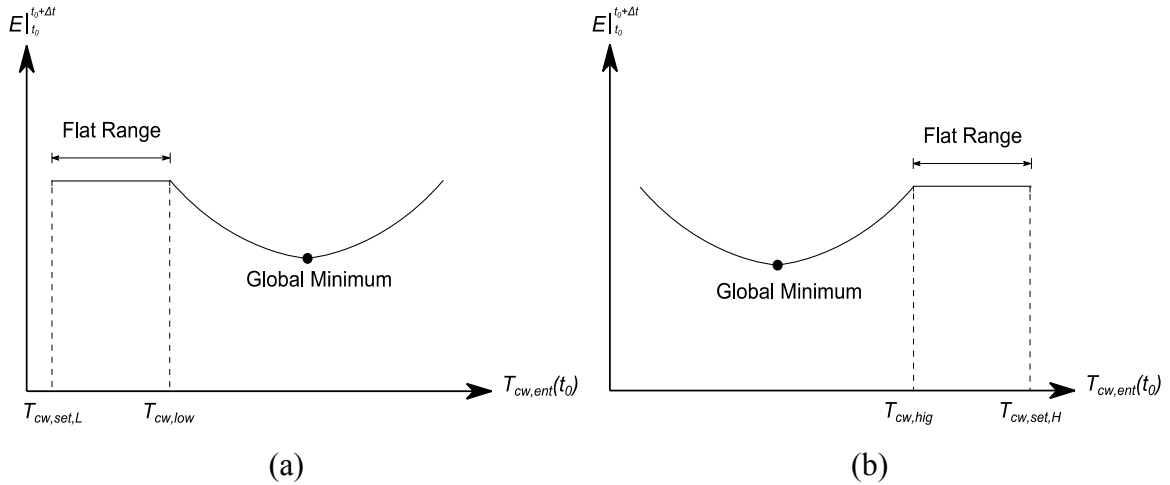


Figure 2-2 Flat ranges in the condenser water set point optimization

In both scenarios, the optimization algorithm will obtain a minimal solution in the flat range since it cannot detect any changes of $E|_{t_0}^{t_0+\Delta t}$ for any $T_{cw,set}$ within the flat range. However, the obtained minimal solution is only valid for the flat range (local minimum). To find the minimal solution for the entire searching space (global minimum), one should start the search outside the flat range.

2.4.2 Current Methods for Selecting Starting Point

To mitigate the local minimal problem in the condenser water set point optimization, it is critical to start the search outside the flat range. Unfortunately, generic starting point selection methods, such as the middle point method, the multiple starting point method, and the previous value method might not be well-suited for avoiding the flat range problem. The middle point method uses the middle point between the low bound and high bound of the independent variable as the starting point. Because it is the simplest method to reduce the distance of the starting point and the global minimum, the middle point method is widely used in optimization problems when only one global minimum is believed to exist [58, 59]. However, for the optimization problems with multiple local minima, the middle point method may lead to a local minimum that is near the middle point.

To deal with this problem, a multiple starting point method was proposed [60]. In this method, multiple starting points are generated randomly (For example, a uniform distribution between the low and high bound for the independent variable). However, it still does not guarantee a global minimum and may increase the searching time with multiple starting points [61].

The previous value method [62] uses the optimal values resulted from the previous search as the starting points of the current search. The previous value method is based on the assumption that the optimal results for two adjacent optimization periods are likely to

be close if the system states and inputs are similar. However, it may not work properly if the optimal results of two optimization periods are significantly different.

Specifically for the condenser water set point optimization, one can also use the highest possible set point as the starting point, $T_{cw,set,sta}$:

$$T_{cw,set,sta} = T_{cw,set,H}. \quad (22)$$

This method can be called as “high point” method. It can mitigate the flat range problem at the low end (Figure 2-2 a) but not the one at the high end (Figure 2-2 b).

2.4.3 Approach Temperature Method

To address the limitations of the current starting point selection methods for the condenser water set point optimization, the author proposes an approach temperature method by considering the physics of the chiller plant. To avoid the flat range problem, $T_{cw,set,sta}$ should satisfy

$$T_{cw,set,sta} \in [T_{cw,low}, T_{cw,hig}]. \quad (23)$$

The challenge is how to predict $T_{cw,low}$ and $T_{cw,hig}$. Although some sophisticated cooling tower performance models [63, 64] can be used for predicting $T_{cw,low}$ and $T_{cw,hig}$, they are too complicated for the purpose of starting point selection. In this study, the author proposes to estimate the $T_{cw,low}$ based on the nominal approach temperature $\Delta T_{app,nom}$, which is the difference between the temperature of condenser water leaving the cooling tower and the outdoor wet bulb temperature at the nominal condition. The predicted $T_{cw,low}$ would be:

$$T_{cw,low}^P = \begin{cases} T_{cw,set,L} & T_{wb} < T_{cw,set,L} - \Delta T_{app,nom} \\ T_{cw,set,H} & T_{wb} > T_{cw,set,H} - \Delta T_{app,nom} \\ \text{round}(T_{wb} + \Delta T_{app,nom}) & \text{Others} \end{cases}, \quad (24)$$

where $\text{round}()$ is the function shown as follows:

$$\text{round}(T) = \text{maximum} \{T_i \in \{T_1, \dots, T_n\} \mid T_i \leq T\}, \quad (25)$$

where $\{T_1, \dots, T_n\}$ is the set of all the possible value for $T_{cw,set}$ defined in equation (3).

The author then sets:

$$T_{cw,set,sta} = T_{cw,low}^P, \quad (26)$$

It is worth mentioning that under certain conditions [65], it is possible that

$$\Delta T_{app} > \Delta T_{app,nom}, \quad (27)$$

where ΔT_{app} is actual approach temperature. This will lead the

$$T_{cw,set,sta} = T_{cw,low}^P < T_{cw,low}. \quad (28)$$

In this case, $T_{cw,set,sta}$ will be located in the flat range.

2.5 Case Study

To evaluate the performances of starting point selection methods and identify how optimization frequency affects the condenser water set point optimization, the author implements the proposed model predictive control in a real chiller plant and performs an offline simulation using the historical cooling load and outdoor wet bulb temperature as the inputs.

2.5.1 Case Description

The studied chiller plant is located in Washington D.C., U.S.A. The chiller plant has a primary-secondary chilled water distribution loop and this optimization focuses on the primary loop. As shown in Figure 2-3, the chiller plant consists of three identical chillers, three identical cooling towers, three identical primary pumps, and three identical condenser water pumps. The chiller capacity is 970 ton. Each chiller has one dedicated

chilled water pump (design power: 22 kW), one dedicated condenser water pump (design power: 75 kW), and one dedicated cooling tower. The nominal chilled water and condenser water flow rate are 91.8 kg/s and 173.5 kg/s. The temperature of chilled water leaving the chiller, $T_{chw,lea}$, is set as 3.89°C. The cooling tower has a fan with the nameplate power as 37 kW, the nominal outdoor wet bulb temperature, $T_{wb,nom}$, is 25.56°C and $\Delta T_{app,nom}$ is 3.89 K. A local controller is used to modulate the speeds of the cooling tower fans to maintain the temperature of the condenser water leaving the cooling towers as 29.44°C. In the condenser water loop, a three-way valve is employed to modulate the condenser flow rates through the cooling towers so that $T_{cw,ent}$ is not less than 15.00°C, which is the lowest temperature can be accepted by the chillers.

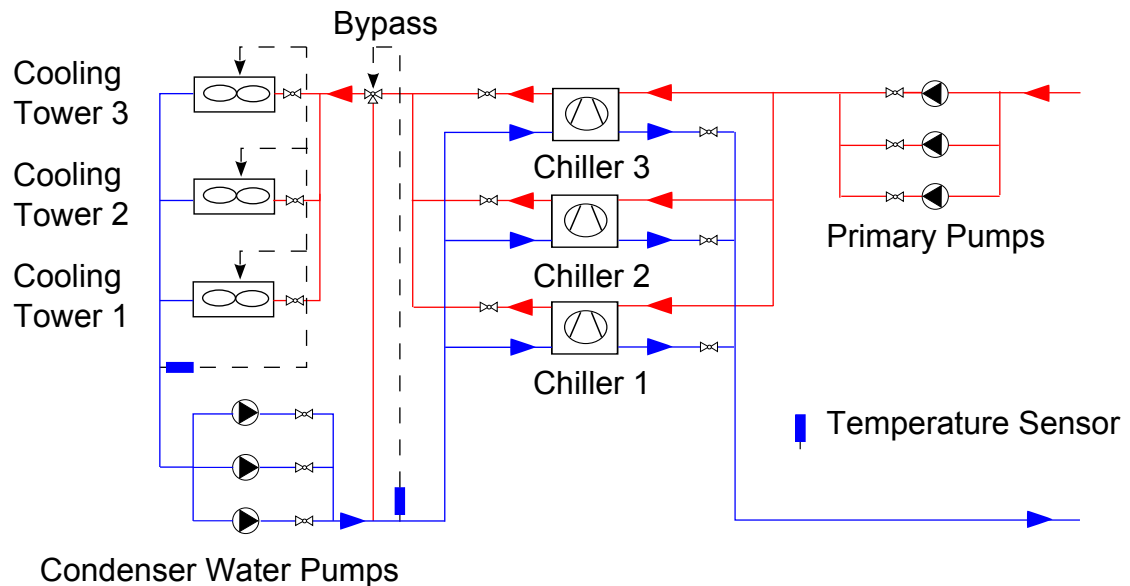


Figure 2-3 The schematic of the studied chiller plant (the primary loop)

A supervisor controller is used to control the chiller operation status according to the measured cooling load. As described in Figure 2-4, there are four operating states for the chiller plant. For instance, “One On” means there is only one chiller in operation. The

three chillers can be turned on or off sequentially. A chiller should not be turned on/off unless the measured cooling load is larger/smaller than a certain critical point plus/minus a dead band, such as 50 ton. The critical points are defined as 90.00% of the sum of the operating chillers' nominal cooling capacity. Besides the dead-band, a waiting period of 900 s is also applied to avoid chiller short cycling.

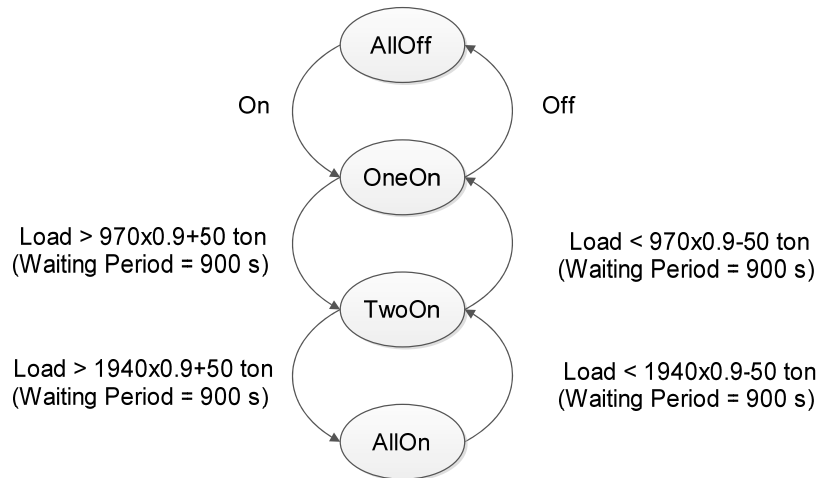


Figure 2-4 The state graph for the supervisor controller

2.5.2 Plant Models

In this study, the author models the chiller plant using component models from the Modelica *Buildings* library [66] and the state graph described in Figure 2-5 with the Modelica *StateGraph2* library [67]. A hierarchical model structure has been applied and Figure 2-5 shows the top-level model, which represents the schematic Figure 2-3. The subsystems for *Chillers*, *Cooling Towers with Bypass* and so on are packaged as single component models in the top-level model. Since this study focuses on the primary loop, the author prescribes the cooling load at the secondary loop using a *Cooling Load* model. Different than the system schematic, the Modelica model also includes the control system, such as the *Supervisor Controller* model. The solid lines represent the pipes and

the dashed lines are the paths for control signals and other input signals, such as weather data and cooling load data.

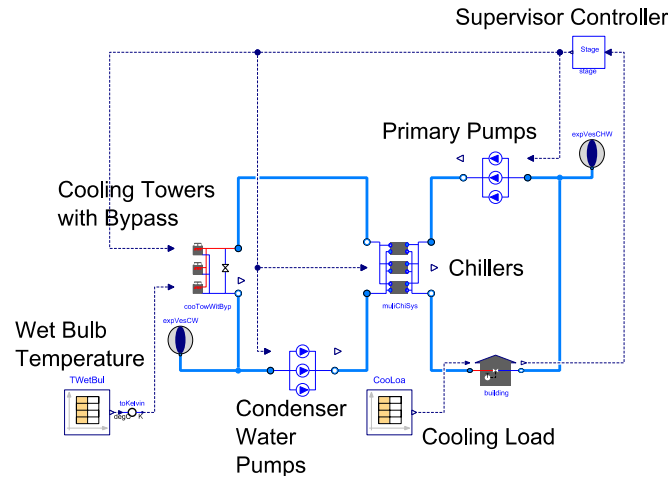


Figure 2-5 Diagram of the top-level Modelica model for the studied chiller plant

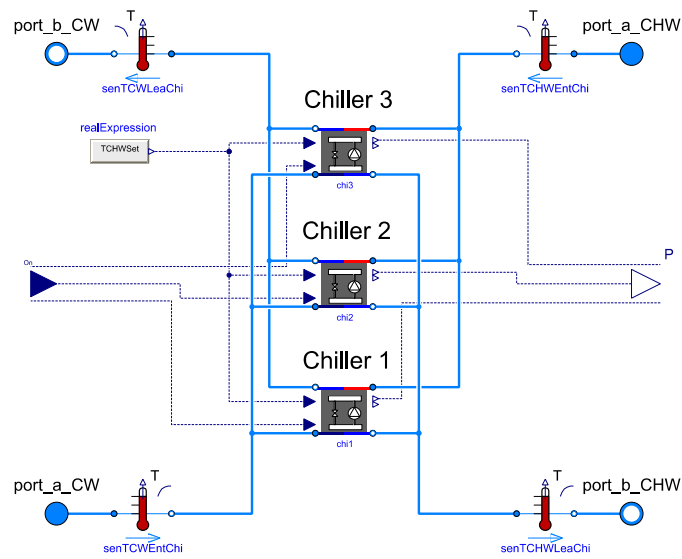


Figure 2-6 Diagram of the subsystem model for the Chillers

Figure 2-6 shows the subsystem model for *Chillers*. The three chillers are connected in parallel and each chiller can be started independently. The inputs for this subsystem include the control signal (ON/OFF) for each chiller, the chilled water supply set point

and the temperature of the chilled and condenser water entering the chillers. The output is the power of each chiller. A *Chillers.Carnot* model in the *Buildings* library is used to calculate the power of each chiller:

$$P_{ch} = P_{ch,nom} PLR \cdot COP_{nom} / \left(\frac{T_{eva}}{T_{con} - T_{eva}} \varepsilon_{carnot} \varepsilon_{PLR}(PLR) \right), \quad (29)$$

where $P_{ch,nom}$ is the nominal power of the chiller, PLR is the partial load ratio (the ratio of the cooling load handled by the chiller to its nominal cooling capacity), COP_{nom} is the chiller's coefficient of performance at the nominal condition, T_{eva} and T_{con} are the temperatures in the evaporator and condenser side of the chiller, respectively. In this study, T_{eva} and T_{con} are assumed to be equal to $T_{chw,lea}$ and $T_{cw,ent}$, respectively. The ε_{carnot} is the Carnot effectiveness (assumed to be constant) and ε_{PLR} is the chiller efficiency due to the part load of compressor, which is a function of PLR :

$$\varepsilon_{PLR}(PLR) = c_1 + c_2 PLR + c_3 PLR^2 + (1 - c_1 - c_2 - c_3) PLR^3, \quad (30)$$

where c_1 , c_2 , c_3 are constant coefficients. In order to mimic the internal capacity control of each chiller, a PI controller is used to modulate PLR for each chiller to maintain $T_{chw,lea}$ as 3.89°C.

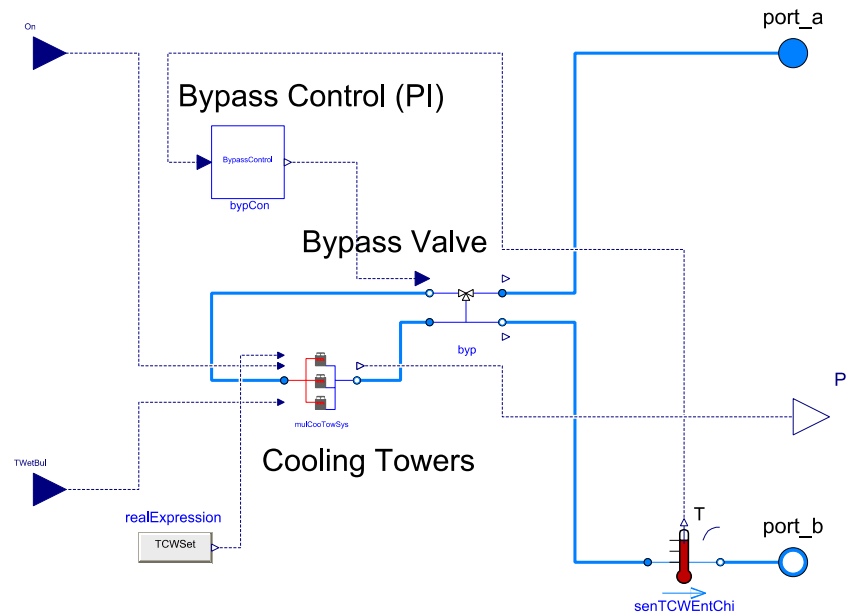


Figure 2-7 Diagram of the subsystem model for the Cooling Towers with Bypass

Figure 2-7 shows the diagram of the *Cooling Towers with Bypass* subsystem model. The inputs of the component include the control signal (ON/OFF) for each cooling tower, the temperature of the condenser water entering the cooling towers, the condenser water set point, and T_{wb} . The output is the power of each cooling tower. The bypass valve and the associated control are also included in this model. The cooling tower is modeled with the model *CoolingTowers.YorkCalc* in the *Buildings* library. The model calculates the approach temperature using a purely-empirical YorkCalc correlation [68]:

$$\begin{aligned}
 \Delta T_{app} = & -0.359741205 - 0.055053608T_{wb} + 0.0023850432T_{wb}^2 + \\
 & 0.173926877\Delta T_r - 0.0248473764T_{wb}\Delta T_r + 0.00048430224T_{wb}^2\Delta T_r - \\
 & 0.005589849456\Delta T_r^2 + 0.0005770079712T_{wb}\Delta T_r^2 - \\
 & 0.00001342427256T_{wb}^2\Delta T_r^2 + 2.8476580111111LGR - \\
 & 0.121765149T_{wb}LGR + 0.0014599242T_{wb}^2LGR + \\
 & 1.680428651T_rLGR - 0.0166920786T_{wb}\Delta T_rLGR -
 \end{aligned} \tag{31}$$

$$\begin{aligned}
& 0.0007190532T_{wb}^2\Delta T_r LGR - 0.025485194448\Delta T_r^2 LGR + \\
& 0.0000487491696T_{wb}\Delta T_r^2 LGR + 0.00002719234152T_{wb}^2\Delta T_r^2 LGR - \\
& 0.065376625555556LGR^2 - 0.002278167T_{wb}LGR^2 + \\
& 0.0002500254T_{wb}^2LGR^2 - 0.0910565458\Delta T_r LGR^2 + \\
& 0.00318176316T_{wb}\Delta T_r LGR^2 + 0.000038621772T_{wb}^2\Delta T_r LGR^2 - \\
& 0.0034285382352\Delta T_r^2 LGR^2 + 0.00000856589904T_{wb}\Delta T_r^2 LGR^2 - \\
& 0.000001516821552T_{wb}^2\Delta T_r^2 LGR^2,
\end{aligned}$$

where ΔT_r is the temperature of the condenser water entering cooling tower minus the temperature of the condenser water leaving cooling tower and LGR is the ratio of the condenser water flow rate to the airflow rate. The fan power P_{tw} is computed as

$$P_{tw} = P_{tw,nom}y^3. \quad (32)$$

where y is the fan speed ratio and $P_{tw,nom}$ is the nominal fan power (the fan efficiency is assumed to be constant). A PI controller is used to adjust y according to $T_{cw,set}$.

The subsystem model for the *Supervisor Controller* is shown in Figure 2-8. The core of the *Supervisor Controller* is a state graph model that is in the middle of the model diagram. It consists of state (oval icon) and transition (bar icon) modules. The state modules are used to represent the four states described in Figure 2-4. The transition module determines when to switch one state to another state. Each transition module has one preceding state and one succeeding state. When the conditions are met, the transition fires.

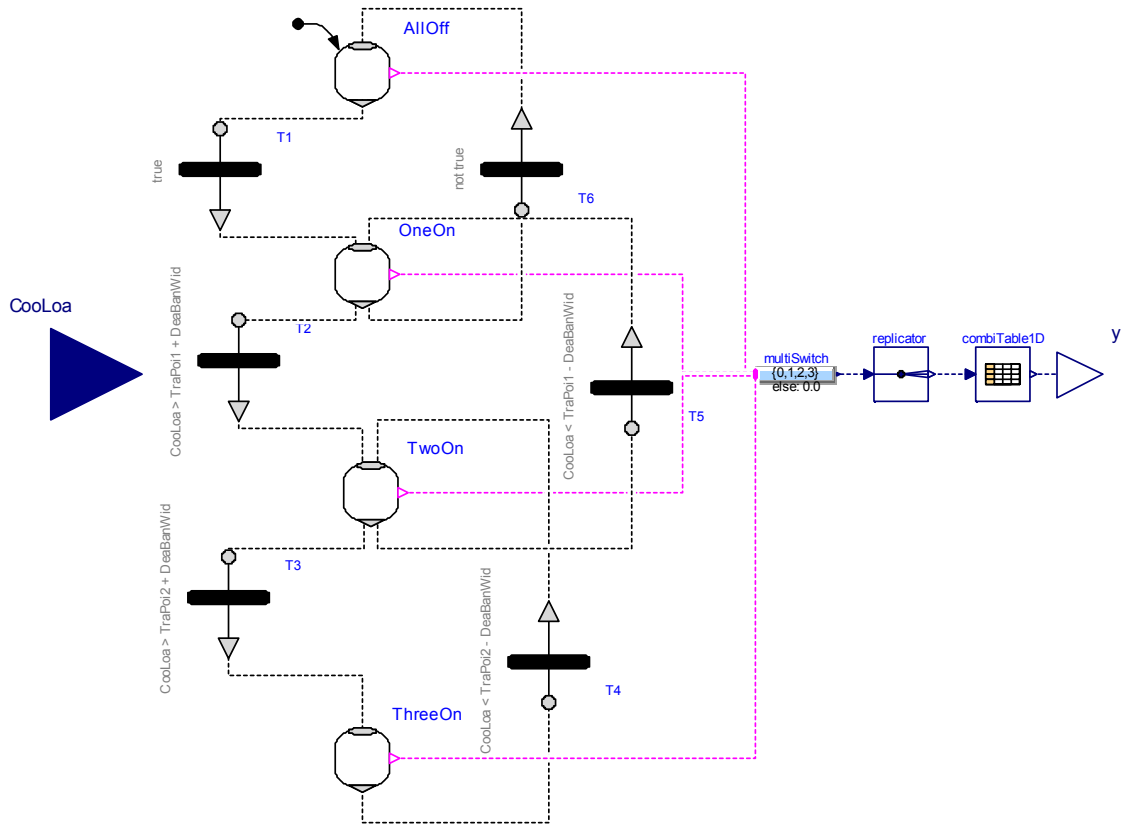


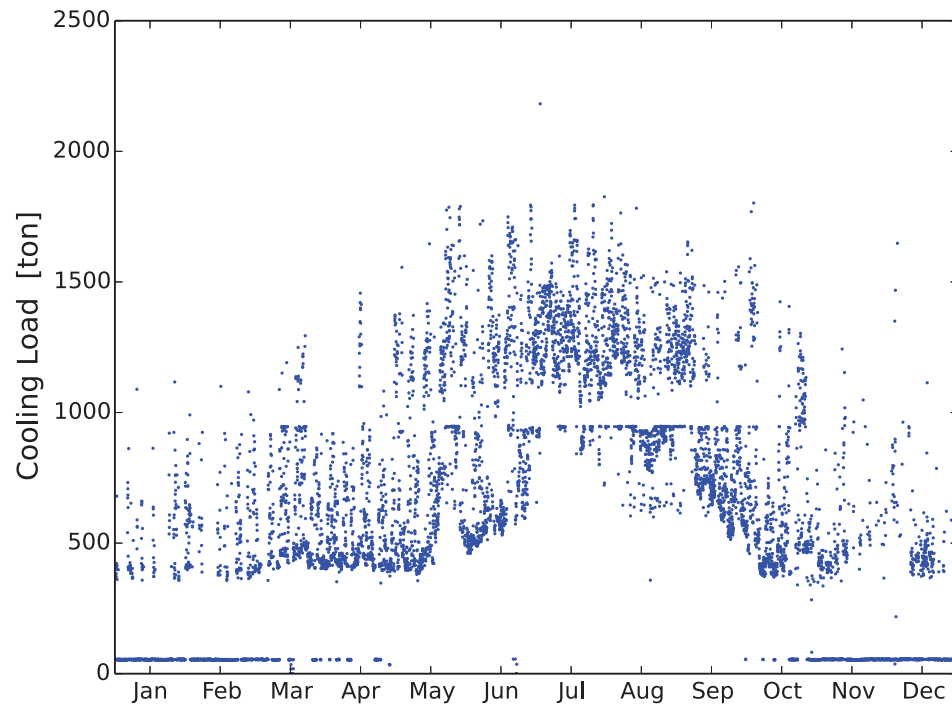
Figure 2-8 Diagram of the subsystem model for the Supervisor Controller

The author calibrates chiller models using the measured data. The author uses the temperature of the condenser and chilled water entering the chillers as input variables and tries to tune the coefficients of the chiller performance curve (c_1, c_2, c_3, c_4 in equation (30)), the design condenser and chilled water temperature so that the difference between the measured and simulated power of chiller can be minimized.

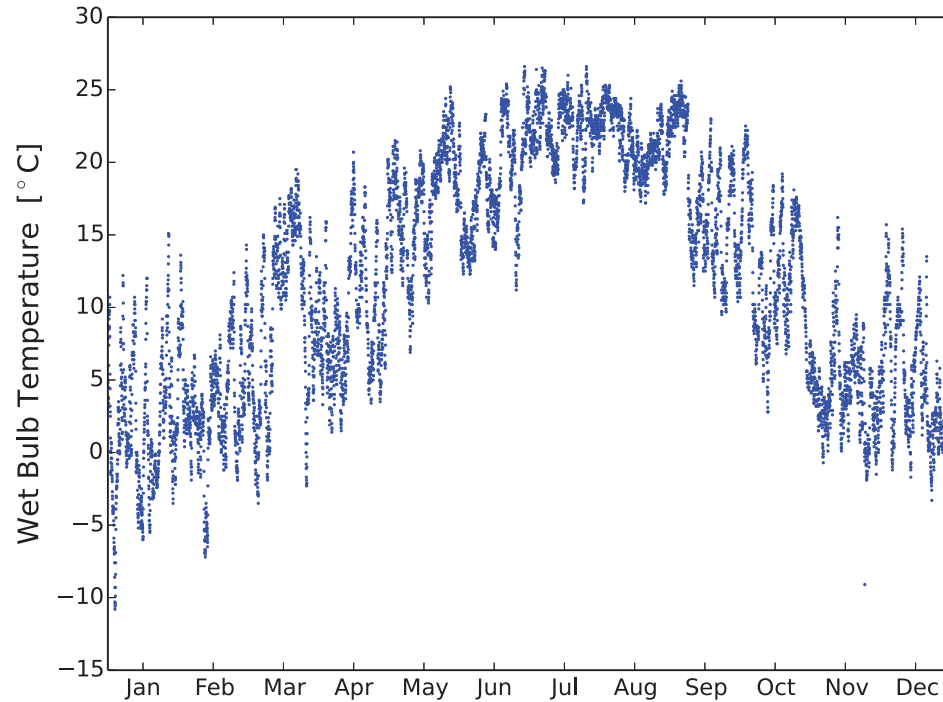
2.5.3 Optimization Settings

In this study, the author uses the GenOpt [69] optimization engine and employs the Hooke Jeeves algorithm. The $\{T_1, \dots, T_n\}$ defined in equation (3) is set to be [15.44, 29.44°C] with an interval of 1°C. The author uses the historic data for \dot{Q} and T_{wb} as the

input variables, which is equivalent to having a perfect prediction model. The perfect prediction model creates an ideal input to evaluate the optimization. Figure 2-9 shows the hourly \dot{Q} and T_{wb} in the year of 2012. The \dot{Q} is obtained from on-site measurement and T_{wb} is from a nearby weather station [70]. Since both \dot{Q} and T_{wb} are hourly data, they are linearly interpolated during one hour to provide the inputs for the dynamic simulation.



(a)



(b)

Figure 2-9 Input data for the optimization (a) cooling load (b) outdoor wet bulb temperature

2.5.4 Evaluation of Starting Point Selection Methods

In this section, the author evaluates the performance of the optimization with four different starting point selection methods: approach temperature, middle point, previous value, and high point. The optimization is performed once an hour for all the methods. An exhaustive search method with a frequency as once an hour (*Hourly ES*) is used as the benchmark.

Table 2-1 compares the accuracy of the optimization with four starting point selection methods compared with the *Hourly ES*, which provides a theoretical optimal solution.

None of the studied optimization starting point selection methods can guarantee the global minimum for all searches. With a better starting point, the search using the approach temperature method can mitigate the local minima problem and has the lowest failure point ratio (the ratio of number of failure searches in finding global optimal to the total number of searches). The failure ratios of the middle point method and the high point method are about twice of the approach temperature method. The previous value method experiences the highest failure points, which is more than three times compared to the approach temperature method. This means that the search with the previous value method is more likely trapped by local minima. However, it is surprising that the energy saving penalties for the failures are significantly smaller compared to the searching failure ratios.

Table 2-1 Comparison of the accuracy using different starting point selection methods

	Approach Temperature	High Point	Previous Value	Middle Point	Benchmark (Exhaustive Search)
Number of Failure Searches	315	814	1,080	715	N/A
Failure Search Ratio	3.59%	9.27%	12.30%	8.14%	N/A
Annual Energy Consumption [kWh]	5,028,148	5,030,700	5,030,545	5,028,436	5,027,758
Annual Energy Saving Ratio	9.67%	9.63%	9.63%	9.67%	9.68%

Table 2-2 compares the computational performances of four methods. Depending on the starting point selection methods, the number of simulations needed by the optimization arranges from 30,989 to 52,285, which is significantly less than 113,658 simulations

required by the exhaustive search. In terms of the computing time, the previous value method has the best performance and it reduces the number of simulations by around 72.73% and computing time by about 55.74% compared to the exhaustive search. The approach temperature method has similar performance as the previous value method. The high point method and the middle point method have lower reduction ratios for both the number of simulation (54.00%-57.82%) and computing time (40.40% - 42.25%).

Table 2-2 Comparison of the computational performance using different starting point selection methods

	Approach Temperature	High Point	Previous Value	Middle Point	Exhaustive Search
Number of Simulation	34,585	52,285	30,989	47,941	113,658
Number of Simulation Reduction Ratio	69.57%	54.00%	72.73%	57.82%	N/A
Computing Time [s]	25,045	32,933	24,459	31,914	55,258
Computing Time Reduction Ratio	54.68%	40.40%	55.74%	42.25%	N/A

To get more insights on when and why each method fails to find the global minimum, the author studies four different scenarios. The first scenario is when \dot{Q} or T_{wb} is low. In this scenario, the flat range is likely to occur at the high end. As shown in Figure 2-10 (a), the flat range is between 27.44°C and 29.44°C. Since the high point method selects $T_{cw,set,H}$ as 29.44°C, it is trapped by the local minima within the flat range. Other methods select a starting point outside the flat range and successfully find the global minimum.

The second scenario occurs when \dot{Q} is extremely low. This can happen in the winter that the chiller is still running to provide cooling for building internal zones, such as computer rooms, even T_{wb} is very low. The flat range then extends to a very low temperature (Figure 2-10 (b)) and both the middle point method and high point method fail to find the global minimum.

The third scenario happens when $T_{wb} < T_{wb,nom}$ and \dot{Q} is relatively high. As mentioned earlier, equation (24) may underestimate $T_{cw,low}$. In that case, the approach temperature method gets stuck in the local minima. For instance, in Figure 2-10 (c), $T_{cw,set,sta}$ given by equation (24) is 24.44°C, which is still in the flat range of [21.44, 24.44°C]. Since the initial search step is 2.00°C, the optimization algorithm finds that both $T_{cw,set} = 22.44^\circ\text{C}$ and 26.44°C cause a higher energy consumption than $T_{cw,set} = 24.44^\circ\text{C}$, but misses the global minimum at 25.44°C. In this case, using a smaller initial search step, such as 1.00°C may avoid the problem. However, this is at the cost of longer searching time.

The fourth scenario appears when the difference between the optimal $T_{cw,set}$ for the adjacent optimization periods is significant. This makes the previous value method fail to reach the global minimum. As shown in Figure 2-10 (d), the previous value method is stuck at 22.44°C, which is the optimal $T_{cw,set}$ for the previous optimization period.

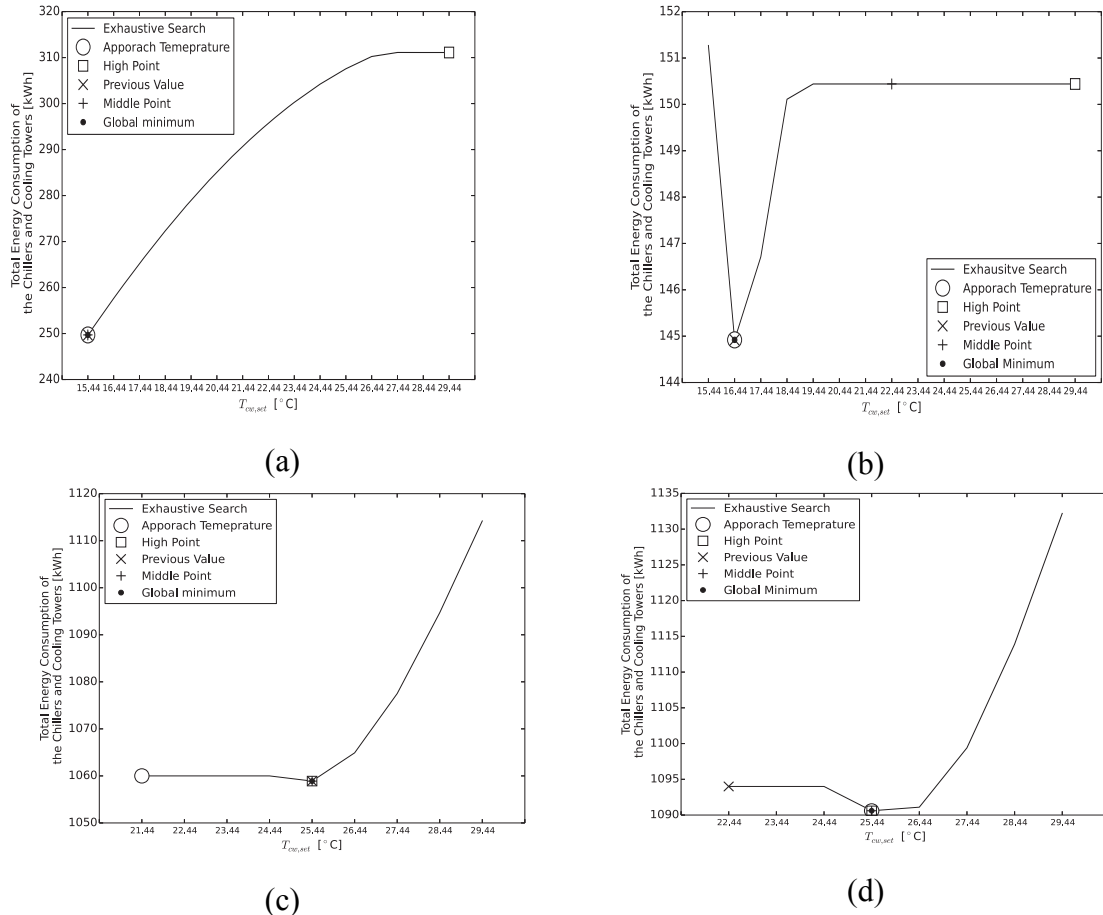


Figure 2-10 The scenarios when different starting point selection methods fail to find the global minimum

To understand why comparably large searching failure ratios only lead to small differences in energy savings, the author analyzes the energy saving penalty due to failing to achieve the optimal condenser water set point. Based on Figure 2-11, for all the methods, more than 90% of the energy saving penalties are less than 5%. As shown in Figure 2-10 (c), the energy saving penalties can only be 0.20%. Thus, although the searching failure ratios of those methods are up to 12.30%, the impact of the searching failures on the total energy savings is not significant.

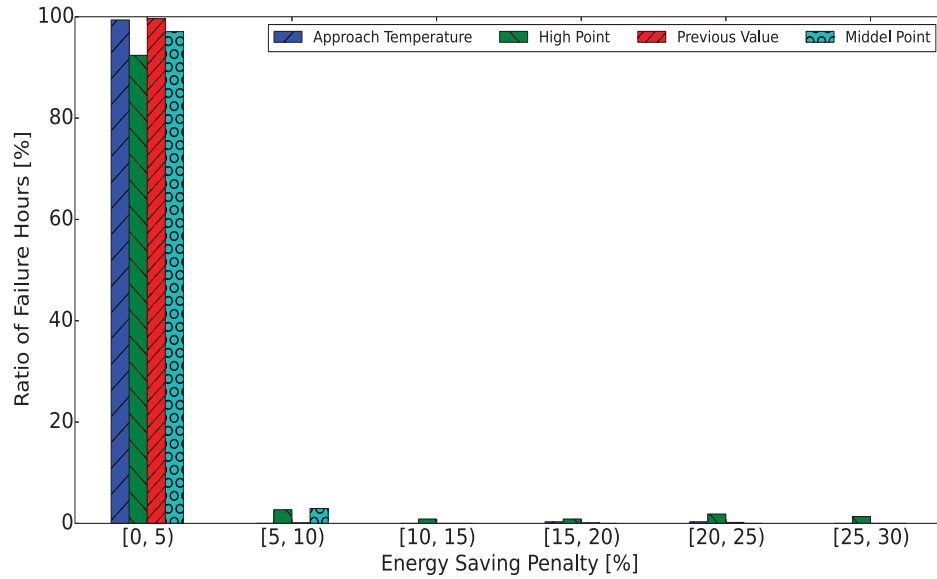


Figure 2-11 The energy saving penalty due to the failure in predicting the optimal condenser water set point

2.5.5 Evaluation of the Optimization Frequency on the Energy Saving

To evaluate the impact of the optimization frequency on the energy savings from the condenser water set point optimization, the author performs optimizations with two different frequencies: once an hour (*Hourly OPT*) and once a day (*Daily OPT*) using perfect predictions of \dot{Q} and T_{wb} . To consider the uncertainties in the load and weather prediction due to a long prediction horizon (one day), the author uses the following equation to generate the synthetic errors.

$$\dot{Q}^* = \dot{Q} + \text{random}(-\Delta\dot{Q}, \Delta\dot{Q}), \quad (33)$$

$$T_{wb}^* = T_{wb} + \text{random}(-\Delta T_{wb}, \Delta T_{wb}), \quad (34)$$

where \dot{Q}^* and T_{wb}^* are the predicted cooling load and outdoor wet bulb temperature with errors, $\Delta\dot{Q} = 20\%\dot{Q}_{nom}$ and $\Delta T_{wb} = 1$ K are the error bands for \dot{Q} and T_{wb} , respectively.

The $\text{random}(a, b)$ is a function that returns a random value between the input range [a,

b]. A daily optimization using \dot{Q}^* and T_{wb}^* as inputs is also tested and the configuration is named *Daily OPT with Error*. The approach temperature starting point method is applied in all configurations.

Table 2-3 compares the performance of the optimization with different optimization frequencies. The *Hourly OPT* provides almost the same solution as the *Hourly ES* with about half of the computing time. By further reducing the number of optimizations, the *Daily OPT* achieves an around 95.00% time reduction with only 0.08% penalty in predicted energy saving than the *Hourly ES*. Compared with the *Hourly OPT*, the *Daily Opt* is about 10 times faster and provides an energy saving only 0.07% less. The reason why the *Daily Opt* does not achieve 24 times faster than the *Hourly OPT* is because the daily simulation costs more time to be solved than the hourly simulation. Even with uncertainties in the \dot{Q} and T_{wb} prediction, the *Daily OPT with Error* gets a similar energy saving compared with the *Daily OPT*.

Table 2-3 Performance comparison of different optimization frequencies

	Hourly OPT	Daily OPT	Daily OPT with Error	Hourly ES (Benchmark)
Annual Energy Consumption [kWh]	5,028,148	5,031,571	5,031,752	5,027,758
Energy Saving Ratio	9.67%	9.60%	9.60%	9.68%
Computing Time [s]	25,045	2,536	2,796	55,258
Computing Time Reduction Ratio	54.68%	95.41%	94.94%	N/A

To understand why the impact of the optimization frequency on the energy savings is not significant; the author investigates the profiles of the inputs for the condenser water set point optimization. The author first looks at the annual distribution of the daily

variation in the outdoor wet bulb temperature. Based on the Figure 2-12, most days (up to around 70.00%) of the year have the daily variations in the outdoor wet bulb temperature that are less than 6.00°C while only very few days (less than 5.00%) have relatively large daily variations (larger than 10.00°C) in the outdoor wet bulb temperature. This means the weather of the studied period in Washington D.C. is relatively temperate with a small daily variation in the outdoor wet bulb temperature. The author then looks at the cooling load distribution, since there are different cooling load profiles for different seasons in the cooling period. The author selects two typical days with different cooling load profiles: one day is from the mild season (April 20th, Friday) and the other day is from the hot season (July 20th, Friday). Both the mild day and the hot day have the daily variation in the outdoor wet bulb temperature less than 6.00°C.

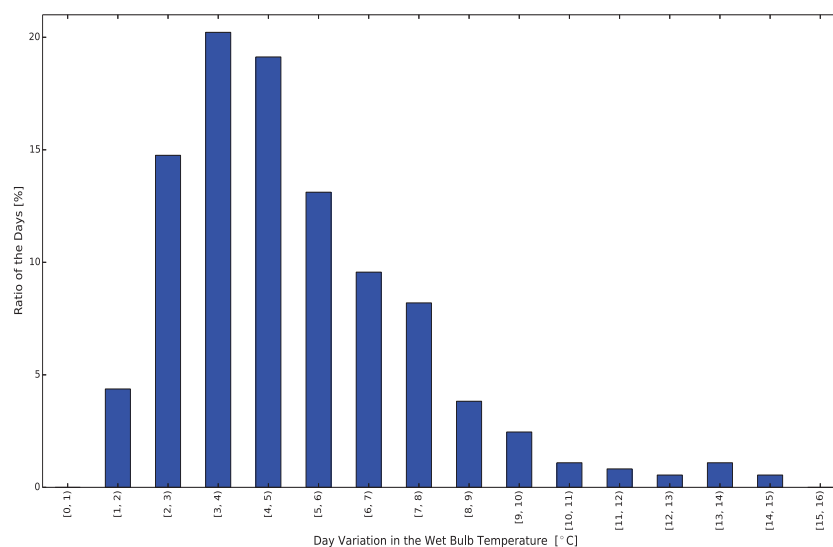


Figure 2-12 The annual distribution of daily variations in the outdoor wet bulb temperature

For the mild day, the cooling load changes from around 400 ton to 900 ton and the outdoor wet bulb temperature is from 11.00°C to 16.00°C (Figure 2-13). The *Hourly OPT* predicts the same results as the *Hourly ES* and a 2,648 kWh (16.14%) energy saving is achieved. The *Daily OPT* produces a slightly different result with an energy savings of 16.13%. The $T_{cw,set}$ is constant as 15.44°C from 0:00 to 13:00 because of the low outdoor wet bulb temperature. The $T_{cw,set}$ begins to increase at 14:00 after T_{wb} passed 15.00°C. At around 17:00, $T_{cw,set}$ suddenly raises to 20.44°C. The reason for the quick increase is that at 17:00, the cooling load decreases from 900 ton to 731 ton and the number of operating chillers reduced from two to one. As a result, the cooling load for the remaining chiller increases from 450 ton to 731 ton. With the increased cooling load, it takes more efforts for the dedicated cooling tower to cool the condenser water to the given $T_{cw,set}$, which makes the optimal $T_{cw,set}$ increased. After 17:00, $T_{cw,set}$ begins to decrease to reflect the reduced cooling load. It returns to 15.44°C at 19:00 and remains unchanged for the rest time. The *Daily OPT* predicts $T_{cw,set}$ as 15.44°C and there are only four hours when the $T_{cw,set}$ by the *Daily OPT* and the *Hourly OPT* are different.

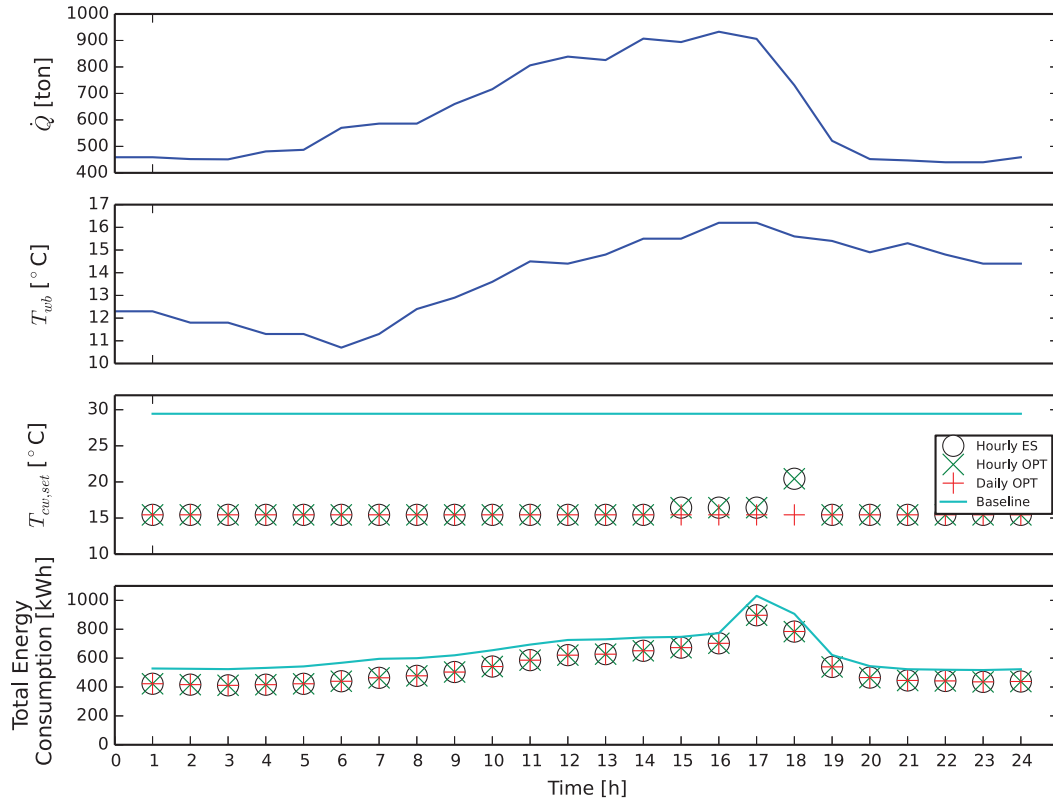


Figure 2-13 The simulation results for April 20, 2012

As shown in Figure 2-14, the cooling load and the outdoor wet bulb temperature for the hot day are higher than those in the mild day in Figure 2-13. Again, the *Hour OPT* predicts the same results as the *Hourly ES*. Basically, the trajectory of $T_{cw,set}$ in the *Hourly ES* follows the change of T_{wb} during that day. The *Daily OPT* predicts $T_{cw,set}$ as 21.44°C. The energy savings from the *Hour OPT* are 682.4 kWh (2.31%) and that for the *Daily OPT* are 681.9 kWh (2.30%). Although there are only three hours when the $T_{cw,set}$ by the *Daily OPT* and the *Hourly OPT* are the same, the differences between the prediction by the *Daily OPT* and the *Hourly OPT* are not larger than 2.00°C.

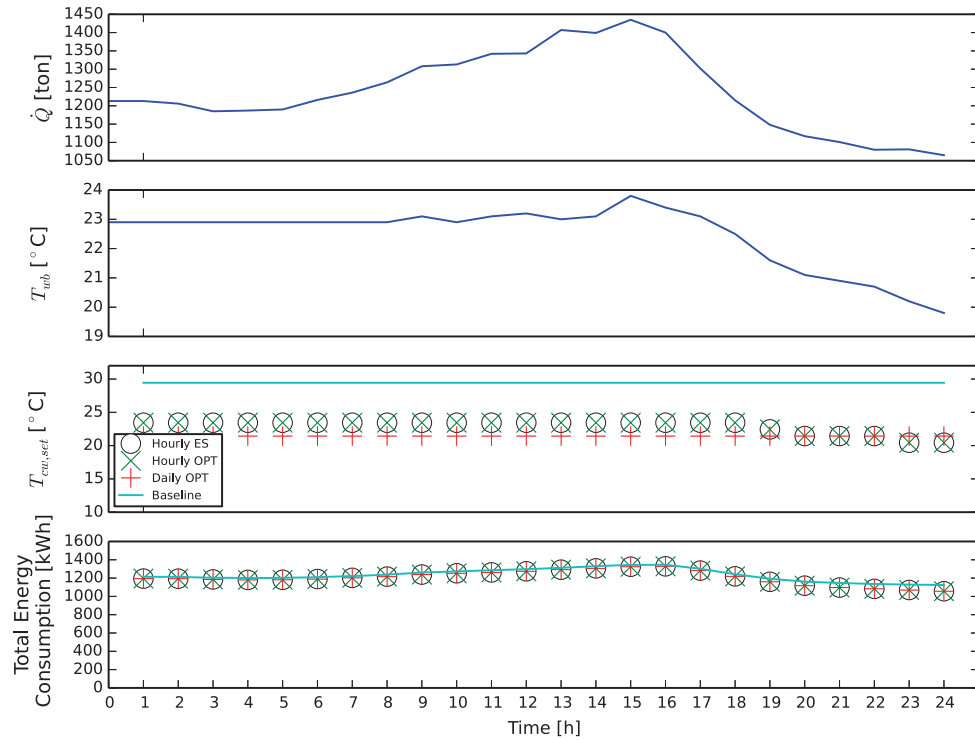


Figure 2-14 The simulation results for July 20, 2012

Based on the above analysis, one can see that despite of different cooling load profiles, the small daily deviation in the outdoor wet bulb temperature makes the difference between the predictions by the *Daily OPT* and the *Hour OPT* not obvious.

2.6 Conclusion

In this chapter, the author proposes and implements a model predictive control for optimizing the condenser water set point. The author evaluates how different starting point selection methods and the optimization frequency affect the condenser water set point optimization results via a case study. Based on the results of the case study, the following conclusions can be drawn:

- 1) Optimization starting point selection does not significantly impact energy savings from the condenser water set point optimization for the studied chiller plant significantly, although it does impact the computing time and the failure rate on finding the global optimum. The previous value method can achieve the fastest searching but it also obtains the largest number of failure. The approach temperature method is recommended since it has a failure rate 2-3 times lower than other methods and its computing time is almost the same as the previous value method.

- 2) The optimization frequency doesn't significantly affect the energy savings from the condenser water set point optimization for the studied chiller plant. This is because the daily variation in the outdoor wet bulb temperature is not large for most of the days in the studied year, which leads to a small difference between the predictions by the *Daily OPT* and the *Hour OPT*.

Chapter 3

Model Predictive Control for Chiller Staging Control

This chapter demonstrates the research on optimizing the model predictive control design for chiller staging.

3.1 Cooling Load based Control for Chiller Staging

Among various configurations of chiller plants, the multiple-chiller plants are the most widely used. For those plants, it is recommended to operate chillers sequentially rather than simultaneously [50]. To operate chillers in sequence, one uses a chiller sequencing control, usually based on the cooling load, to bring chillers online or offline. Depending on the approach to indicate the cooling load, the chiller sequencing control can be categorized as: the return chilled water temperature based control, the bypass flow based control, the direct power based control, and the Cooling Load based Control (CLC) [71]. Among them, the CLC is considered to be the most promising because other approaches employ the use of indirect indicators of the cooling load (e.g. the return chilled water temperature, the volume flow rate at bypass of secondary loop, and the chiller power), which may not be proportional to the cooling load [72]. The CLC directly calculates the cooling load using the chilled water flow rate and the difference between the chilled water return temperature and supply temperature [73].

In the CLC, one chiller will not be brought online/offline unless the cooling load is larger/smaller than the total available cooling capacity of the operating chillers. The

total available cooling capacity of i operating chillers can be referred as a Critical Point (CP):

$$CP_i = \sum_{j=1}^i CC_{act,j}, \quad (35)$$

where $CC_{act,j}$ is the actual cooling capacity of the j th chiller. In the real world implementation, the nominal capacity of the chiller, $CC_{nom,j}$, is conventionally used to represent $CC_{act,j}$. Thus, equation (35) can be converted into:

$$CP_i = \eta \sum_{j=1}^i CC_{nom,j}, \quad (36)$$

where η is the safety factor (e.g., 90%) to mitigate the risk of insufficient cooling supply during the chiller start-up period. Besides, a state machine [74] can also be used to facilitate the implementation of the CLC. To avoid a chiller short circling, a waiting time t_{wait} and a dead band CP_{db} are usually employed. For instance, Figure 3-1 shows a conventional CLC for a chiller plant with three identical chillers. The transition between states indicates adding or reducing the number of the operating chillers.

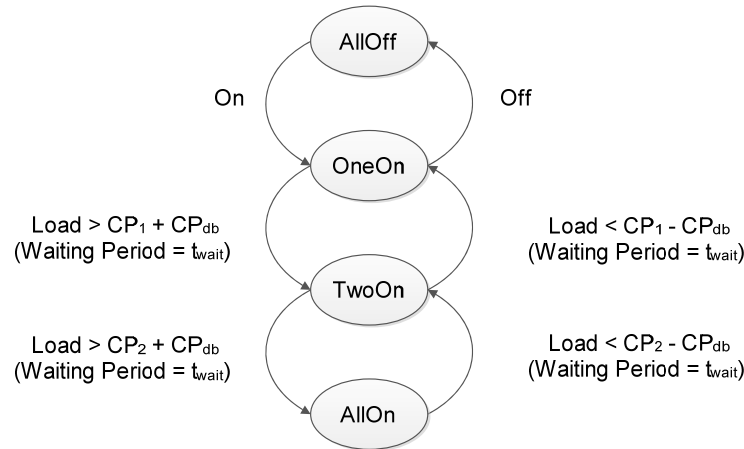


Figure 3-1 The state graph of a conventional CLC for a chiller plant with three identical chillers

3.2 Chiller Staging Optimization

Although widely used, the conventional CLC has limitations and can't guarantee the minimal energy consumption by the chiller plants. To improve the energy efficiency of the chiller plants, researchers proposed various CLC optimization approaches [72, 73, 75-94]. Generally speaking, those approaches can be divided into two groups: studies to optimize the load distribution and studies to identify the optimal number of operating chillers. The author will discuss the concept and the limitations of each group as follows.

The first group aims to optimize the load distribution among the chillers. The conventional CLC turns on an additional chiller only when the cooling load approaches the total nominal cooling capacity of the operating chillers. This means that chillers will work at the highest *PLR*. However, the ASHRAE Handbook [50] points out that a higher *PLR* does not necessarily mean a higher operational efficiency. The chiller's operational efficiency is usually measured by the coefficient of performance (*COP*), which is the ratio of the cooling energy provided by the chiller to its power consumption. Figure 3-2 shows that the highest *COPs* may occur at relatively low *PLRs* for three different chillers.

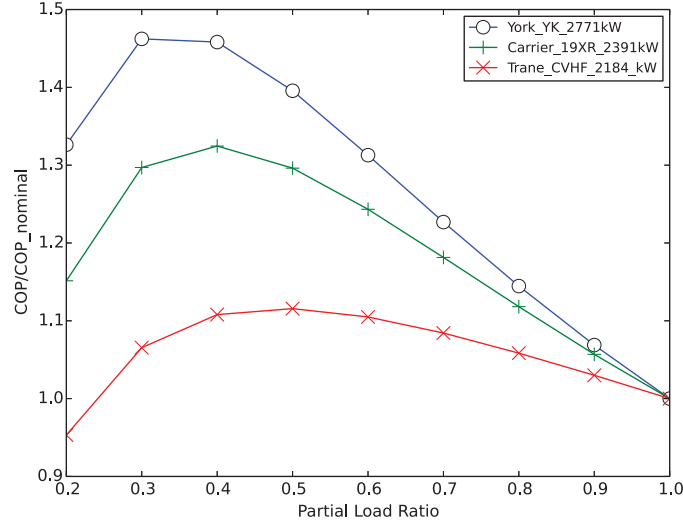


Figure 3-2 The relationship between PLRs and the relative COPs for three different chillers calculated according to the chiller dataset provided by EnergyPlus [42]

To achieve the optimal load distribution, researchers developed model-based optimization approaches to adjust the *PLR* of each chiller individually according to a given cooling load [75-88]. Some studies aimed to maximize a summation of the operating chillers' *COP* as follows [75, 76, 78, 88]:

$$J = \max(\sum_{i=1}^M COP_i), \quad (37)$$

$$s.t. \quad \sum_{i=1}^M PLR_i CC_{nom,i} = \dot{Q}, \quad (38)$$

where COP_i and PLR_i are the *COP* and *PLR* of the i th chiller, respectively. The M is the number of the chillers in the chiller plant. They utilized a regressed *PLR-COP* curve in equation (39) to calculate the COP_i under the PLR_i :

$$COP_i = \sum_{j=0}^m a_j PLR_i^j, \quad (39)$$

where a_j is the j th constant coefficient and m is the number of the constant coefficients.

Other approaches tried to minimize the sum of the chillers' power as follows [77, 79-87]:

$$J = \min(\sum_{i=1}^M P_{ch,i}), \quad (40)$$

$$s.t. \quad \sum_{i=1}^M PLR_i CC_{nom,i} = \dot{Q}, \quad (41)$$

where $P_{ch,i}$ is the power of the i th chiller. The regressed Power- PLR curve in equation (42) is employed to calculate $P_{ch,i}$:

$$P_{ch,i} = \sum_{j=0}^n b_j PLR_i^j, \quad (42)$$

where b_j is the j th constant coefficient and n is the number of the constant coefficients.

Both the above approaches use the $PLRs$ as the independent variables to directly/indirectly reduce the total power of the chillers. However, it is difficult to implement the PLR control in the real world application since the PLR can only be indirectly controlled. Some scholars improved the above approaches by replacing the $PLRs$ with other relevant controllable parameters, such as the chilled water flow rates through each chiller [90, 91], the temperature set points of the chilled water leaving each chiller [92, 93], and the combination of the previous two parameters [94]. However, these approaches still have some limitations. For instance, the approaches of adjusting the chilled water flow rate through chillers can only be applied to the chiller plant equipped with chillers and pumps that can handle variable chilled water flow rates. In addition, these approaches only consider the impact of the load distribution on the chiller power. However, for plants with dedicated pumps and dedicated cooling tower for each chiller, the load distribution also impacts the pump power and the cooling tower power. Without considering the impacts on the pump power and the cooling tower power, these approaches can't guarantee the minimal energy consumption for the entire chiller plant.

The second group is associated with the optimization on the number of the operating chillers. As mentioned above, the conventional CLC uses the chillers' nominal cooling capacities to represent the chillers' actual cooling capacities. However, the actual cooling capacity of a chiller varies by its operating conditions [72, 73]. As shown in Figure 3-3, a chiller's capacity increases up to 110% of its nominal capacity when the temperature of the condenser water entering the chiller ($T_{cw,ent}$) decreases from 23.89°C (nominal condition) to 18.89°C. Therefore, it is possible that a chiller's actual cooling capacity is larger than its nominal capacity and so does the entire multi-chiller plant. In this case, the chiller plant can meet a higher cooling load without turning on an additional chiller. Since people usually have a dedicated primary chilled water pump and a dedicated condenser water pump for each chiller, reducing the number of the operating chillers can save energy from the dedicated pumps [50].

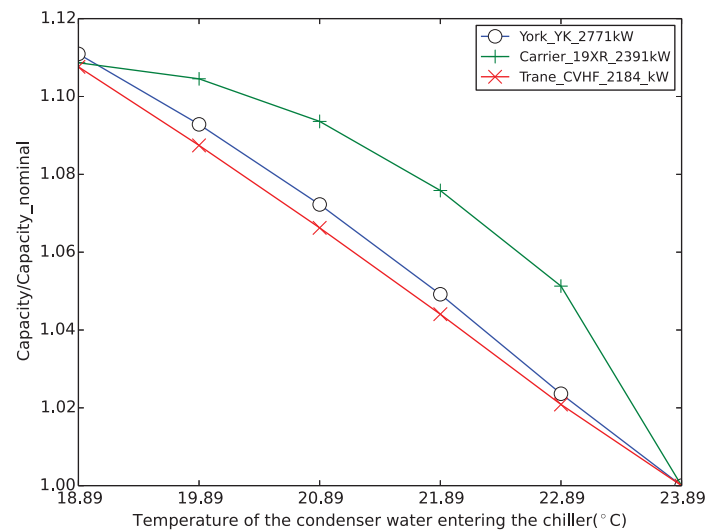


Figure 3-3 The relationship between the temperature of the condenser water entering the chiller and the relative cooling capacity for three different chillers calculated according to the chiller dataset provided by EnergyPlus [42]

To identify the optimal number of the operating chillers, some researchers proposed to reset the CPs based on the estimation of the actual cooling capacity [72, 73, 89]. They calculated $CC_{act,i}$ using the operating parameters of the chiller (such as the pressure in the evaporator, compressibility factor and so on) at a given operating condition. Although these approaches may reduce the pump energy consumption, they can't guarantee the minimal energy consumption of the entire chiller plant including chillers, cooling towers and pumps. For instance, by increasing the CPs according to the calculated cooling capacities, it is possible to reduce the number of the operating chillers. In that case, the PLR of each operating chiller has to increase to meet the same cooling load with fewer chillers. As mentioned above, the increased $PLRs$ may lead to lower $COPs$.

To summarize, there are deficiencies in the existing CLC optimization approaches. In addition, although the optimization of the load distribution and the optimization of the number of the operating chillers interact with each other, they were only studied separately in previous studies. In response to these issues, the author proposes three new CLC optimization approaches. The first approach is to optimize the load distribution by adjusting the CPs . The second approach is to optimize the number of the operating chillers by modulating the CPs and the condenser water set point. The third approach combines the first two approaches aiming to achieve more energy savings with a holistic solution.

3.3 New Approaches for the CLC Optimization

3.3.1 General Assumptions

In this study, the author considers a water-cooled chiller plant with M chillers and N cooling towers. Each chiller has a dedicated constant speed chilled water pump and a dedicated constant speed condenser water pump. The towers have variable speed cooling tower fans controlled by the same condenser water set point. The other control parameters besides the CPs and $T_{cw,set}$, such as set points for the temperature of the chilled water leaving the chillers, $T_{chw,set}$, are constant. Thus, the total power of chillers, pumps, and cooling towers, P_{tot} , at time t can be described as follows:

$$P_{tot}(t) = \sum_i^M (P_{ch,i}(t) + P_{pu,i}(t)) + \sum_j^N P_{tw,j}(t) \quad (43)$$

$$= f_1(T_{cw,set}(t), CP_1(t), \dots, CP_{M-1}(t), \dot{Q}(t), T_{wb}(t), \vec{S}(t)),$$

where $P_{pu,i}$ and $P_{tw,j}$ is the power of the dedicated chilled water pump and the dedicated condenser water pump for the i th chiller and the j th cooling tower, respectively. Then the energy consumption of the chiller plant for a period from t_0 to $t_0 + \Delta t$, $E_{tot}|_{t_0}^{t_0+\Delta t}$, is

$$E_{tot}|_{t_0}^{t_0+\Delta t} = \int_{t_0}^{t_0+\Delta t} P_{tot}(t) dt = \int_{t_0}^{t_0+\Delta t} f_1(T_{cw,set}(t), CP_1(t), \dots, CP_{M-1}(t), \dot{Q}(t), T_{wb}(t), \vec{S}(t)) dt. \quad (44)$$

The outdoor wet bulb temperature and the cooling load during the period of $[t_0, t_0 + \Delta t]$ can be obtained from the weather forecast and by using regression models, respectively. Then one can use the predicted cooling load, \dot{Q}^P , and the predicted outdoor wet bulb temperature, T_{wb}^P , to represent \dot{Q} and T_{wb} in the optimization:

$$\dot{Q}(t) = \dot{Q}^P(t), \quad (45)$$

$$T_{wb}(t) = T_{wb}^P(t). \quad (46)$$

The author assumes $CP_i(t)$ and $T_{cw,set}(t)$ are constant during the period of $[t_0, t_0 + \Delta t]$:

$$T_{cw,set}(t) = T_{cw,set}(t_0), \quad (47)$$

$$CP_i(t) = CP_i(t_0). \quad (48)$$

In addition, since $\vec{S}(t)$ is a function of $\vec{S}(t_0)$, equation (44) can be converted into:

$$E_{tot}|_{t_0}^{t_0+\Delta t} = \int_{t_0}^{t_0+\Delta t} f_2(T_{cw,set}(t_0), CP_1(t_0), \dots, CP_{M-1}(t_0), \dot{Q}^P(t), T_{wb}^P(t), \vec{S}(t_0)) dt. \quad (49)$$

3.3.2 The New Approaches

1) Approach 1: Optimal Load Distribution

For the load distribution optimization, the author assumes $T_{cw,set}$ is constant, thus equation (49) can be changed to:

$$E_{tot}|_{t_0}^{t_0+\Delta t} = \int_{t_0}^{t_0+\Delta t} f_3(CP_1(t_0), \dots, CP_{M-1}(t_0), \dot{Q}^P(t), T_{wb}^P(t), \vec{S}(t_0)) dt. \quad (50)$$

The author uses the CPs to replace $PLRs$ as the independent variables to minimize $E_{tot}|_{t_0}^{t_0+\Delta t}$. Based on equation (50), the optimization problem can be defined as

$$J = \min(E_{tot}|_{t_0}^{t_0+\Delta t}) = \min\left(\int_{t_0}^{t_0+\Delta t} f_3(CP_1(t_0), \dots, CP_{M-1}(t_0), \dot{Q}^P(t), T_{wb}^P(t), \vec{S}(t_0)) dt\right), \quad (51)$$

$$s.t. \quad CP_1^{min} < CP_1(t_0) \leq \eta \sum_{j=1}^1 CC_{nom,j}, \quad (52)$$

$$CP_{i-1}(t_0) < CP_i(t_0) \leq \eta \sum_{j=1}^i CC_{nom,j} \quad (i > 1), \quad (53)$$

where CP_1^{min} is the low bound for $CP_1(t_0)$. The $\dot{Q}^P(t)$, $T_{wb}^P(t)$ and $\vec{S}(t_0)$ are the input variables while $CP_1(t_0), \dots, CP_{M-1}(t_0)$ are the independent variables in the optimization.

Approach 1 does not consider the change of chiller cooling capacities by the operating conditions, thus the high bounds for CPs are determined as $\eta \sum_{j=1}^i CC_{nom,j}$.

Compared to the existing optimal load distribution approaches [75-88], Approach 1 has the following advantages: first, it is easier for implementation since CPs can be directly adjusted; second, the impact of the load distribution on the energy consumption by the cooling towers and the pumps is considered in the objective function. Thus, Approach 1 can lead to a better energy saving for the entire chiller plant.

2) Approach 2: Optimal Number of the Operating Chillers

For the cooling capacity based CPs reset, the author changes the reset into an optimization problem based on equation (49) to minimize $E_{tot}|_{t_0}^{t_0+\Delta t}$:

$$J = \min(E_{tot}|_{t_0}^{t_0+\Delta t}) = \min\left(\int_{t_0}^{t_0+\Delta t} f_2(T_{cw,set}(t_0), CP_1(t_0), \dots, CP_{M-1}(t_0), \dot{Q}^P(t), T_{wb}^P(t), \vec{S}(t_0))dt\right), \quad (54)$$

$$s.t. \quad T_{cw,set,L} \leq T_{cw,set}(t_0) \leq T_{cw,set,H}, \quad (55)$$

$$\eta \sum_{j=1}^i CC_{nom,j} \leq CP_i(t_0) \leq CP_i^{max}, \quad (56)$$

where CP_i^{max} is the high bound for CP_i . The $\dot{Q}^P(t)$, $T_{wb}^P(t)$ and $\vec{S}(t_0)$ are the input variables. The $T_{cw,set}$ is selected as an independent variable because $T_{cw,set}$ can be used to regulate $T_{cw,ent}$ which in turn affects the actual cooling capacity of the chillers. The CPs can directly impact the number of the operating chillers and the associated pumps. To reduce the number of the operating chillers and the operating pumps, the author uses $\eta \sum_{j=1}^i CC_{nom,j}$ as the low bound for CPs and allowed CPs to be higher values up to CP_i^{max} .

Because the chiller cooling capacities vary by operating conditions, it is possible that one may not be able to provide sufficient cooling if the estimated CP_i^{max} is larger than

the actual maximum capacity. In that case, one may save energy by reducing the number of the operating chillers and the associated pumps, but the thermal comfort in the demand side would be sacrificed since provided cooling is insufficient. The author uses the deviation of temperature of chilled water leaving the chiller, $T_{chw,lea}$, from $T_{chw,set}$ as an indicator to determine if sufficient cooling is supplied. The deviation, $D_{chw,lea}$, is calculated by

$$D_{chw,lea} = \int_{t_0}^{t_0+\Delta t} |T_{chw,lea}(t) - T_{chw,set}| dt \quad (57)$$

Ideally, $D_{chw,set}$ should be equal to 0. However, the deviation may also be caused by the waiting time in the CLC, which is inevitable. With that in mind, the author designs the following constraint:

$$D_{chw,lea} \leq D_{chw,lea,base}, \quad (58)$$

where $D_{chw,set,base}$ is $D_{chw,set}$ at the baseline in which no optimization occurs.

To summarize, the optimization can be described as:

$$J = \min(E_{tot}|_{t_0}^{t_0+\Delta t}) = \min\left(\int_{t_0}^{t_0+\Delta t} f_2(T_{cw,set}(t_0), CP_1(t_0), \dots, CP_{M-1}(t_0), \dot{Q}^P(t), T_{wb}^P(t), \vec{S}(t_0)) dt\right), \quad (59)$$

$$s.t. \quad T_{cw,set,L} \leq T_{cw,set}(t_0) \leq T_{cw,set,H}, \quad (60)$$

$$\eta \sum_{j=1}^i CC_{nom,j} \leq CP_i(t_0) \leq CP_i^{max}, \quad (61)$$

$$D_{chw,lea} \leq D_{chw,lea,base}. \quad (62)$$

Approach 2 considers the impact of the CP s reset on the energy performance of the chillers, the cooling towers and the pumps. Thus it can guarantee the minimal energy consumption for the entire chiller plant, which may not be achieved by the existing CP s reset approaches [72, 73, 89].

3) Approach 3: A Holistic Solution for the CLC

It is possible to save more energy by combining Approach 1 and Approach 2. In this holistic approach, the CLC optimization problem can be defined as:

$$J = \min\left(E_{tot}|_{t_0}^{t_0+\Delta t}\right) = \min\left(\int_{t_0}^{t_0+\Delta t} f_2(T_{cw,set}(t_0), CP_1(t_0), \dots, CP_{M-1}(t_0), \dot{Q}^P(t), T_{wb}^P(t), \vec{S}(t_0))dt\right), \quad (63)$$

$$s.t. \quad T_{cw,set,L} \leq T_{cw,set}(t_0) \leq T_{cw,set,H}, \quad (64)$$

$$CP_1^{min} < CP_1(t_0) \leq CP_1^{max}, \quad (65)$$

$$CP_{i-1}(t_0) < CP_i(t_0) \leq CP_i^{max} \quad (i > 1), \quad (66)$$

$$D_{chw,lea} \leq D_{chw,lea,base}. \quad (67)$$

The $\dot{Q}^P(t)$, $T_{wb}^P(t)$ and $\vec{S}(t_0)$ are the input variables while $T_{cw,set}(t_0)$, $CP_1(t_0), \dots, CP_{M-1}(t_0)$ are the independent variables.

3.3.3 Implementation

The CLC optimizations described in Approach 1, Approach 2 and Approach 3 are all constrained optimization problems. The commonly used technologies for solving the constrained optimization problems include the barrier function method and the penalty function method [95]. On one hand, the barrier function method imposes a punishment on the value of the objective function if the value of the objective function approaches the feasible region boundary. On the other hand, the penalty function method adds a term to the objective function and the added term generates a negative impact on the objective function when constraints are violated. In our CLC optimization, the author adopts the penalty function method. For example, the optimization problem in Approach 3 can be converted into:

$$J^* = \min(\int_{t_0}^{t_0+\Delta t} f_2(T_{cw,set}(t_0), CP_1(t_0), \dots, CP_{M-1}(t_0), \dot{Q}^P(t), T_{wb}^P(t), \vec{S}(t_0))dt + k \cdot \text{maximum}(0, D_{chw,lea} - D_{chw,lea,base})) \quad (68)$$

$$s.t. \quad T_{cw,set,L} \leq T_{cw,set}(t_0) \leq T_{cw,set,H} \quad (69)$$

$$CP_1^{min} < CP_1(t_0) \leq CP_1^{max} \quad (70)$$

$$CP_{i-1}(t_0) < CP_i(t_0) \leq CP_i^{max} \quad (i > 1), \quad (71)$$

where k is the iteration index of one optimization and $\text{maximum}(0, D_{chw,lea} - D_{chw,lea,base})$ is the term for the penalty function method.

The author then uses the software environment mentioned in Chapter 2 to implement the optimization problems described in Approach 1, Approach 2 and Approach 3.

3.4 Case Study

3.4.1 Case Description

1) Configuration of the Chiller Plant

The author studies a chiller plant with the same configuration with that shown in Figure 2-3. The model of the chiller is a York_YK2771kW, which has the nominal cooling capacity as 2,771 kW (788 ton). Each chiller has one dedicated chilled water pump, one dedicated condenser water pump, and one dedicated cooling tower. For the cooling tower, the design fan power is 37 kW (50 HP) and the actual fan power is assumed to be proportional to the cubic of the fan speed ratio. The nominal outdoor wet bulb temperature and the nominal approach temperature are 23.89°C (75.00°F) and 0.89°C (1.60°F), respectively. The chilled water and the condenser water pumps are constant speed pumps and their design powers are 34 kW and 47 kW, respectively. In the condenser water loop, a three-way valve is employed to modulate the condenser flow rates through the cooling towers so that the temperature of the condenser water entering

the chiller, $T_{cw,ent}$ will not be less than 12.78°C (55.00°F), which is the lowest $T_{cw,ent}$ can be accepted by the chillers.

A supervisor controller is used to control the chiller operation status according to the measured cooling load. The control sequence is described as Figure 3-1 with CP_1 and CP_2 fixed as 709 ton and 1,418 ton, respectively. The dead band (50 ton) and a waiting period (900 s) are also applied.

2) System Model

For this study, the system model is almost the same with that described in section 2.5.2. However, the author replaces the *Chillers.Carnot* model with the *Chillers.ElectricEIR* model, both the models are from Modelica *Buildings* library [66]. In addition, the performance curves of York_YK2771kW from the chiller dataset provided by EnergyPlus [42] are adapted in the *ElectricEIR* model.

3) Optimization Setting

In this study, the author uses the Hooke Jeeves algorithm [96] in the GenOpt [69] optimization engine to perform the searching of the optimal CPs and the optimal condenser water set point. The optimization is set to be performed every day. The author sets the safety factor $\eta = 90\%$ for all proposed approaches. For Approaches 2 and 3, the author sets the lowest allowable condenser water set point to be 13.89°C and CP_i^{max} to be $1.1CC_{nom}$. The intervals for $T_{cw,set}$, CP_1 and CP_2 are 1°C, 78.8 ton and 78.8 ton,

respectively. Table 3-1 summaries the settings used in the baseline and proposed approaches.

Table 3-1 Settings for each CLC optimization approach

CLC Optimization Approaches	$T_{cw,set}$ [°C]	CP_1 [ton]	CP_2 [ton]
Baseline	Fixed as	709	1418
Approach 1	23.89	[0, 709]	[CP_1 , 1,418]
Approach 2	[13.89,	[709, 867]	[1,418, 1,734]
Approach 3	23.89]	[0, 867]	[CP_1 , 1,734]

The author uses real historic data for \dot{Q} and T_{wb} shown in Figure 2-9. In real world implementation, one can obtain the predicted cooling load by using regression models and the outdoor wet bulb temperature from weather forecast.

3.4.2 Results

1) Annual Simulation

Figure 3-4 shows the annual energy saving of the three CLC optimization approaches compared to the baseline. Approach 1 can reduce the annual chiller energy consumption by 4.9%. However, the energy consumption of the cooling towers and the pumps are increased (-5.8% and -8.6% in saving, respectively). Thus, the total energy saving ratio is only 0.5%. Approach 2 achieves a total energy saving around 5.3%. The energy use of the chillers and the pumps are reduced by 8.6% and 2.0%, respectively. Meanwhile, the cooling tower energy use is significantly increased (-41.8% in saving). As expected, Approach 3 provides the highest annual total energy saving (around 5.6%). The chiller energy saving ratio is the highest as 11.8% with the cost of the highest cooling tower

energy consumption (-43.8% in saving). In addition, the pump energy also rises slightly (-3.7% in saving).

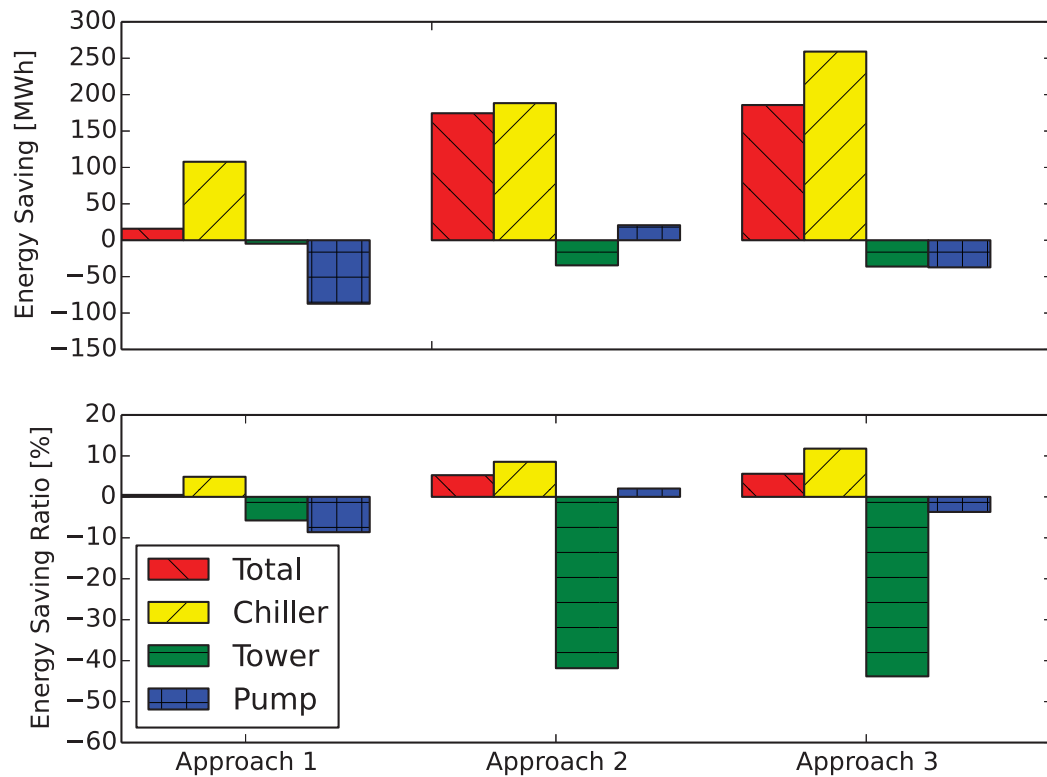


Figure 3-4 Comparison of the energy savings by different approaches

To understand when the energy saving occur, the author performs the detailed analysis. As shown in Figure 3-5, the chiller energy consumption is saved mainly in the summer (May to September) for Approach 1. The cooling tower energy consumption sometimes decreases and sometimes increases. The pump energy consumption increases in the summer, which indicates that the number of the operating chillers is mainly increased to achieve an optimal load distribution. The total energy consumption decreases mainly in the summer. However, at a very few days, the total energy consumption even increases. The explanation is that the initial values of the state vectors (such as the chiller operating status) are different from that in the baseline at these days. Thus, it is possible

that Approach 1 may generate higher total energy consumption. For example, in October 27, there are two chillers operating at the beginning for Approach 1 while there is only one for the baseline. The total energy consumption increases for Approach 1 compared with the baseline is around 0.2%.

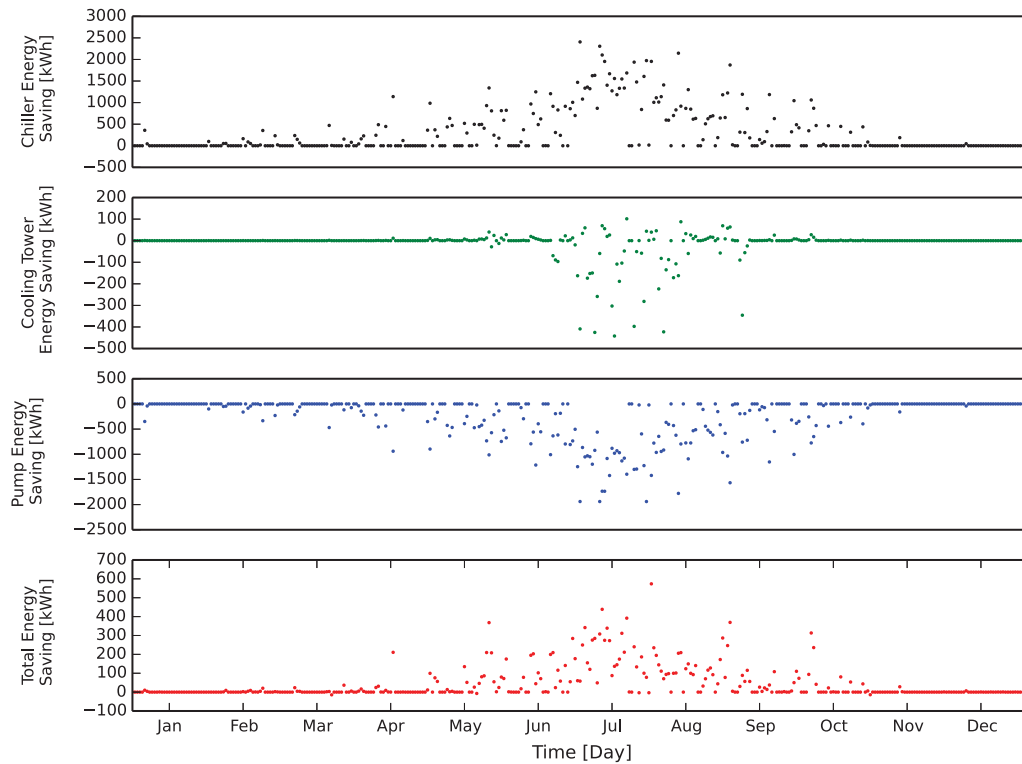


Figure 3-5 Daily energy saving by Approach 1

For Approach 2, the chiller energy consumption is saved mainly in the non-summer season (Figure 3-6). The cooling tower energy consumption increases in the non-summer season due to the lower $T_{cw,set}$. The pump energy consumption is also saved in the non-summer season, which implies that the number of the operating chillers is mainly decreased. Since the studied chillers have higher efficiency at the part loads thus the energy saving from the chiller should be mainly due to the lower $T_{cw,ent}$.

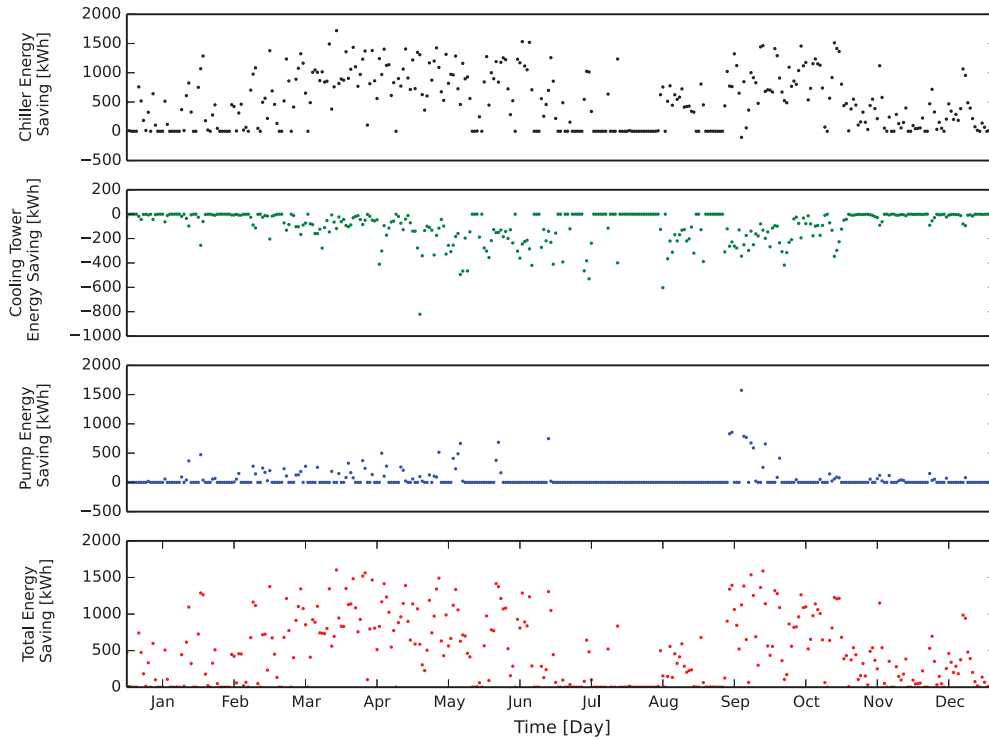


Figure 3-6 Daily energy saving by Approach 2

As shown in Figure 3-7, the chiller energy consumption is saved for the most of time in the studied year for Approach 3, which can be attributed to both the optimal load distribution and the lower $T_{cw,ent}$. The cooling tower energy consumption mostly increases. It is also interesting to see that cooling tower energy consumption reduces sometimes in the summer. The pump energy consumption increases or reduces around the year. In the summer, the pump energy consumption usually increases which indicates that more chillers are operating compared with the baseline. In the rest time, the pump energy consumption reduces which means the cooling load is met with few chillers.

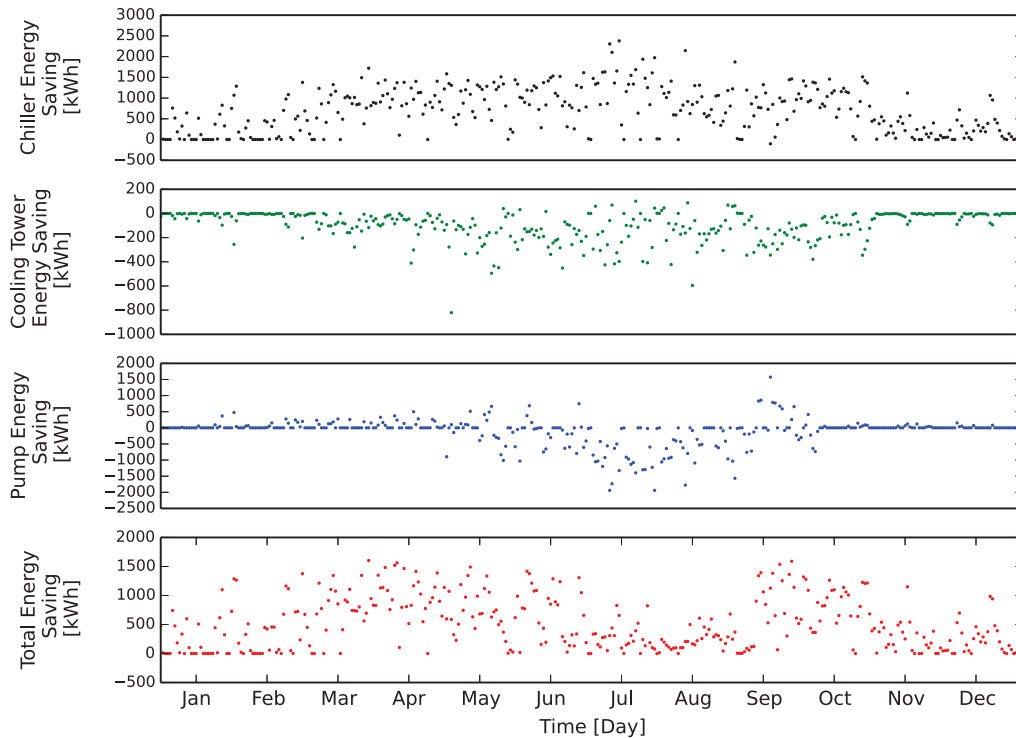


Figure 3-7 Daily energy saving by Approach 3

Based on the above analysis, it can be found that:

- Approach 1's energy savings from chillers is mostly offset by the increased energy used by the pumps. This means that the optimal load distribution approach should be performed on chiller plants with high efficiency condenser water pumps and high efficiency chilled water pumps.
- Approach 2 can save the pump energy for about 2.0% and the chiller energy for about 8.6%. The pump energy decreases because of the reducing number of the operating chillers while the chiller energy use saving is mainly due to the lower temperature of the condenser water entering the chiller.

- Approach 3 can increase the energy saving by combining the previous two approaches, but the total energy saving is less than the summation of their savings. Approach 3 can save the energy used by the chillers, the cooling towers as well as the pumps. In the summer, it increases the number of the operating chillers to save energy for the chillers and the cooling towers. In the non-summer season, it reduces the operating chiller number so that the pump energy saving can be obtained.

2) Typical Days

In order to further identify how energy saving for different components is achieved at different seasons, the author analyzes the performance of Approach 3 for one non-summer day and one summer day. As shown in Figure 3-8, the cooling load in the non-summer day (April 9) ranges from around 400 ton to 800 ton and the outdoor wet bulb temperature is within the range from around 5°C to 10°C. The optimal CP_1 and CP_2 predicted by Approach 3 are 867 ton and 1,418 ton while the optimal $T_{cw,set}$ is 13.89°C. Since the cooling load is always lower than 817 ton, there is only one chiller operating for Approach 3. However, for the baseline, since the cooling load is larger than 759 ton at around 13:00, the number of the operating chillers increases to 2 accordingly and then decreases to 1 around 17:00 when the cooling load is less than 659 ton. There is almost no deviation of $T_{chw,lea}$ from $T_{chw,set}$ for both Approach 3 and the baseline.

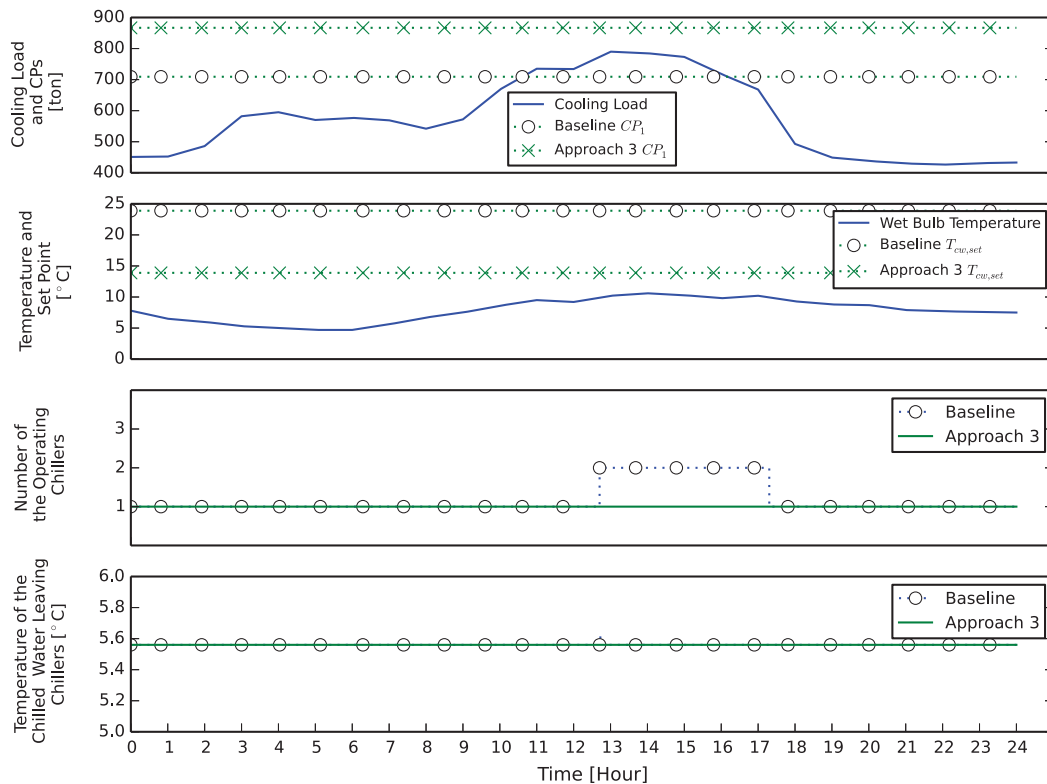


Figure 3-8 Simulated system statuses for a non-summer day

As shown in Figure 3-9, the hourly chiller energy consumption by Approach 3 is significantly less than the baseline over the day since the chiller is more efficient with cooler condenser water achieved by lowering the $T_{cw,set}$. However, having a lower $T_{cw,set}$ significantly increases the cooling tower energy consumption. The pump energy is the same for Approach 3 as that for the baseline except the period when there is two operating chillers for the baseline. Since the chiller energy and the pump energy dominate the chiller plant energy consumption, Approach 3 always requires less energy than the baseline.

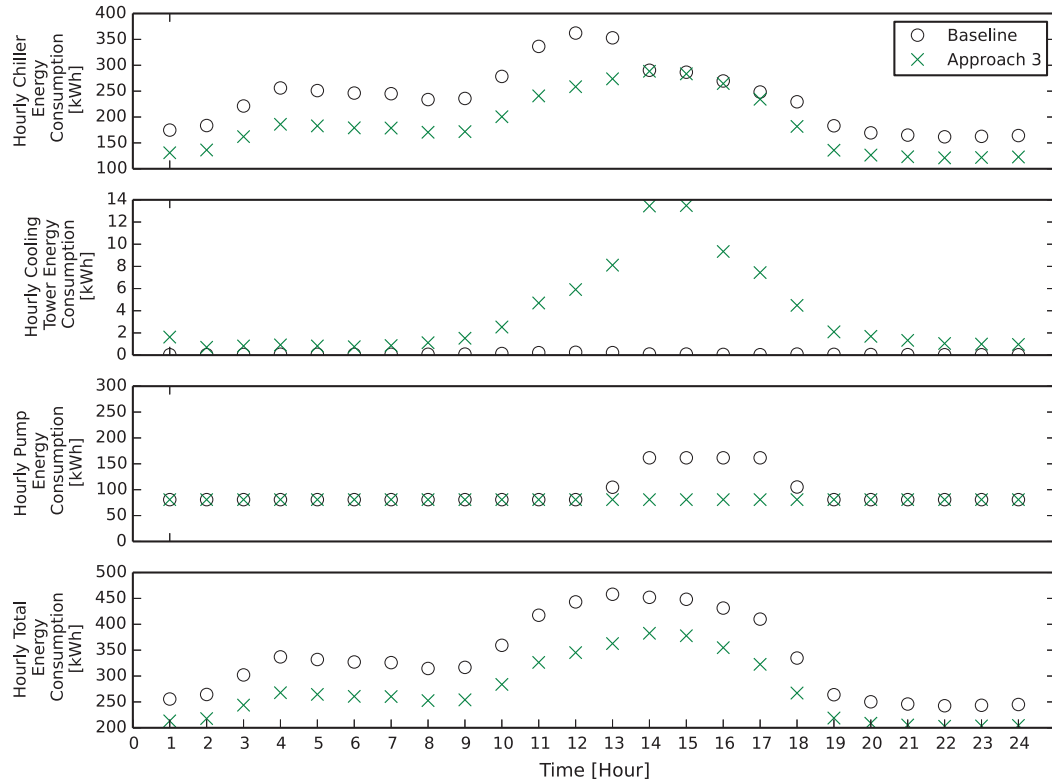


Figure 3-9 Simulated energy consumptions for a non-summer day

As shown in Figure 3-10, the cooling load in the summer day (July 20) ranges from around 1,000 ton to 1,500 ton and the outdoor wet bulb temperature is within the range from around 20 to 25°C. The optimal CP_1 and CP_2 predicted by Approach 3 are 709 ton and 1,182 ton compared to the baseline value of 709 ton and 1,418 ton. The optimal $T_{cw,set}$ predicted by Approach 3 is 23.89°C, which is the same as the baseline. At the beginning, there are three chillers operating for Approach 3. The cooling load decreases to be less than 1,132 ton at around 19:00 and one of the operating chillers is turned off. For the baseline, the number of the operating chillers is two at the beginning and then turns to three at around 14:00. At around 15:30, it turns back to two. No significant deviation of $T_{chw,lea}$ from $T_{chw,set}$ for both Approach 3 and the baseline is observed.

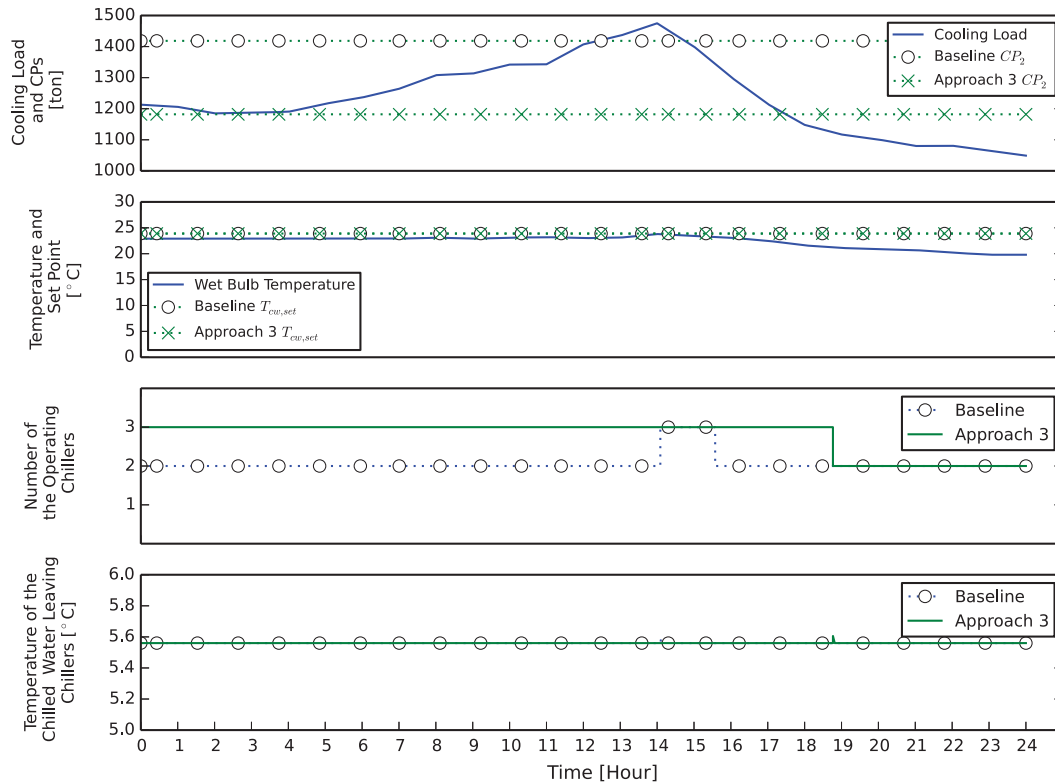


Figure 3-10 Simulated system statuses for a summer day

As shown in Figure 3-11, the hourly chiller consumption for Approach 3 is significantly less than that for the baseline mostly because the chillers are more efficient at lower $PLRs$ enabled by an additional chiller. When the number of the operating chillers is the same (e.g. 20:00-24:00), the chiller energy is the same for both Approach 3 and the baseline.

The cooling tower energy consumption is smaller for Approach 3 than that for the baseline for most of the day since running three towers at lower speed is more energy efficient than running two towers at a higher speed. However, in the period from 14:00 to 16:00, the cooling tower energy consumption for the baseline is smaller. The reason is that at this period, the outdoor wet bulb temperature is relatively higher and the cooling

towers are not able to maintain $T_{cw,ent}$ as the set point. In that case, adding the number of the operating cooling towers would not affect the load ratio of each cooling tower (always be full load) and thus the cooling tower energy consumption is increased as a result.

The pump energy is mostly higher for Approach 3 than that for the baseline because additional pumps are running for the additional chiller. However, the total energy consumption for Approach 3 is smaller than that in the baseline for the most time of the day because the energy saving from the chillers and the cooling towers can offset the additional energy consumption by the pumps.

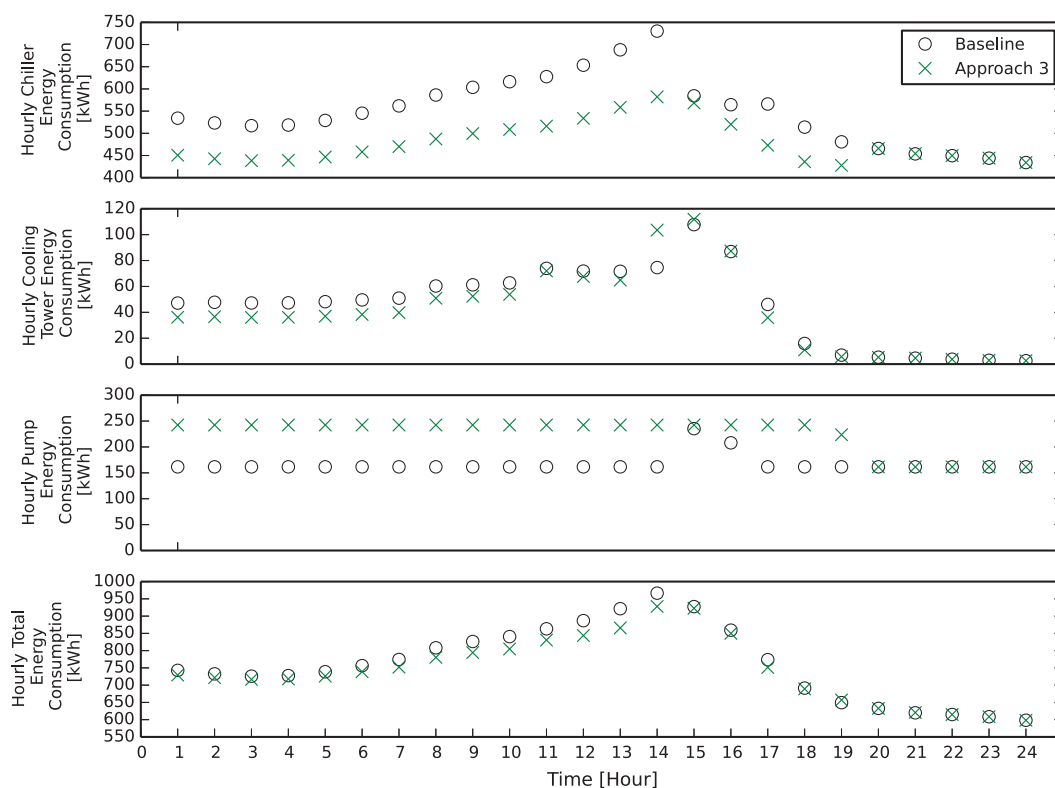


Figure 3-11 Simulated energy consumptions for a summer day

3.5 Conclusion

In this chapter, the author proposes three new CLC optimization approaches to enhance the CLC. Approach 1 is to optimize the load distribution by adjusting the *CPs*. Approach 2 is to optimize the number of the operating chillers by modulating the *CPs* and the condenser water set point. Approach 3 is the combination of the first two approaches. The results suggest that the three approaches for optimizing the chiller sequencing control can all result in energy savings with little risk. The results also suggest that one needs to look at both the energy savings in the chillers as well as the increased energy use by other components of the chiller plant in the chiller sequencing control optimization. Among the three approaches, Approach 3 achieves the highest energy saving because it considers the trade-off among the energy consumption by the chillers, the cooling towers and the pumps. In the summer, one can make more chillers operating to achieve higher energy efficiency for the chillers and the cooling towers. In the non-summer season, one can reduce the number of the operating chillers to save the pump energy consumption.

The new CLC optimization approaches can be directly implemented in the real chiller plant for resetting the *CPs* and/or the condenser water set point. They can also be used as references to help the operators manually adjust the chiller sequencing control.

Chapter 4

A Bayesian Network Model for the Cooling Load Prediction in the Model Predictive Control

Chapter 4 presents research on cooling load prediction.

4.1 Cooling Load Prediction Methods

Predicting cooling load is essential to model predictive control methods [28, 97]. However, it is challenging to accurately predict the cooling load because it is affected by many factors, such as the weather conditions and the internal activities of a building. In addition, the relationship between the cooling load and those factors is complicated and nonlinear.

There are two approaches to predicting the cooling load of a building. One is to use building energy simulation tools such as DOE-2 [41], EnergyPlus [42], and TRNSYS [43]. Those tools predict the cooling load based on a physical description of the buildings. Although those tools have been successfully used to predict the cooling load [98, 99], they require detailed information about building characteristics, such as the thermal conductivity of the envelope as well as the operation schedules of the occupants, to build the model. That information, however, may not be available. In addition, those energy simulation tools are also time-consuming and resource-intensive for implementing in the model predictive control methods.

The other approach involves using regression models to predict the cooling load according to the pre-defined factors of building operations. These regression models include neural networks models [100-103], auto-regressive with exogenous inputs models [104], support vector machine models [105, 106], hourly cooling load factor methods [107], previous-prediction-error-based online load prediction methods [108], and analytic hierarchy process methods [109]. These regression models can be trained by the historical data regarding the cooling load as well as pre-defined factors. Compared to the building energy simulation tools, these regression models do not require detailed information about building characteristics. In addition, they can predict the cooling load instantaneously with few computational resources, which facilitates implementation. Due to those advantages, the regression models are preferable when the historical data is available [102].

However, the regression models also have limitations. The first limitation is that the performance of the regression models is sensitive to the settings of those models. For example, Chapelle, Vapnik, et al. [110] found that the values of parameters in the support vector machine model can dramatically affect the performance of this model. However, determining the best settings for those regression models requires a deep understanding of the mechanism of each model, which poses a serious challenge to large-scale applications.

The second limitation is that the reliability and accuracy of those regression models mainly depend on the amount of training data that is available. If the actual situation

significantly deviates from the training data range, the predicted results may even become unreasonable [108]. Therefore, researchers tend to collect as much training data as possible. However, training data may be limited—more training data may not exist, or the cost to collect it may be extremely high. Thus, for those situations, it is worth studying the relationship between the amount of training data available and the accuracy of the regression models so an appropriate amount of training data can be determined.

Aside from the limitations of those regression models, there is another problem that is seldom considered during the evaluation of those regression models. This problem is how uncertainties in cooling load prediction affect the prediction results. The uncertainties may occur in the training data. For example, the cooling load measurement is error-prone [89]. The uncertainties are likely to occur in the prediction of pre-defined factors. For example, the outdoor dry bulb temperature is usually selected as one factor for prediction cooling load, and regression models tend to rely on the weather forecast service to predict the outdoor dry bulb temperature. However, a significant difference between the predicted outdoor dry bulb temperature and the actual one may exist due to microclimate effects. Given these possibilities, it is necessary to quantitatively assess how those uncertainties affect the cooling load prediction.

To address the first limitation of existing regression models, this chapter proposes a Bayesian network model that does not involve a complicated setting process. Bayesian network models have been used in the building industry for different purposes. For instance, Jesen et al. [111] employed a Bayesian network model to estimate the effects of

the thermal indoor environment on the mental performance of office workers. Toftum et al. [112] used a Bayesian network model to calculate how the indoor temperature set point affected the performance of occupants and building energy consumption. O'Neil [113] utilized a Bayesian network model to establish the system model for building systems. However, no study on the results of applying the Bayesian network model in cooling load prediction seems to have been published. To address the second limitation of existing regression models, this chapter quantitatively describes the relationship between the amount of training data and cooling load prediction accuracy via a case study. This case study also evaluates how the uncertainties in predefined factors affect cooling load prediction.

4.2 Bayesian Network Model

4.2.1 Theory

As shown in Figure 4-1, a typical Bayesian network model includes two components: nodes and arcs. The nodes (e.g., X_a to X_f) represent variables that make up the system of analysis. A node that impacts other nodes is called a parent node (e.g., X_a and X_f), and a node that is impacted by other nodes is called a child node (e.g., X_b and X_d). A node can be both a parent node and a child node (e.g., X_b and X_c). The arcs indicate the relationships between the nodes, which are quantified as conditional probabilities. In the following section, the node X_c will serve as an example of how a Bayesian network model works.

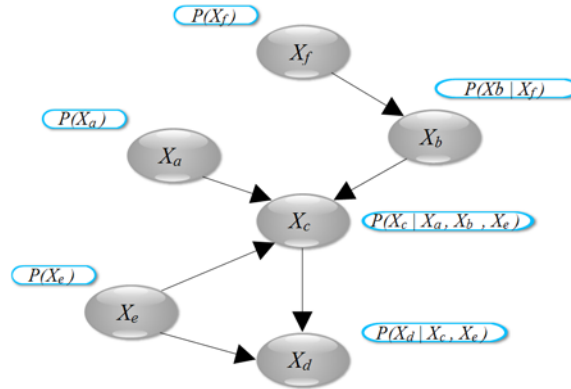


Figure 4-1 The structure of a typical Bayesian Network model

Node X_c has three parent nodes— X_a , X_b , and X_e —which means

$$X_c = f(X_a, X_b, X_e). \quad (72)$$

Here, it is assumed that the values of X_a , X_b , and X_e are within the sets $[x_{a,L}, x_{a,H}]$, $[x_{b,L}, x_{b,H}]$, and $[x_{e,L}, x_{e,H}]$, respectively. The ranges of X_a , X_b , and X_e can be split into smaller sections: $[x_{a,L}, x_{a,H}]$ is split into m sections: $A_1 = [x_{a,L}, x_{a,1})$, ..., and $A_m = [x_{a,m-1}, x_{a,H}]$; $[x_{b,L}, x_{b,H}]$ is split into n sections: $B_1 = [x_{b,L}, x_{b,1})$, ..., and $B_n = [x_{b,n-1}, x_{b,H}]$; and $[x_{e,L}, x_{e,H}]$ is split into o sections: $E_1 = [x_{e,L}, x_{e,1})$, ..., and $E_o = [x_{e,o-1}, x_{e,H}]$. The conditional possibility that $X_c = x_{c,i}$, when the values of X_a , X_b , and X_e are within the set $\{X_a \in A_j \cap X_b \in B_k \cap X_e \in E_l\}$, can be calculated as

$$P(X_c = x_{c,i} / (X_a \in A_j \cap X_b \in B_k \cap X_e \in E_l)) = P(X_c = x_{c,i} \cap X_a \in A_j \cap X_b \in B_k \cap X_e \in E_l) / P(X_a \in A_j \cap X_b \in B_k \cap X_e \in E_l), \quad (73)$$

Then the expectation of X_c , when the values of X_a , X_b , and X_e are within the set $\{X_a \in A_j \cap X_b \in B_k \cap X_e \in E_l\}$, can be calculated by

$$E(X_c / (X_a \in A_j \cap X_b \in B_k \cap X_e \in E_l)) = \sum_i^p x_{c,i} P(X_c = x_{c,i} / (X_a \in A_j \cap X_b \in B_k \cap X_e \in E_l)), \quad (74)$$

where $x_{c,1}, \dots, x_{c,p}$ are the observed values of X_c .

If one assumes that the value of X_c , when the values of X_a , X_b , and X_e are within the set $\{X_a \in A_j \cap X_b \in B_k \cap X_e \in E_l\}$, is equal to its expectation, then one can obtain the following equation:

$$X_c = f(X_a, X_b, X_e) \cong E(X_c / (X_a \in A_j \cap X_b \in B_k \cap X_e \in E_l)) \quad (75)$$

Based on the above analysis, the value of X_c for the given values of X_a , X_b , and X_e can be determined according to equation (68) if the conditional probabilities are known.

These probabilities are calculated with the following equations:

$$P(X_c = x_{c,i} \cap X_a \in A_j \cap X_b \in B_k \cap X_e \in E_l) = \frac{\text{num}(X_c = x_{c,i} \cap X_a \in A_j \cap X_b \in B_k \cap X_e \in E_l)}{\text{num}_{tot}}, \quad (76)$$

$$P(X_a \in A_j \cap X_b \in B_k \cap X_e \in E_l) = \frac{\text{num}(X_a \in A_j \cap X_b \in B_k \cap X_e \in E_l)}{\text{num}_{tot}}, \quad (77)$$

where $\text{num}(X_c = x_{c,i} \cap X_a \in A_j \cap X_b \in B_k \cap X_e \in E_l)$ is the number of training data points in which the values of X_c , X_a , X_b , and X_e are within the set $\{X_c = x_{c,i} \cap X_a \in A_j \cap X_b \in B_k \cap X_e \in E_l\}$, $\text{num}(X_a \in A_j \cap X_b \in B_k \cap X_e \in E_l)$ is the number of training data points in which the values of X_a , X_b , and X_e are within the set $\{X_a \in A_j \cap X_b \in B_k \cap X_e \in E_l\}$, and num_{tot} is the number of total training data points.

Thus, equation (67) can be simplified as

$$\begin{aligned} P(X_c = x_{c,i} / (X_a \in A_j \cap X_b \in B_k \cap X_e \in E_l)) \\ = \frac{\text{num}(X_c = x_{c,i} \cap X_a \in A_j \cap X_b \in B_k \cap X_e \in E_l)}{\text{num}(X_a \in A_j \cap X_b \in B_k \cap X_e \in E_l)}. \end{aligned} \quad (78)$$

4.2.2 The Procedure for Developing the Bayesian Network Model

The typical procedure of developing the Bayesian Network model consists of four steps.

Step 1: The first step is to determine the parent nodes for the studied child nodes. Selecting the parent nodes requires a careful balance between model accuracy and accessibility. On one hand, including parent nodes tends to give better prediction results; on the other hand, the parent nodes should also be easy to obtain so that the efforts of implementation can be minimized.

Step 2: Based on the identified parent nodes in Step 1, one selects the training dataset and determines how to split this dataset. After the split is completed, one calculates the conditional probabilities according to equation (78).

Step 3: After one obtains conditional probabilities from Step 2, one calculates the expectations for the studied child nodes according to equation (74).

Step 4: To facilitate the implementation of the Bayesian network model, one must convert the expectations for child nodes and the corresponding sets of parent nodes into a multiple-dimensional reference table. This table is used to represent the conditional probabilistic expressions based on relative column position in the association list.

4.2.3 The Bayesian Network Model for Cooling Load Prediction

To develop the Bayesian network model for cooling load prediction, the first step is to determine the parent nodes. The cooling load for the buildings is usually affected by factors such as the weather condition and the building's internal activities. Depending on the type of building, the weather condition and internal activities affect the total cooling load in different ways. For example, in data centers, the cooling load is dominated by the heat gain from the IT equipment, and the impact of the weather condition is negligible. However, for buildings with a constant and high fresh air requirement (such as the clean rooms), the cooling load is mainly used for cooling the fresh air. In that case, the cooling load is mainly determined by the weather condition.

To facilitate large-scale application of the Bayesian network model, this study considers both the weather condition and the internal activities in the design of a cooling load prediction method. The outdoor dry bulb temperature and the outdoor wet bulb temperature are used to represent the weather condition. For the internal activities, the days are divided into three categories (shown in Table 4-1) and the category numbers are used to reflect the internal activities of the day-level period. It is expected that days in the same category have a similar internal activity pattern. In addition, the hour index (0,...,23) is employed to reflect change in the internal activities within one day.

Table 4-1 The category of days

Day Category Number	Day Category name	Description
1	Working Day	Official working day of the week. For typical office buildings, the working days are from Monday to Friday
2	Holiday	The days when no works are done. For typical office buildings, the working days are from Saturday to Sunday
3	Event Day	The days when events (e.g. ceremonies) occur

Based on the above analysis, the Bayesian network model is built for cooling load prediction as shown in Figure 4-2.

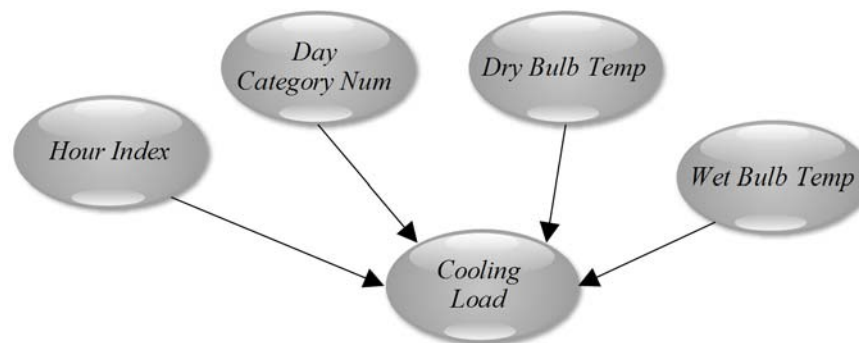


Figure 4-2 The structure of Bayesian Network model for the cooling load prediction

It is possible that the training data may not cover the full range for the parent nodes. In that case, the Bayesian network model cannot predict the output. To address this issue, the linear interpolation and the nearest extrapolation methods are applied in the Bayesian network model. For example, one may use the Bayesian network model to predict the hourly cooling load for the following 5 hours: $\dot{Q}_1, \dot{Q}_2, \dot{Q}_3, \dot{Q}_4, \dot{Q}_5$. However, due to the

limitations of the training data, the Bayesian network model can only generate \dot{Q}_2 , \dot{Q}_4 , and \dot{Q}_5 . To predict \dot{Q}_1 and \dot{Q}_3 , the following equations were therefore used:

$$\dot{Q}_1 = \dot{Q}_2, \quad (79)$$

$$\dot{Q}_3 = \frac{\dot{Q}_4 - \dot{Q}_2}{2}(3 - 2) + \dot{Q}_2, \quad (80)$$

For the Bayesian network model, it is necessary to split the training data. In the case of this study, two of the parent nodes (day category number and the hour index) are discrete. For the other two parent nodes (outdoor dry bulb temperature and outdoor wet bulb temperature), a fixed interval (2°C) was used to split the full range of these temperature data: for the outdoor dry bulb temperature, the split ranges are $[0, 2), \dots, [40, \infty]$; for the outdoor wet bulb temperature, the split ranges are $[0, 2), \dots, [30, \infty]$.

4.3 Case Study

In this case study, the Bayesian network model was applied in the prediction of the cooling load for a university campus located in Annapolis, Maryland, U.S.

4.3.1 Training and Testing Data

To generate the training and testing data for the cooling load prediction, the hourly cooling load data for the campus were collected via the building automation systems of the central cooling system. In addition, the hourly outdoor dry bulb temperature and the outdoor wet bulb temperature were obtained from a weather station located on the campus. The day category number was determined according to the academic calendar, which is available on the university website. The collected cooling load, the outdoor dry

bulb temperature data, the outdoor wet bulb temperature, and the day category number are shown in Figure 4-3. They cover two periods: 09/09–11/02/2014 and 04/27–09/20/2015. These two periods represent a typical cooling season for the studied campus. The two periods consist of 29 weeks (although data gaps exist), among which one week (09/06–12/2015) was selected as the testing period to evaluate the cooling load prediction while the remaining 28 weeks served as the training period.

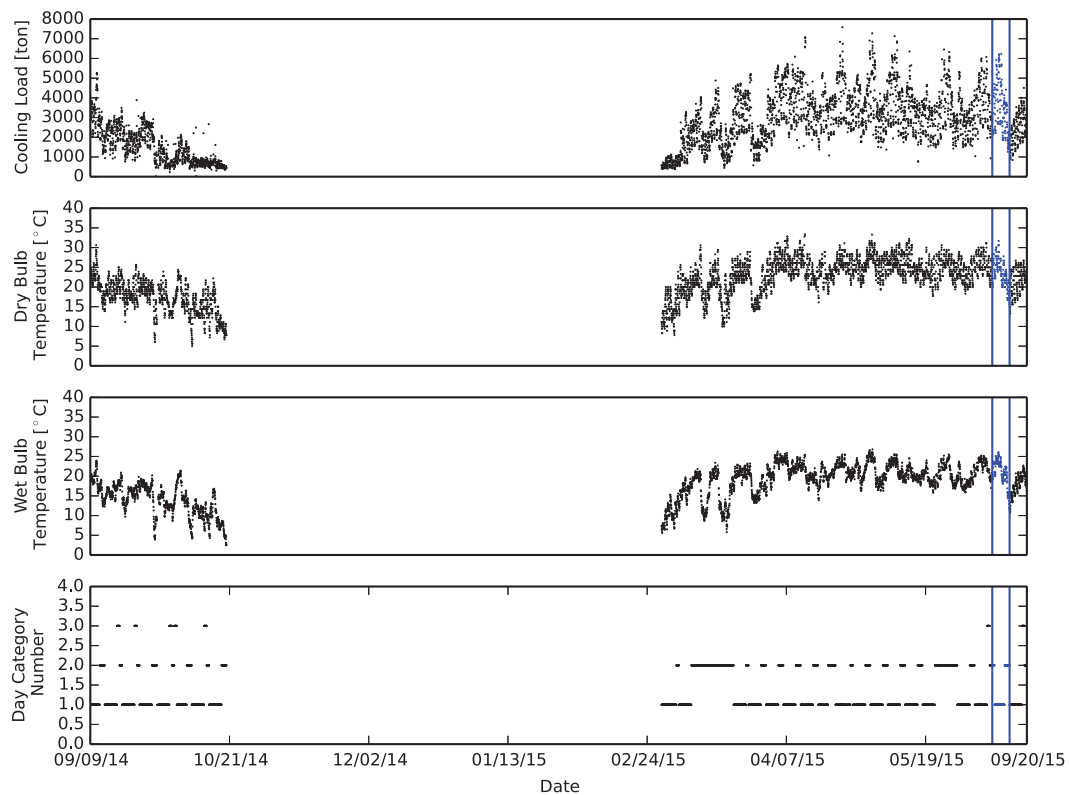


Figure 4-3 The training and testing dataset (blue = testing data; the rest = training data)

4.3.2 Other Regression Models

To better evaluate the performance of the proposed Bayesian network model in cooling load prediction, a support vector machine model is applied in the cooling load

prediction. For a comprehensive introduction to the support vector machine model, please refer to [105]. The reason to select the support vector machine model is that previous studies show that this model is better than other regression models, such as the neural network model [105]. The current study uses the Python Package scikit-learn [114] to implement the support vector machine model, and the inputs for the support vector machine model are the same as those of the Bayesian network model. For the support vector machine model, the kernel function is selected as the Gaussian function since it is recommended by [105]. The other settings are set as default values.

4.3.3 Evaluation Merits

To quantitatively evaluate the prediction accuracy, the author employ the coefficient of determination, denoted R^2 , and the root mean squared error (RMSE). R^2 is calculated by

$$R^2 = 1 - \frac{\sum_i^{pnum} (\dot{Q}_{p,i} - \dot{Q}_{m,i})^2}{\sum_i^{pnum} (\dot{Q}_{m,i} - \overline{\dot{Q}_m})^2}, \quad (81)$$

where $\dot{Q}_{p,i}$ and $\dot{Q}_{m,i}$ are the i th predicted and measured cooling load, $pnum$ is the prediction number, and $\overline{\dot{Q}_m}$ is the mean value of $\dot{Q}_{m,i}$. Basically, the more closely R^2 approaches 1, the better the prediction accuracy is. The RMSE is calculated by

$$RMSE = \sqrt{\frac{\sum_i^{pnum} (\dot{Q}_{p,i}/\dot{Q}_{m,i} - 1)^2}{pnum}}. \quad (82)$$

4.3.4 The Impact of the Training Data on the Cooling Load Prediction

To quantitatively describe the relationship between the amount of training data and the cooling load prediction results, the following studies were performed:

- The 28 weeks in the training period were indexed from 1 to 28 according to the time (shown in Figure 4-4). The week for index 27 is the week immediately before the testing week.

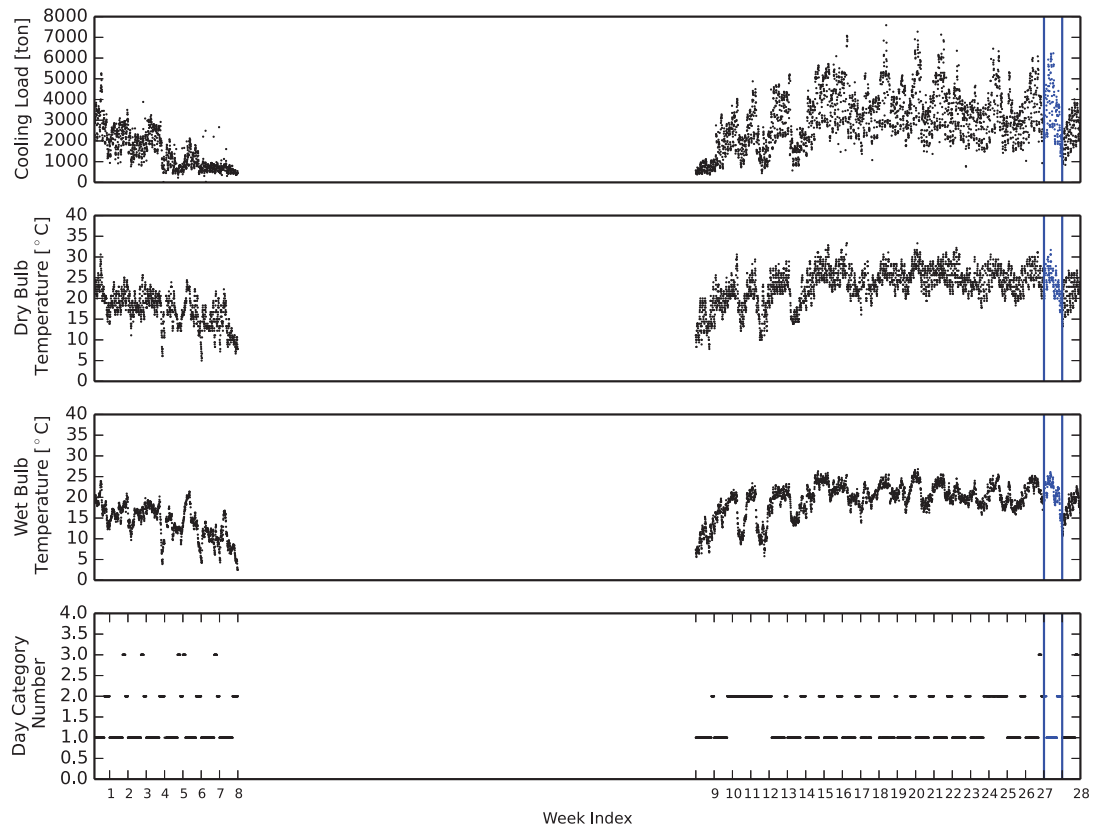


Figure 4-4 The week indexes of the training data

- The 28-week training data were distributed into 14 groups, shown in Table 4-2.
- The Bayesian network model and support vector machine model were trained using training data from each group.

Table 4-2 the groups for the training data

Groups	The Week Number	Number of Data
1	26,27	276
2	24,25,26,27	554
3	22,23,24,25,26,27	872
4	20,21,22,23,24,25,26,27	1,188
5	18,19,20,21,22,23,24,25,26,27	1,463
6	16,17,18,19,20,21,22,23,24,25,26,27	1,756
7	14,15,16,17,18,19,20,21,22,23,24,25,26,27	2,079
8	12,13, 14,15,16,17,18,19,20,21,22,23,24,25,26,27	2,413
9	10,11,12,13, 14,15,16,17,18,19,20,21,22,23,24,25,26,27	2,743
10	8,9,10,11,12,13, 14,15,16,17,18,19,20,21,22,23,24,25,26,27	3,077
11	6,7,8,9,10,11,12,13, 14,15,16,17,18,19,20,21,22,23,24,25,26,27	3,413
12	4,5,6,7,8,9,10,11,12,13, 14,15,16,17,18,19,20,21,22,23,24,25,26,27	3,735
13	2,3,4,5,6,7,8,9,10,11,12,13, 14,15,16,17,18,19,20,21,22,23,24,25,26,27	4,071
14	1,2,3,4,5,6,7,8,9,10,11,12,13, 14,15,16,17,18,19,20,21,22,23,24,25,26,27,28	4,379

The following plotting was then made based on the group information shown in Table 4-2 and the results for the cooling load prediction:

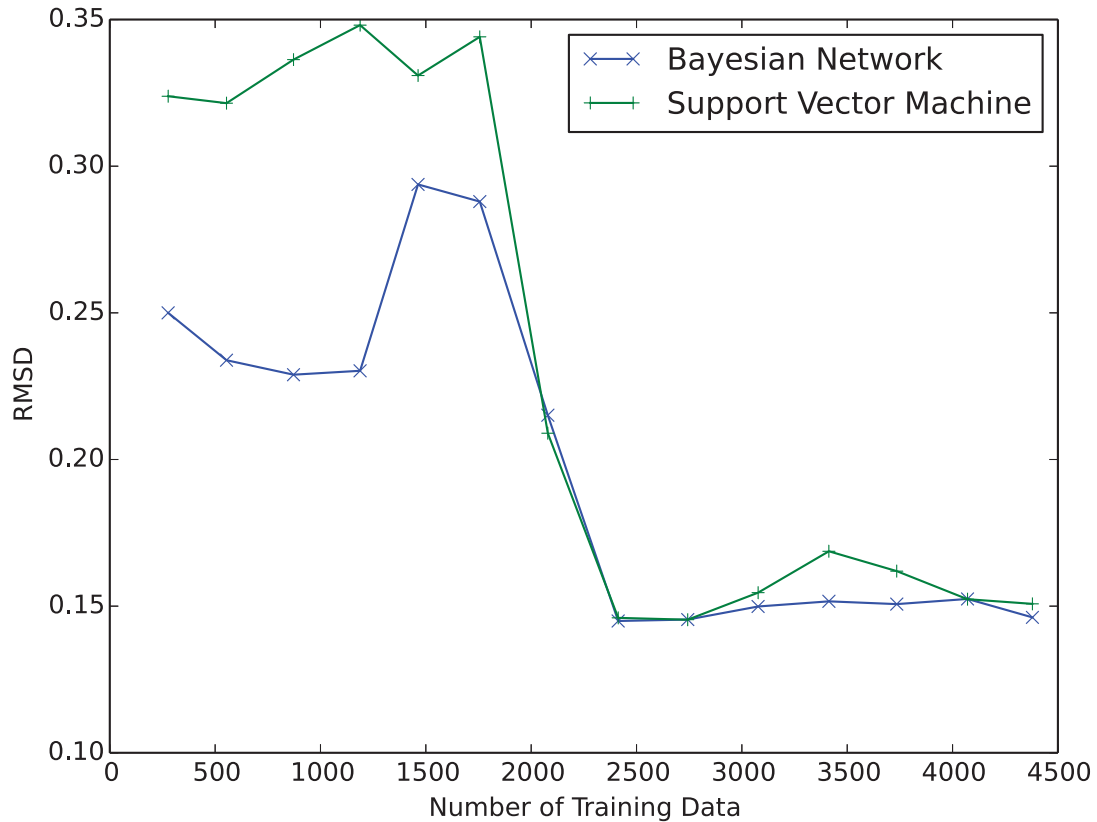


Figure 4-5 The relation between the amount of training data and the RMSD for the cooling load prediction

Based on Figure 4-5, it is apparent that:

- 1) By increasing the scope of training data collected from 2 weeks to 28 weeks, the RMSD of the Bayesian network model and the support vector machine model can be reduced from 0.25 to 0.15 and from 0.32 to 0.15, respectively.
- 2) More training data does not guarantee better results. When the amount of the training data changes from 16 weeks (2,413 data) to 28 weeks, the RMSD of the Bayesian network model and the support vector machine model even increase slightly.

To demonstrate the details of the cooling load prediction, the results of the Bayesian network model and the support vector machine model (shown in Figure 4-6) were plotted for a volume of training data spanning 16 weeks. Generally speaking, both the Bayesian network model and the support vector machine model can predict changes in the cooling load during the testing period. The R^2 of the two models are 0.84 and 0.83, which are quite close. However, for some periods, such as the middle of the week of 09/09/2015, significant deviations between the cooling load prediction and measurement exist for both two models. One possible reason for that discrepancy is that during those periods, cooling load changed dramatically due to the occupants' activities. However, the factors selected to represent the occupancy activities may be too simple to reflect the dramatic changes in those short periods.

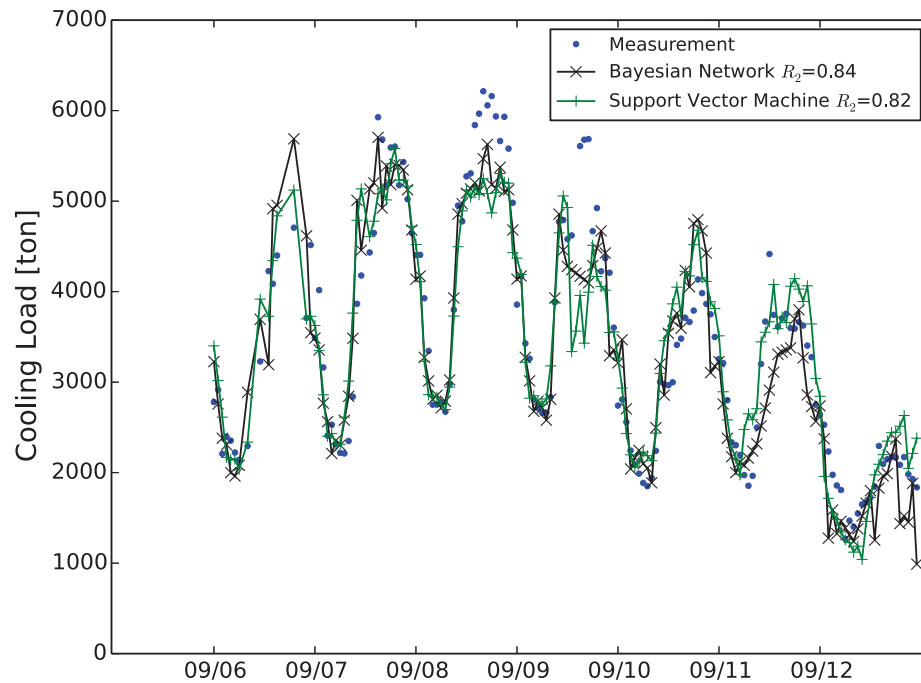


Figure 4-6 The cooling load prediction results (16 weeks training data)

4.3.5 The Impact of the Uncertainties on the Cooling Load Prediction

To quantitatively describe the relationship between the amount of training data and the cooling load prediction, the following studies were performed.

- The following equation was used to generate synthetic errors to mimic the uncertainties in the weather forecasting:

$$T^* = T + T_{sta,er} + ran(-0.5,0.5), \quad (83)$$

where T^* is predicted as the outdoor dry/wet bulb temperature with error, T is the predicted outdoor dry/wet bulb temperature without error, $T_{sta,er}$ is the static error while $ran(-0.5,0.5)$ is used to represent the dynamic error, and $ran(a,b)$ is a function that returns a random number from the range $[a,b]$.

In this study, it is assumed that the on-site outdoor dry/wet bulb temperature is noise-free. Based on this assumption, the synthetic errors can be calculated according to different static error settings. An example for predicted outdoor dry/wet bulb temperature with error when synthetic error is 2°C is shown as Figure 4-7.

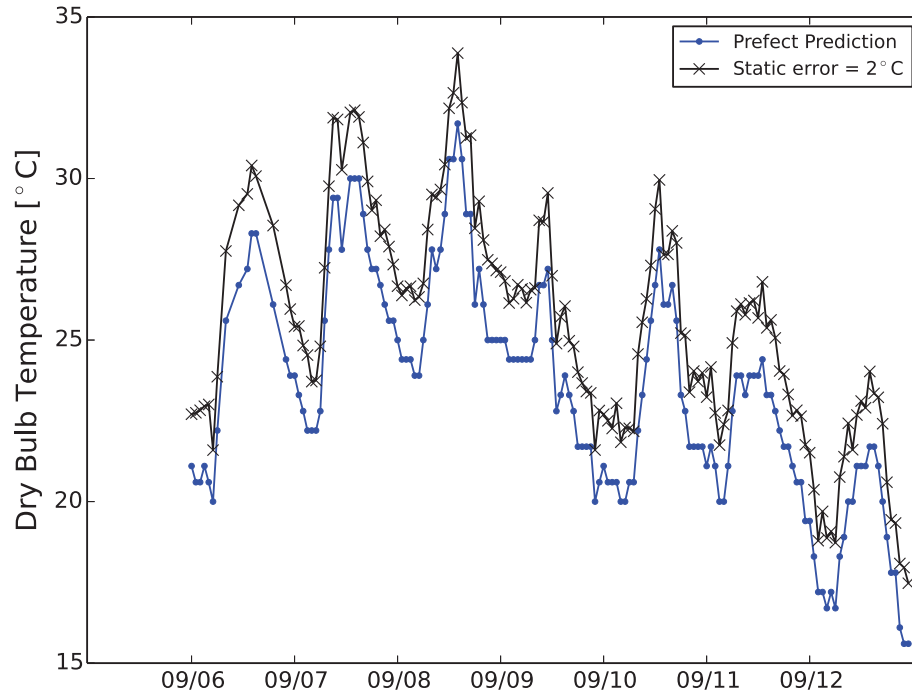


Figure 4-7 The uncertainties in the weather forecast (static error is 2°C)

- The Bayesian network model and the support vector machine model were then used to predict the cooling load for the testing period, when the synthetic errors were considered for the outdoor dry bulb temperature and the outdoor wet bulb temperature. To mimic different error conditions, $T_{sta,er}$ was changed from -2°C to 2°C with an interval of 0.5°C. Sixteen weeks of training data was used.

The results for the cooling load prediction with errors in inputs are shown in Figure 4-8. When the static error equals 0, the RMSD for the Bayesian network model and the support vector machine model are 0.15 and 0.17, which are slightly larger than the RMSDs when there are no errors in the inputs (a 15% and 5% increase, respectively). When the static error changes from 0°C to -2°C, the RMSD for the Bayesian network

model and the support vector machine model increases by 45% and 58%, respectively; when the static error changes from 0°C to 2°C, the RMSD for the Bayesian network model and the support vector machine model increases by 41% and 42%, respectively.

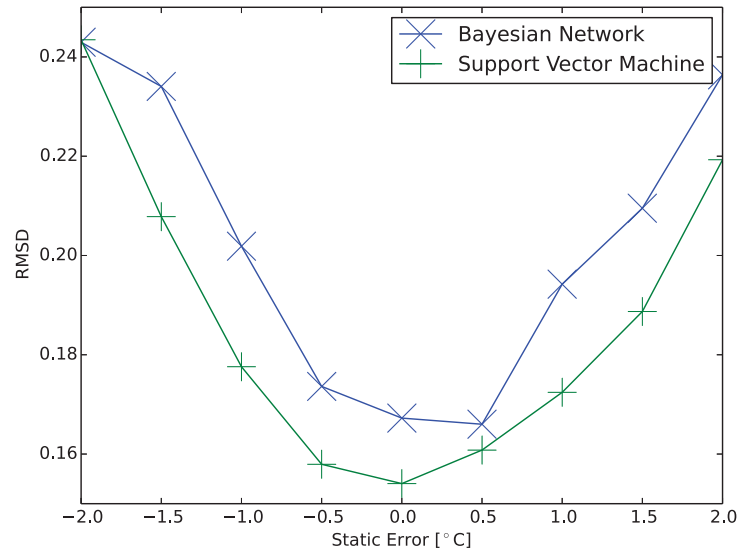


Figure 4-8 The cooling load prediction with error in inputs

4.4 Conclusion

A Bayesian network model may be effective in predicting cooling load. The results of the case study evaluating the performance of this model on predicting cooling load point to the following conclusions:

- 1) The Bayesian network model can achieve a very close performance to that of the support vector machine model in terms of accuracy and reliability. However, the Bayesian network model is easier to implement.
- 2) The accuracy of the cooling load prediction is not always proportional to the amount of training data available. Sixteen weeks of training data actually

generated a slightly better prediction by both the Bayesian network model and the support vector machine model than 28 weeks of training data for the studied case.

- 3) The accuracy of the cooling load prediction can be significantly affected by the uncertainties in the inputs.

Chapter 5

A Bayesian Network Model for the Optimization of a Chiller Plant's

Condenser Water Set Point

Chapter 5 elaborates the research on the condenser water set point optimization with a regression-model-based-control method.

5.1 Regression-Model-based-Control Methods to Optimize the Condenser Water Set Point

As described in Chapter 2, researchers have proposed various regression-model-based-control methods to optimize the condenser water set points [19, 23, 30]. For example, Sun and Reddy [19] used a linear regression model to predict the optimal condenser water temperature set points according to the outdoor wet bulb temperature and the cooling load:

$$T_{cw,set,opt} = a_1 + a_2 T_{wb} + a_3 \frac{\dot{Q}}{\dot{Q}_{nom}}, \quad (84)$$

where the a_1 , a_2 , and a_3 are regression coefficients.

Yu and Chan [23] developed a polynomial regression model to predict the optimal condenser water temperature set points based on the outdoor wet bulb temperature and the cooling load in order to consider the nonlinearity in the actual system:

$$T_{cw,set,opt} = b_1 + T_{wb} + b_2 \frac{\dot{Q}}{\dot{Q}_{nom}} + b_3 \left(\frac{\dot{Q}}{\dot{Q}_{nom}}\right)^2, \quad (85)$$

where the b_1 , b_2 , and b_3 are regression coefficients.

Although fast and simple, the existing regression-model-based-control methods often do not achieve the optimal energy savings due to the low accuracy in predicting the optimal condenser water set points. It is likely that suboptimal condenser water set points are predicted mainly due to difficulties in representing the nonlinear relationships in the chiller and the cooling tower operation with linear or polynomial regression models.

5.2 Bayesian Network Model for Condenser Water Set Point Optimization

To address the limitations of linear or polynomial regression models, the author proposes a Bayesian Network model. Bayesian Network models have been employed in the building industry for other applications as show in Chapter 4. To the author's best knowledge, however, no research has been reported on the application of a Bayesian Network model for the optimal selection of the condenser water set point of a chiller plant.

For chiller plants, if the thermal and hydraulic dynamics are assumed to be negligible, the total power of the chillers and cooling towers, P_{sum} , can be described as

$$P_{sum} = f_1(T_{cw,set}, \dot{Q}, T_{wb}), \quad (86)$$

Based on Equation (86), the author defines the following optimization problem,

$$J = \min(P_{sum}) = \min(f_1(T_{cw,set}, \dot{Q}, T_{wb})). \quad (87)$$

The input variables are the cooling load and the outdoor wet bulb temperature, the optimized variable is the condenser water set point and the objective function is the total power of the chillers and cooling towers. Thus, the problem is to find the optimal

condenser water set point, $T_{cw,set,opt}$, that minimizes the total power of the chillers and cooling towers as a function of the cooling load and the outdoor wet bulb temperature:

$$T_{cw,set,opt} = f_2(\dot{Q}, T_{wb}). \quad (88)$$

Based on equation (88), the author builds a Bayesian Network model shown in Figure 5-1. In this Bayesian Network model, the parent nodes are the cooling load and the outdoor wet bulb temperature, which are continuous variables. To perform the discretization for those variables, the author selects the discretization interval as 100 Ton and 1.0°C for the cooling load and the outdoor wet bulb temperature, respectively. The child node is the optimal condenser water set point and is limited in a certain range to avoid obviously negative impacts on the chiller operation (overcooling or overheating). In this case, the range is set to be [15.1, 26.1] (°C).

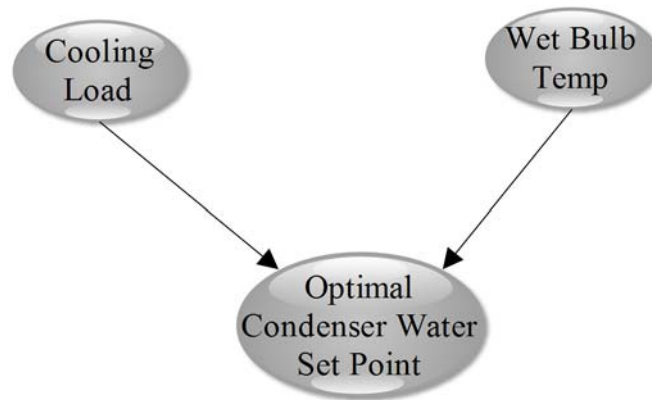


Figure 5-1 The structure of the Bayesian Network model for the optimization of the condenser water set point

5.3 Case Study

As a case study, the author considers the chiller plant shown in Figure 2-3. The model of the chiller is a Trane_CVHF_2799kW, which has the nominal cooling capacity as

2,799 kW (796 ton). For the cooling tower, the design fan power is 37 kW (50 HP) and the actual fan power is assumed to be proportional to the cubic of the fan speed ratio. The nominal outdoor wet bulb temperature and the nominal approach temperature are 26.11°C (79.00°F) and 1.11°C (2°F), respectively. Each chiller has one dedicated chilled water pump, one dedicated condenser water pump and one dedicated cooling tower.

The control sequence for the chillers is described as Figure 3-1 with CP_1 and CP_2 fixed as 796 ton and 1,592 ton, respectively. The dead band and the waiting period are assumed to be 0.

To evaluate the proposed Bayesian Network model, the author compares its performance with that of two regressing models: one is a linear regression model defined by (84), and the other one is a polynomial model defined as

$$T_{cw,set,opt} = c_1 + c_2 T_{wb} + c_3 \frac{\dot{Q}}{\dot{Q}_{nom}} + c_4 \left(\frac{\dot{Q}}{\dot{Q}_{nom}} \right)^2, \quad (89)$$

where c_1 , c_2 , c_3 , and c_4 are regression coefficients. Equation (8) is derived from the equation (85). In equation (85), the coefficient of the outdoor wet bulb temperature is 1, which means when the outdoor wet bulb temperature changes by 1.0°C, the optimal condenser water set point will also change by 1.0°C. However, with different characteristics of chillers and cooling towers, it is possible that the relationship between the optimal condenser water set point and the outdoor wet bulb temperature changes by chiller plants. With that in mind, the author treats the coefficient of the outdoor wet bulb temperature as one regression coefficient in equation (8). Similar to the proposed Bayesian Network model, the optimal condenser water set points predicted by the regression models are also limited in the range [15.1, 26.1] (°C).

The regression coefficients in the linear and the polynomial models are estimated by the ordinary least squares method [115]. The ordinary least squares method estimates the unknown parameters in regression models by solving the following optimization problem:

$$J = \min(\sum_{i=1}^{N_{ob}} (y_i - \hat{y}_i)) = \min(f(r_1, \dots, r_n)), \quad (90)$$

where y_i is the i th observed value of the dependent variable, \hat{y}_i is the corresponding predicted value of the dependent variable by the recession model, N_{ob} is the number of the observed values, and r_1, \dots, r_n are the regression coefficients.

5.3.1 The Training Dataset

To generate a training dataset for the proposed Bayesian Network model and the linear and polynomial regression models, the author uses the following approach shown in Figure 5-2:

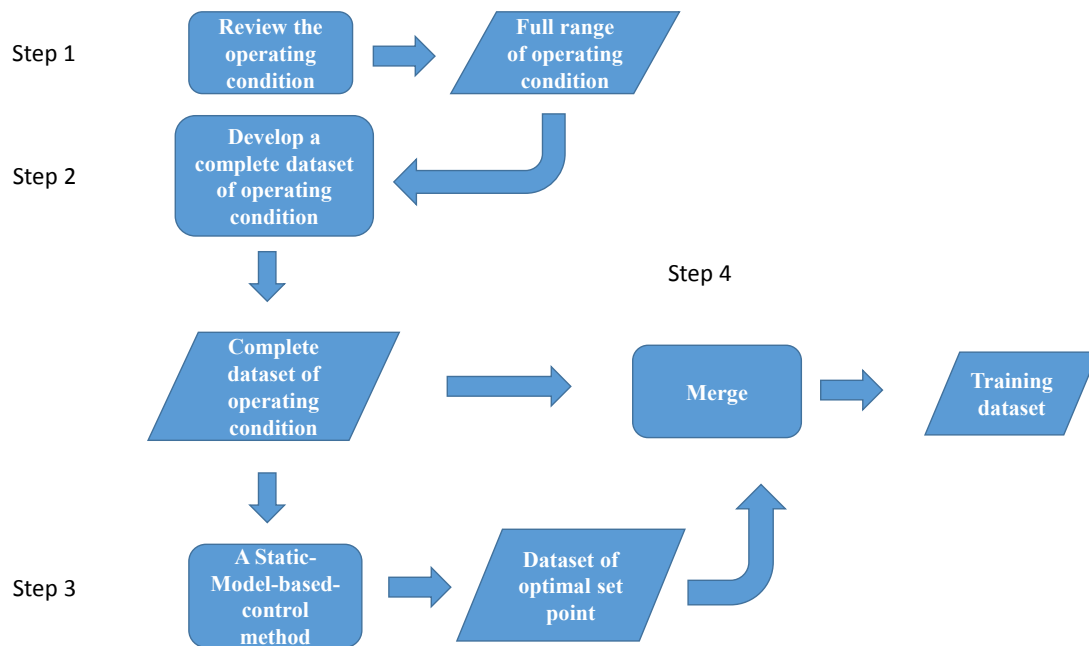


Figure 5-2 The procedure for generating a training dataset

In Step 1, the author reviews the studied chiller plant's typical operating condition. Over the course of a year, the author finds the cooling load ranges from 0 to around 2000 Ton while the outdoor wet bulb temperature changes from around -11.0°C to 25.0°C .

In Step 2, the author develops a complete dataset for the cooling loads and the outdoor wet bulb temperatures based on their ranges obtained in Step 1. In the dataset, the cooling load range is [50, 2000] (Ton) with an interval of 50 ton and the outdoor wet bulb temperature range is $[-11.0, 25.0]$ ($^{\circ}\text{C}$) with an interval of 0.5°C .

In Step 3, the complete set for the cooling load and the outdoor wet bulb temperature is used as the inputs for a static-model-based-control method to find the corresponding optimal condenser water set points. For the static-model-based-control method, the optimization problem is the same as that defined in equation (87). The author models the studied chiller plant with Modelica [116] so that the values of the objective function under different condenser water set points can be obtained by the system model. For this study, the system model is almost the same with that described in section 3.4.1. However, the performance curves of Trane_CVHF_2799kW from the chiller dataset provided by EnergyPlus [42] are adapted in the *ElectricEIR* model and the system dynamics is also ignored. To guarantee that the optimal solution can be achieved, the author uses an exhaustive search method to evaluate all the possible condenser water set points. We limit the selection range in the range for the possible condenser water set points as $[15.1^{\circ}\text{C}, 26.1]$ ($^{\circ}\text{C}$). The interval for this range is set to be 0.1°C since the accuracy level of water temperature sensor is normally 0.1°C in real practice.

In Step 4, the generated optimal condenser water set points are merged with the complete dataset for the cooling load and the outdoor wet bulb temperature data to develop a complete training dataset.

5.3.2 Testing

To evaluate the performances of the proposed Bayesian Network model and the linear and polynomial regression models, the author uses them to predict the optimal condenser water set points for two testing months: one mild month (April 2012) and one summer month (July 2012) in Washington D.C.. The two months represent the mild season and the summer season, respectively. The historic hourly data of the cooling load from an on-site measurement of three office buildings and the outdoor wet bulb temperature from a nearby weather station [70] are used. The data is shown in Figure 5-3 and Figure 5-4.

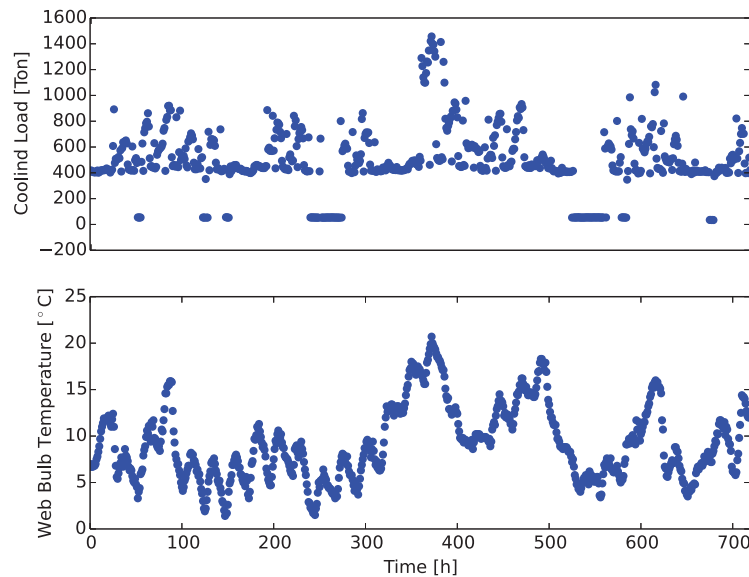


Figure 5-3 The hourly cooling load and outdoor wet bulb temperature data for the mild month in Washington D.C.

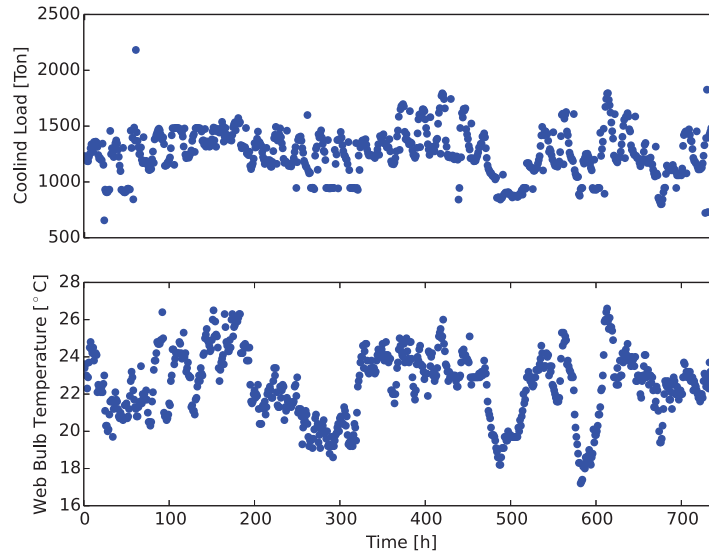


Figure 5-4 The hourly cooling load and outdoor wet bulb temperature data for the summer month in Washington D.C.

To evaluate the performance of the Bayesian Network model, the author also uses the static-model-based-control method (section 5.3.1) to predict the true optimal condenser water set points for the testing periods.

To investigate how the condenser water set point prediction affects the energy performance of the studied chiller plant, the author calculates the total power used by the chillers and the cooling towers according to the predicted condenser water set point via simulation. The system model is the same as that in the static model based control method (section 5.3.1). The author then calculates the energy consumption by the chillers and the cooling towers during the testing period by the following equation:

$$E = \sum_i^m 3600P_{sum}(i), \quad (91)$$

where $P_{sum}(i)$ is the total power used by the chillers and the cooling towers at the i th hour while m is the number of hour in the testing period.

5.3.3 Results

1) General Result

The general simulation results are shown as Table 5-1. In the mild month (April 2012), the Bayesian Network model predicts the optimal condenser water set point with a Root Mean Square Deviation (RMSD) of 0.2°C to the real optimum. As a result, the energy saving ratio for the Bayesian Network model (25.92%) is close to the theoretically upper limit (26.04%). On the contrary, both the linear and the polynomial models have a relatively large error with a RMSD of 2.3°C. The large errors in condenser water set point predictions by the linear and the polynomial models lead to less energy savings (up to 12,500 kWh) than the Bayesian Network model.

Table 5-1 The general result for the testing set

		Bayesian Network Model	Linear Regression Model	Polynomial Regression Model	Model-based Optimization Method
Mild Month	RMSD [°C]	0.2	2.3	2.3	N/A
	Energy Consumption [kWh]	133,477	145,954	146,022	133,271
	Energy Saving Ratio	25.92%	19.00%	18.96%	26.04%
Summer Month	RMSD [°C]	0.3	3.3	3.3	N/A
	Energy Consumption [kWh]	486,117	511,345	511,139	485,262
	Energy Saving Ratio	1.39%	-3.73%	-3.69%	1.56%

(In the baseline, the condenser water set point is fixed as 26.1°C)

In the summer month (July 2012), the accuracy of the Bayesian Network model in predicting the optimal condenser water set points is also close to the real optimum with a RMSD of 0.3°C. Thus, the decrease in the energy saving ratio by the Bayesian Network model compared to the theoretically upper limit is only 0.17%. On the other hand, the linear and the polynomial models have relatively poor predictions with a RMSD of 3.3°C. The poor predictions of the linear and polynomial models result in even more energy than the baseline with increases by 3.73% and 3.69%, respectively. In other words, plants using these two models will consume up to 25,200 kWh more energy compared to the one using the Bayesian Network model.

The above analysis shows that the performance of the Bayesian Network model is much better than that of the linear and the polynomial models in predicting the optimal condenser water set points for both the mild month and the summer month. Moreover, larger prediction errors of the linear and the polynomial models tend to increase the energy consumption.

2) Typical Days

In order to understand how the optimal condenser water set point predictions affect the plant operation, the author selects two typical days from the two months: a mild day (April 20th, Friday) and a summer day (July 20th, Friday). In the mild day, the cooling load changes from around 400 Ton to 900 Ton and the outdoor wet bulb temperature was from 11.0°C to 16.0°C (Figure 5-5). The condenser water set points predicted by the Bayesian Network model are quite close to the optimal solution (predicted by the model-

based optimization scheme). The highest deviation is 0.7°C . The linear and the polynomial models have similar condenser water set point predictions and the condenser water set points predicted by those two methods are always larger than that the optimal solution. As a result of different condenser water set point predictions, the Bayesian Network model, the linear model, and the polynomial model achieve 20.41%, 15.66% and 15.63% daily energy savings for the chillers and cooling towers, respectively. As a reference, the model-based optimization method achieves a 20.66% daily energy saving.

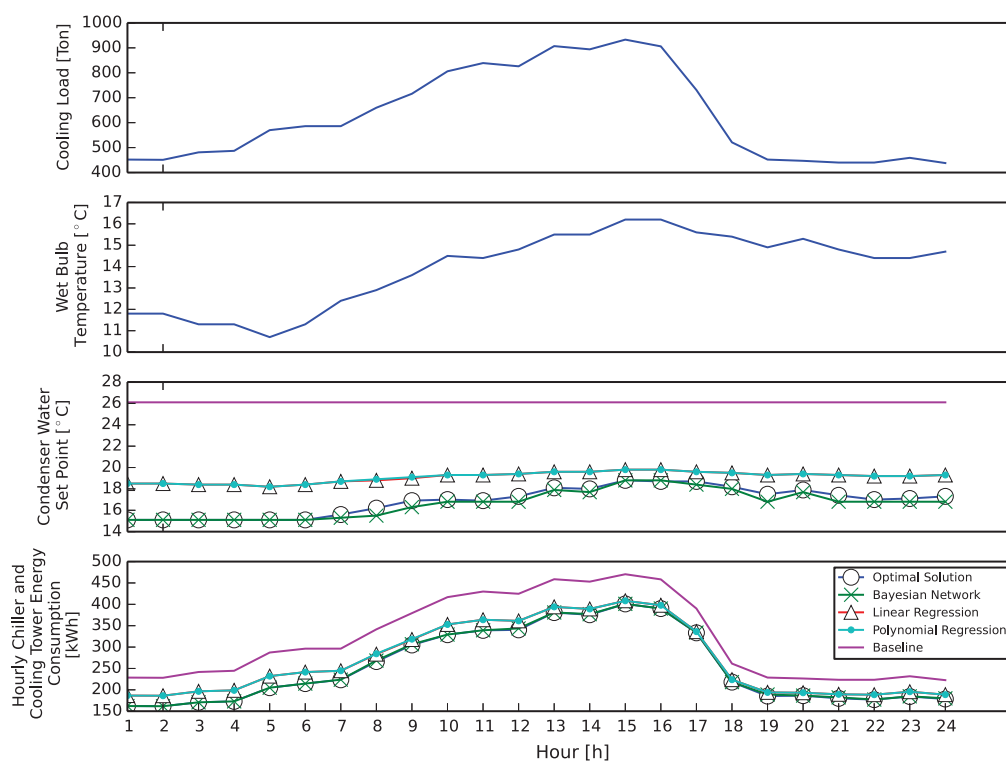


Figure 5-5 The cooling load, outdoor wet bulb temperature, predicted condenser water set point, and the total chiller and cooling tower energy consumption of the mild day

As shown in Figure 5-6, the cooling load and outdoor wet bulb temperature in the summer day are higher than those in the mild day in Figure 5-5. Since the condenser

water set point should be always higher than the outdoor wet bulb temperature, there is smaller room for optimizing the condenser water set points with higher outdoor wet bulb temperature. Thus, the optimal solution only achieves a 1.25% daily energy saving for the chillers and the cooling towers in the summer day. The Bayesian Network model achieves a condenser water set point prediction relatively closer to the optimal solution. The condenser water set points predicted by the linear and polynomial models are much lower than that by the optimal solution and sometimes are even less than the outdoor wet bulb temperature, which is not possible. In consequence, the Bayesian Network method achieves a 0.87% daily energy saving while both the linear and polynomial models increase the daily energy consumption for the chillers and the cooling towers by 5.08%.

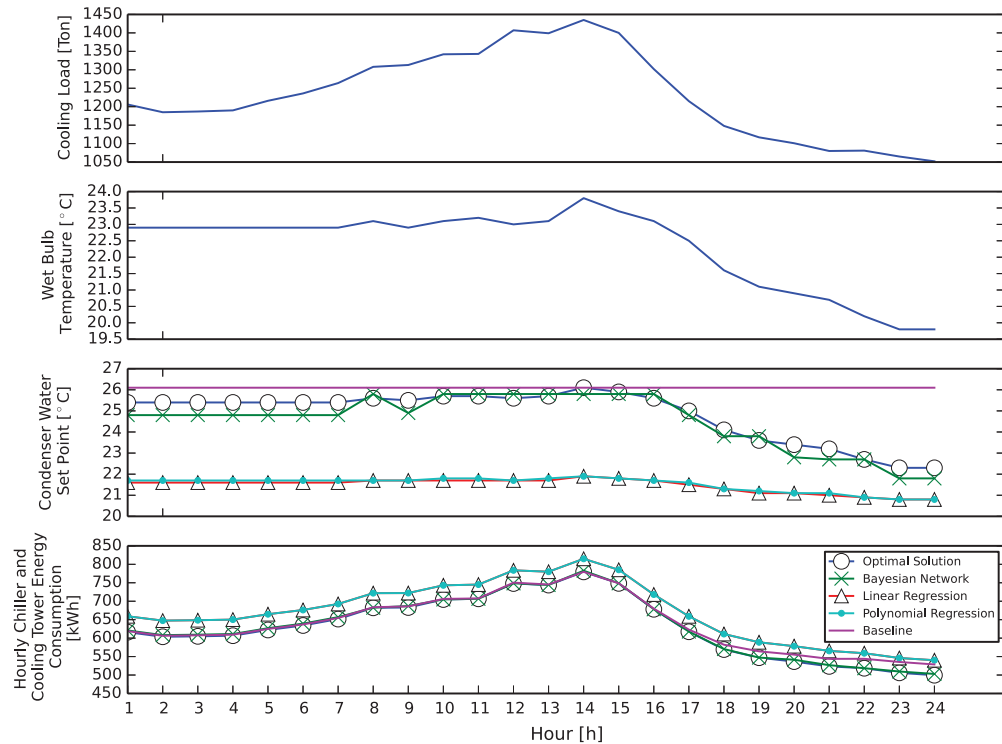


Figure 5-6 The cooling load, outdoor wet bulb temperature, predicted condenser water set point, and the total chiller and cooling tower energy consumption of the summer day

5.4 Conclusion

In this chapter, the author proposes a Bayesian Network model for predicting the optimal condenser water set points. The author compares the performance of the Bayesian Network model with those of a linear model and a polynomial model via a case study. Based on the results of the case study, one can draw the following conclusions:

- 1) The Bayesian Network model is able to represent the relationship between the cooling load, the outdoor wet bulb temperature, and the corresponding optimal condenser water set points with a good accuracy. It may be a promising approach for fast selection of the optimal condense water set point;

- 2) The Bayesian Network model can significantly increase the energy saving by the condenser water set point optimization compared to the linear and the polynomial models.

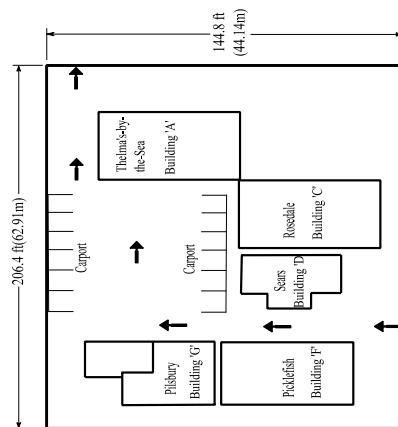
Chapter 6

Modeling for a Net Zero Energy Community

Chapter 6 discusses the research on modeling a community-level system that serves a net zero energy community.

6.1 The Studied System

The system investigated in this study is a real community energy system, which is an integration of multiple building systems. This system serves the Historic Green Village (HGV), which is a net zero energy community in Anna Maria Island, Florida. As shown in Figure 6-1, the HGV consists of five mixed-use (retail, residential, and office) commercial buildings.



(a) Building Layout



(b) Google Street View

Figure 6-1 Historic Green Village on Anna Maria Island, FL

To satisfy the energy demand of these buildings, the community energy system consists of three subsystems: electric, water-source heat pump, and domestic hot water (Figure 6-2).

The electric subsystem includes the solar photovoltaic (PV) panels, electric load, and distribution network. The electric subsystem interacts with the power grid. The water-source heat pump subsystem includes water-to-air heat pumps and a single ground-coupled water loop with two boreholes. The heat pumps provide cooling and heating energy to all buildings within the community. The domestic hot water subsystem includes three solar thermal domestic water heaters. The domestic hot water subsystem is also coupled with heat pumps for the purpose of heat recovery. The following sections will demonstrate the details of the electric subsystem and the water-source heat pump subsystem.

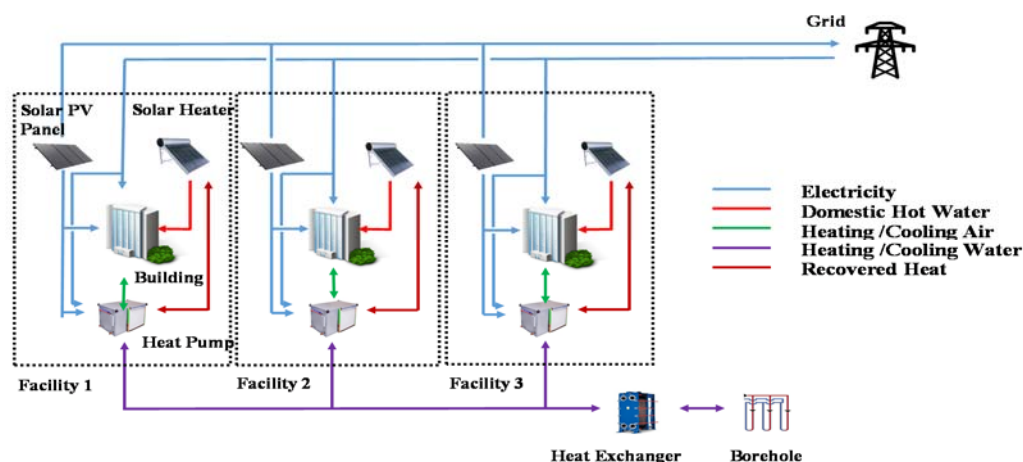


Figure 6-2 The schematic of the studied building system

Figure 6-3 shows the schematic of the electric subsystem. Electricity is produced by the solar PV panels, which are installed on the roof of the Sea (A), Rosedale (C), Sears (D), Picklefish (F), Pillsbury (G), Carport, and Warehouse (another house outside the

HGV). Inverters are installed in the PV system to enable the connection with the service panels. (The voltage of the output electricity is 120/240 VAC). The interaction between the electric subsystem and the grid is realized by transformers. If transformers detect that demand load is not satisfied, the electricity generated by the solar PV panels will flow to the service panels to satisfy demand load. If load is satisfied, the electricity will flow out to the grid.

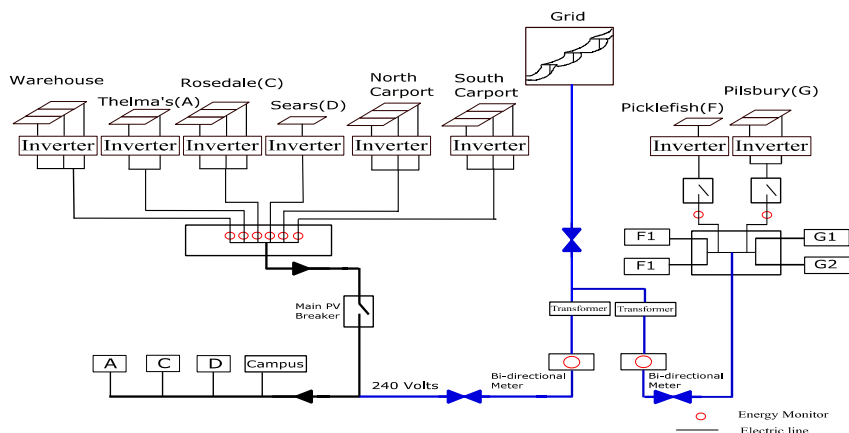


Figure 6-3 The schematic of power distribution of HG

The water-source heat pumps subsystem is shown in Figure 6-4. The ground-coupled water loop consists of a heat exchanger and two boreholes. The boreholes penetrate a layer of limestone rock and are four hundred and fifty feet deep. The ground-coupled water loop connects with nine heat pumps, which provide cooling and heating to the buildings. Each heat pump has two dedicated circulating pumps (Table 6-1 shows detailed information about the pumps). In addition, the water loop also provides cooling for the refrigeration units in the general store. To ensure that the loop temperature stays

within the design range, a variable speed well pump controls the flow rate of the ground water through the main heat exchanger, based on the exit water temperature.

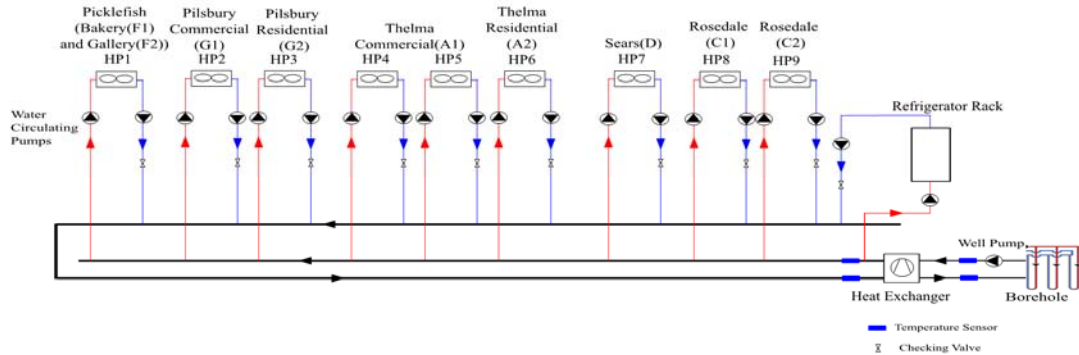


Figure 6-4 The schematic of HG V Ground Loop

Table 6-1 The specification of circulation pumps

Heat Pump	Circulation Pump Model	Flow Rate [kg/s]	Head (m)
HP1	BGM 3655	8.83×10^{-1}	20.73
HP2	UP26-116F	5.68×10^{-1}	18.90
HP3	UP26-116F	5.68×10^{-1}	18.90
HP4	UP26-116F	5.05×10^{-1}	19.20
HP5	UP26-116F	5.68×10^{-1}	18.90
HP6	UP26-116F	5.68×10^{-1}	18.90
HP7	UP26-116F	5.68×10^{-1}	18.90
HP8	UP26-116F	5.68×10^{-1}	18.90
HP9	UP26-116F	5.68×10^{-1}	18.90

6.2 The Proposed Research

Aiming to improve the operational efficiency of the studied building system, the author proposes performing the research described in Figure 6-5:

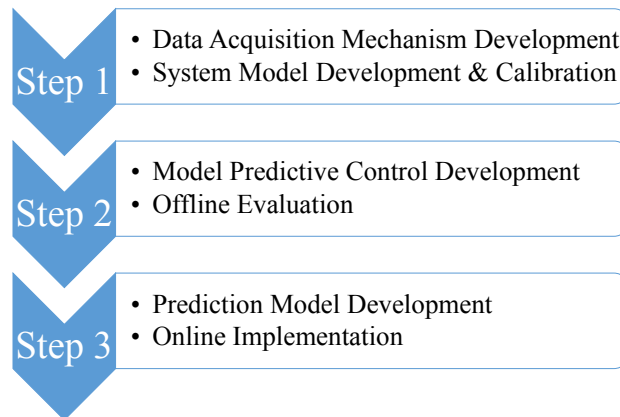


Figure 6-5 The proposed research for HGV

In the first step, a data acquisition mechanism that enables automatic collection of the operational data will be developed. The collected data can be used in the calibration of the system models. It can be also used as inputs for model predictive controls. In addition, the system models of the building system will be developed and calibrated.

The second step first involves developing the model predictive control method and then implementing the method using the software environment proposed in Chapter 2. After that, an offline simulation will be performed to evaluate the model predictive control method. In the offline simulation, the measured data such as the cooling load will be used as the inputs. The offline simulation will facilitate quantification of the potential energy savings and test whether the proposed model predictive control method is robust.

In the third step, the prediction model will be developed. The prediction model provides the inputs, such as the weather conditions, the thermal load, and hot water usage, to the model prediction control in the online operation. The prediction model will be built using the Bayesian network model proposed in Chapter 4. After the prediction model is trained and verified, the prediction model and the model predictive control will be combined and implemented in the real controllers to achieve energy savings in the real world.

This research remains ongoing, and at the time of writing, the first step is in progress. The following sections will report the preliminary results for the first step.

6.3 Data Acquisition

Developed by the partner Amzur Technologies, the data acquisition mechanism shown in Figure 6-6 consists of three parts: on-site measurement, database, and Web interface. The on-site measurement collects data from sensors and meters that are installed on site; the database receives data from the on-site measurement and stores the data for future uses. The Web interface provides a graphic interface by which the building operators can easily check the operation status. In addition, it also provides APIs (application program interfaces) for Python. The APIs can enable a seamless connection between the data acquisition and the proposed software environment for the predictive control model.

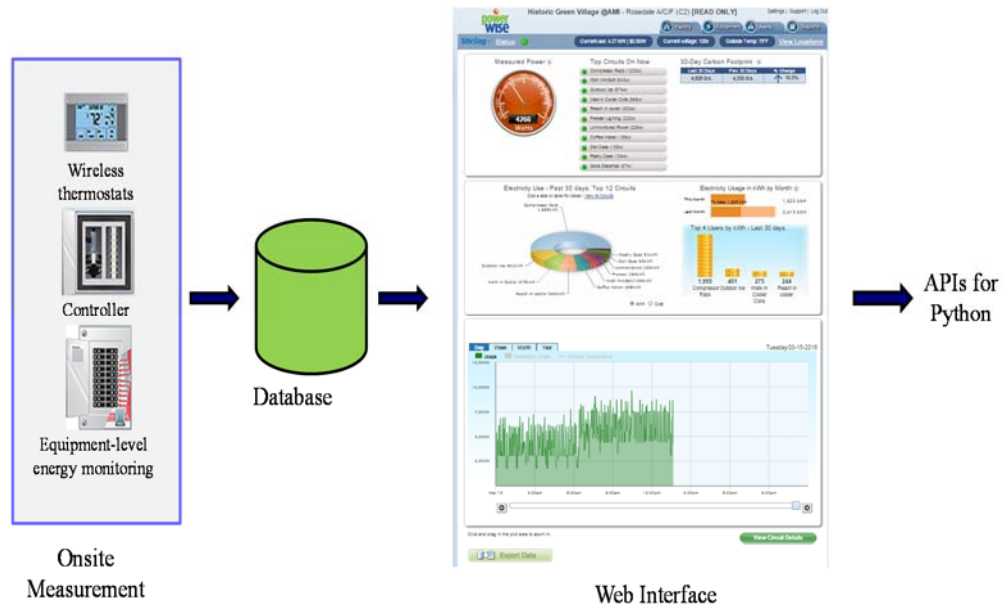


Figure 6-6 the data acquisition mechanism

6.4 System Modeling

6.4.1 The Partitioning Modeling Method

The studied community energy system is a typical multidisciplinary dynamic system. The modeling and simulation of such a complex system can be challenging, preventing the developed model's predictive control environment from being directly applied in this system. The difficulties stem from two aspects of its modeling and simulation: First, the interactions between different subsystems lead to a complicated structure for the system models, which makes it difficult to implement and debug the models; second, the simulation tends to be computationally intensive because a small time step should be used to catch the dynamics of the subsystem.

To address the above challenges, the author proposes dividing the studied community system into different groups, as shown in Figure 6-7. The energy/mass/information

connections between different groups are modeled with corresponding buses. This technique has two benefits: first, it allows the system model to be easily separated in order to perform the unit testing, which permits the quick detection of bugs; second, by splitting the system model into different groups, it allows one to solve the time integration of different groups with different time step sizes: for groups with fast dynamics, one can use small time step sizes to capture the fast changes; while for those with relatively slow dynamics, one can use large time steps to reduce the computing time. Then, the connections between different groups can be realized by co-simulation interfaces such as Functional Mock-up Interface [117].

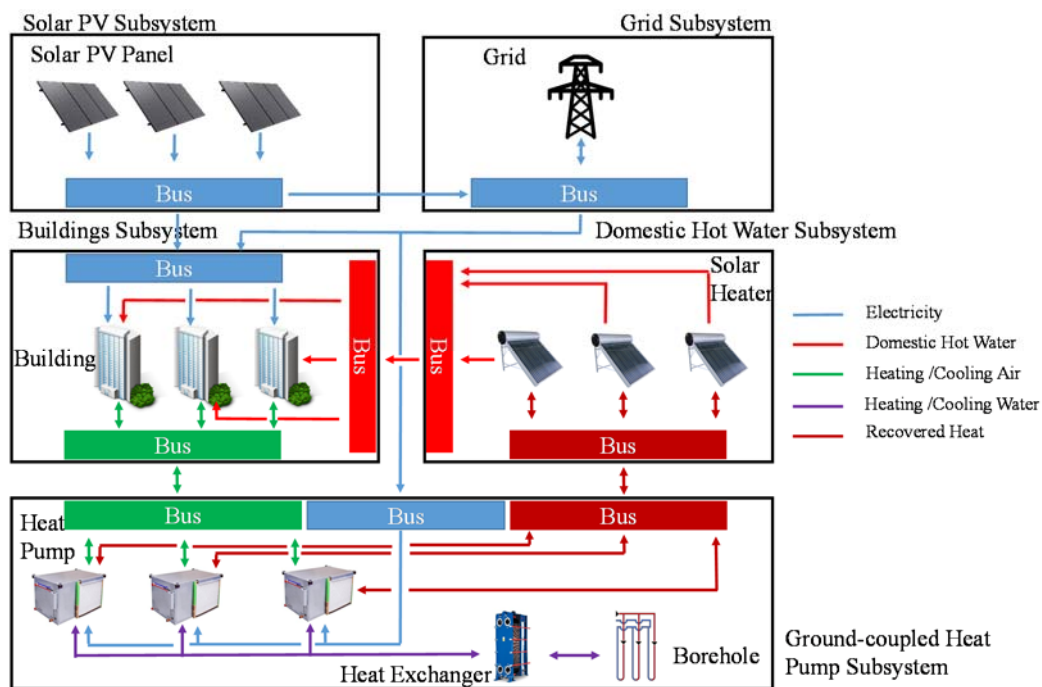


Figure 6-7 The structure for the system model

Following the grouping modeling concept, models were successfully developed for two groups: the ground-coupled heat pump subsystem and the solar PV subsystem.

6.4.2 The Ground-Coupled Heat Pump Subsystem

Figure 6-8 shows the top-level model of the ground-coupled heat pump subsystem. The model inputs include outside air temperatures, room air temperature set points, switching of cooling/heating mode, set temperature of the water leaving the heat pump, cooling/heating load profiles, and other device parameters. The main model outputs are the energy consumption of individual heat pumps and room air temperature. The key of this subsystem model is the heat pump.

Figure 6-9 shows the details of the heat pump model: (a) shows the top-level model for the heat pump module, while (b) and (c) show the models of the waterside and airside equipment of the heat pump module, respectively.

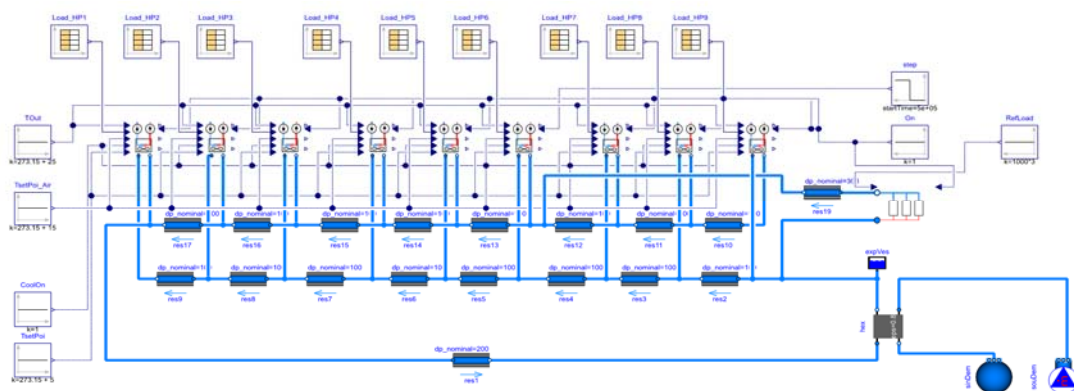


Figure 6-8 Diagram of top level model of the heat pump subsystem

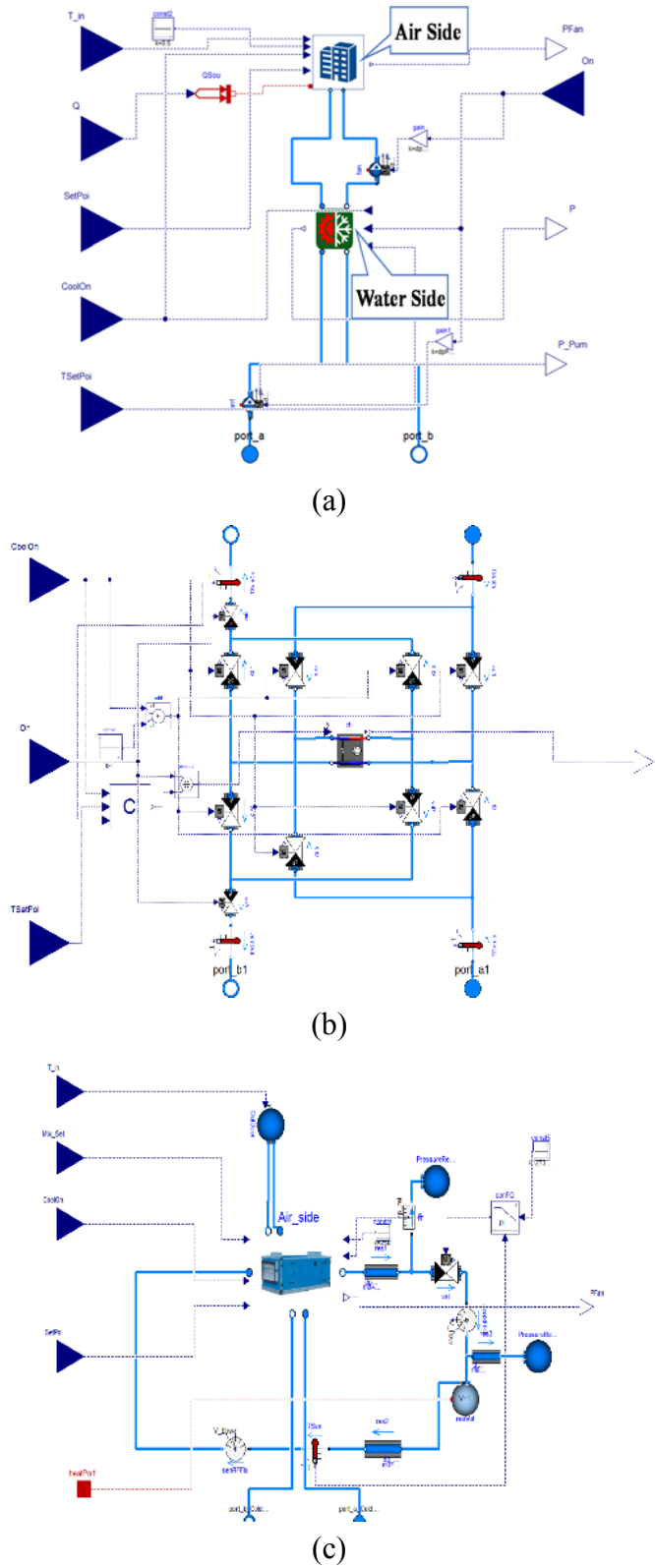


Figure 6-9 Diagram of heat pump module: (a) heat pump; (b) air side; (c) water side

6.4.3 The Solar PV Subsystem

Figure 6-10 shows the diagram of the top-level model of the solar PV subsystem, which consists of several single PV panel models. The single PV panel model takes the direct and diffuse solar radiation, which is calculated according to the inclined angle of the panel and the weather condition, as inputs. This model computes the active power generated by the PV panel as

$$P = Af_{act}\eta G\eta_{DCAC}, \quad (92)$$

where A is the panel area; f_{act} is the fraction of the aperture area; η is the constant panel efficiency; G is the total solar irradiation, which is the sum of direct and diffuse irradiation; and η_{DCAC} is the constant efficiency of the conversion between the direct current and the alternating current.

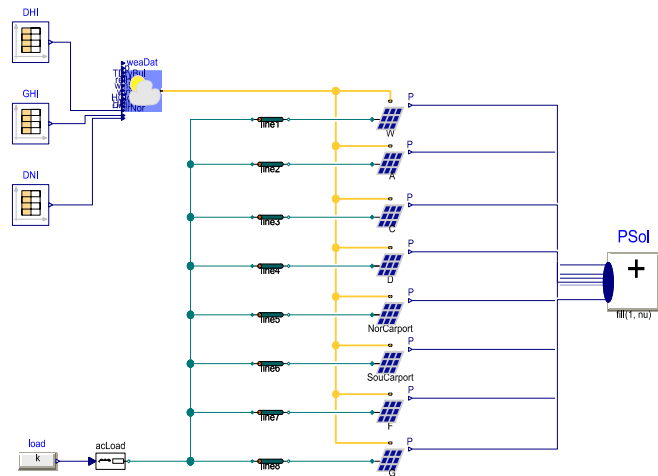


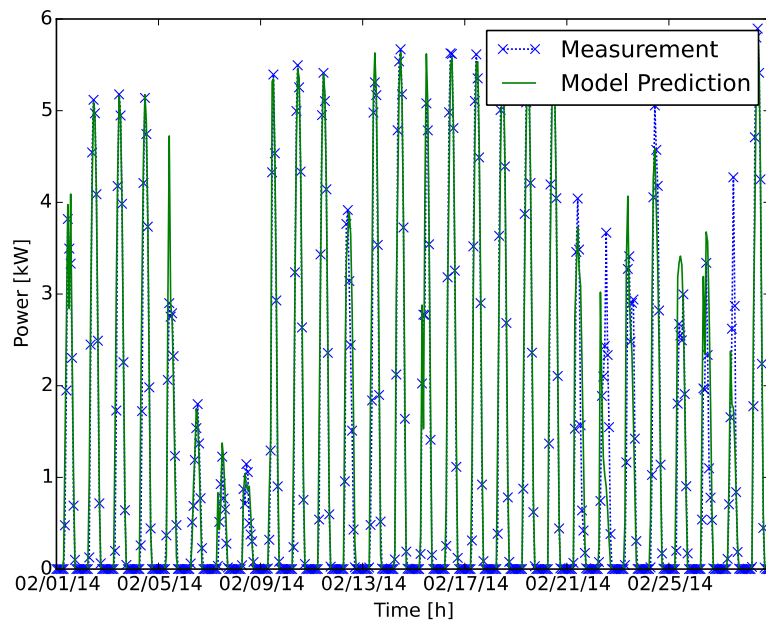
Figure 6-10 Diagram of top level model of the solar subsystem

6.5 Preliminary Simulation Results

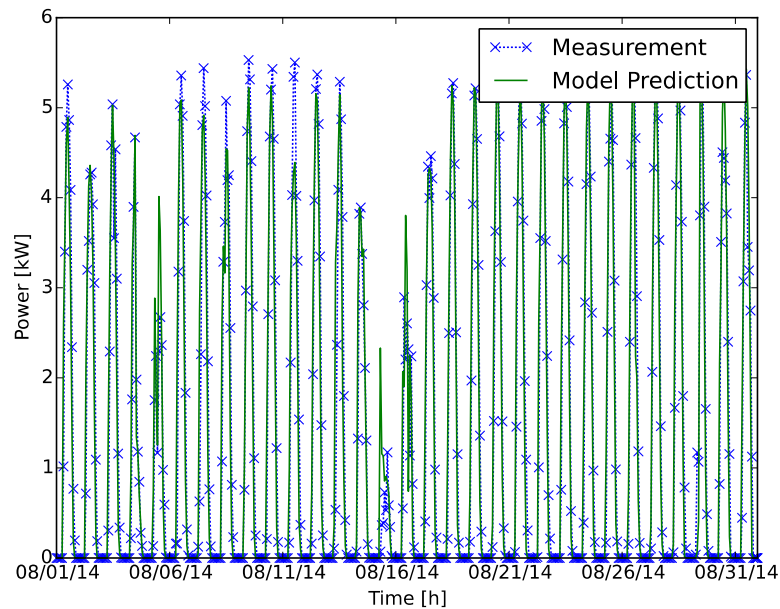
Although the Historic Green Village has installed many sensors, the collected data is only sufficient for the evaluation of a solar PV subsystem. To evaluate the performance of the developed model for the solar PV subsystem, the following study was performed:

- Historic data was used for solar radiation as the inputs for one PV module in the solar PV subsystem in order to perform the simulation.
- The simulation output was compared with the measurement.

As shown in Figure 6-11, in the comparison of the simulation output with the measurement, it is clear that for both two studied months, the model predicts results that are quite close to the measurement.



(a)



(b)

Figure 6-11 Simulated and measured energy production of PVs in building

Warehouse in winter (a) and summer (b) of 2014

6.6 Conclusion

This chapter reports the preliminary work of developing a model predictive control for a net zero energy community. The simulation results show that the developed solar PV model can predict close results compared to the measurement.

Chapter 7

Conclusion and Future Work

This chapter concludes the finding of this dissertation and provides suggestions for future study.

7.1 Conclusion

In this dissertation, a software environment for implementing the model predictive control in buildings is proposed. Using the software environment, model predictive control methods for the condenser water set point and the chiller staging are implemented and optimized. In addition, this dissertation generates a new method for cooling load prediction, which is a critical input of the model predictive control methods for buildings. Furthermore, a new regression-model-based-control method for optimizing the condenser water set point is proposed. Finally, preliminary steps for modeling an integrated community system that serves a net zero energy community are presented.

Based on the studies performed in this dissertation, the following conclusions can be drawn:

- 1) For the model predictive control of the condenser water set point optimization, the selection of the initial point for searching has a significant impact on the optimization's accuracy and runtime. The proposed method is recommended, since it can result in the lowest number of optimization failure points and a reasonably good speed. In addition, for the studied chiller plant located in the

climate with mild daily changes in outdoor wet bulb temperature, the frequency of the condenser water set point resetting does not affect the energy savings significantly. Thus, one can adopt a lower frequency to simplify the control.

- 2) For the chiller staging control, the results clearly show that there is a trade-off among the energy consumption of the chillers, cooling towers, and pumps for the studied chiller plant. Depending on the season, one can adjust the number of operating chillers to reduce the total energy consumption of the chillers, cooling towers, and pumps. By considering the trade-off in the design of the model predictive control for chiller staging, one can achieve better energy savings.
- 3) For the cooling load prediction, the proposed Bayesian network model can achieve a close performance to the support vector machine model in terms of accuracy and reliability. However, the Bayesian network model is easier to implement because it does not include a tuning process. For both the Bayesian network model and the support vector machine model, the accuracy of the cooling load prediction is not always proportional to the amount of training data available, and it may be significantly affected by the uncertainties in the inputs.
- 4) For optimizing the condenser water set point, the proposed Bayesian network model is able to predict comparable results to the physics-model-based control method. Thus, it can achieve much better energy savings compared to the existing regression-model-based-control methods, which rely on a linear or polynomial

regression model. This is likely because the Bayesian network model is more suitable for nonlinear relationships.

- 5) For the modeling of an integrated community system, the preliminary results show that the developed PV subsystem model is able to predict relatively accurate results.

7.2 Future Works

Suggestions for further study include:

- 1) In the system modeling of the studied chiller plant, the author ignored the heat gains from the ambient environment and equipment (e.g., the heat generated from the operating pumps). It is recommended to consider those heat gains in system modeling so that a more realistic representation of the studied chiller plant can be achieved.
- 2) This dissertation evaluates the impacts of the starting point selection and the resetting frequency on the energy savings from the condenser water set point optimization through a single case. It will be interesting to extend the evaluation to chiller plants with different load profiles and weather conditions. Based on such studies, researchers can gain a better understanding of the relationships between the starting point selection, the resetting frequency, and the energy savings from the condenser water set point optimization.

- 3) In this dissertation, the evaluation of the three model predictive control approaches for chiller staging is limited to application in the chiller plants with a constant primary chilled water flow rate and identical chillers. It is recommended to assess the performance of the three approaches on chiller plants with variable primary chilled water flow rates and non-identical chillers.
- 4) For cooling load prediction, both the Bayesian network model and the support vector machine model are unable to catch the changes in cooling load for some periods. This may be because the hour index and the day number category may not be able to represent the occupancy activities in short periods of time. It will be beneficial to investigate how to further improve the cooling load prediction by using alternative factors to represent the occupancy activities. In addition, it will also be interesting to study the possibility of increasing the accuracy by predicting the sensible cooling load and the latent cooling load separately.
- 5) For chiller plants with thermal storage devices or larger distribution loops, researchers may need to consider the dynamics of the chiller plants by introducing the time and state vectors as parent nodes in the Bayesian network model. In addition, studies should also be performed to determine if it is feasible to apply the Bayesian network model in the optimization of other control parameters, such as the critical points for chiller staging, and if the Bayesian network model can achieve better results than the linear or polynomial models in predicting the optimal values for those parameters.

- 6) For the research on the net zero energy community, the recommended future work will complete the proposed research mentioned in section 6.2. An evaluation should also be performed to learn to what extent the partitioning modeling method could speed up the simulation. In addition, it is also recommended to study whether it is possible to apply the Bayesian network model in the operational optimization to simplify the implementation.

WORKS CITED

- [1] U.S. Department of Energy. Buildings Energy Data Book. <<https://catalog.data.gov/dataset/buildings-energy-data-book>> (accessed May 15. 2014).
- [2] U.S. Energy Information Administration. The State Energy Data System. <<http://www.eia.gov/state/seds/>> (accessed March 9. 2016).
- [3] Wetter M. A View on Future Building System Modeling and Simulation In: Hensen JLM, Lamberts R, editors. Building Performance Simulation for Design and Operation, UK: Routledge; 2011.
- [4] Gordon JM, Ng KC, Chua HT, Lim CK. How Varying Condenser Coolant Flow Rate Affects Chiller Performance: Thermodynamic Modeling and Experimental Confirmation. Appl Therm Eng 2000;20(13):1149-59.
- [5] T.Taylor S. Primary-Only vs.Primary-Secondary Variable Flow Systems. ASHRAE J 2002;44(2):25-9.
- [6] P.Bahnfleth W, Peyer E. Variable Primary Flow Chilled Water Systems: Potential Benefits and Application Issues. Pennsylvania State University; 2004.
- [7] Lee WL, Lee SH. Developing a Simplified Model for Evaluating Chiller-system Configuration. Appl Energ 2007;84(2007):290-306.
- [8] Shimoda Y, Nagota T, Isayama N, Mizuno M. Verification of Energy Efficiency of District Heating and Cooling System by Simulation Considering Design and Operation Parameters. Build Environ 2008;43(2008):569-77.

- [9] Yu FW, Chan KT. Strategy for Designing More Energy Efficient Chiller Plants Serving Air-conditioned Buildings. *Build Environ* 2007;42(2007):3737-46.
- [10] K.L.Chan R, W.M.Lee E, K.K.Yuen R. An Integrated Model for the Design of Air-cooled Chiller Plants for Commercial Buildings. *Build Environ* 2010;46(2011):196-209.
- [11] R.V.Rao, V.K.Patel. Optimization of Mechanical Draft Counter Flow Wet-cooling Tower using Artificial Bee Colony Algorithm. *Energ Convers Manage* 2011;52(7):2611-22.
- [12] A.Tirmizi S, P.Gandhidasan, M.Zubair S. Performance Analysis of a Chilled Water System with Various Pumping Schemes. *Appl Energ* 2012;100(2012):238-48.
- [13] Chang Y, Chieng PC, Lu JT, Chan TS, Chen CL, Lee CW. Energy Saving Analysis of Variable Primary Flow System with Screw Chiller. *International Journal of Electronics Communications and Electrical Engineering* 2012;2(12):25-42.
- [14] Ali M, Vukovic V, Sahir MH, Fontanella G. Energy Analysis of Chilled Water System Configurations using Simulation-based Optimization. *Energ Buildings* 2013;59(2013):111-22.
- [15] Maehara N, Shimoda Y. Application of the Genetic Algorithm and Downhill Simplex Methods (Nelder–Mead Methods) in the Search for the Optimum Chiller Configuration. *Appl Therm Eng* 2013;61(2):433-42.
- [16] W.Furlong J, T.Morrison F. Optimization of Water-Cooled Chiller-Cooling Tower Combinations. *CTI Journal* 2013;26(1):12-9.
- [17] Lu L, Cai W, Soh YC, Xie L, Li S. HVAC System Optimization - Condenser Water Loop. *Energ Convers Manage* 2004;45(4):613-30.

- [18] Yao Y, Lian Z, Hou Z, Zhou X. Optimal Operation of a Large Cooling System based on an Empirical Model. *Appl Therm Eng* 2004;24(16):2303-21.
- [19] Sun J, Reddy A. Optimal Control of Building HVAC&R Systems using Complete Simulation-based Sequential Quadratic Programming (CSB-SQP). *Build Environ* 2005;40(5):657-69.
- [20] Yu FW, Chan KT. Optimum Condenser Fan Staging for Air-cooled Chillers. *Appl Therm Eng* 2005;25(14-15):2204-18.
- [21] Hydeman M, Zhuo G. Optimizing Chilled Water Plant Control. *ASHRAE J* 2007;54(3):56-74.
- [22] Ma Z, Wang S, Xu X, Xia F. A Supervisory Control Strategy for Building Cooling Water Systems for Practical and Real Time Applications. *Energy Convers Manage* 2008;49(8):2324-36.
- [23] Yu FW, Chan KT. Optimization of Water-cooled Chiller System with Load-based Speed Control. *Appl Energy* 2008;85(2008):931-50.
- [24] Ma Z, Wang S, Xiao F. Online Performance Evaluation of Alternative Control Strategies for Building Cooling Water Systems Prior to In Situ Implementation. *Appl Energy* 2009;86(2009):712-21.
- [25] Ma Z, Wang S, Xu X, Xia F. An Optimal Control Strategy for Complex Building Central Chilled Water Systems for Practical and Real-time Applications. *Build Environ* 2009;44(6):1188-98.
- [26] F.W.Yu, K.T.Chan. Economic Benefits of Optimal Control for Water-cooled Chiller Systems Serving Hotels in a Subtropical Climate. *Energy Buildings* 2010;42(2):203-9.

- [27] Huang X, Xu J, Wang S. Operation optimization for centrifugal chiller plants using continuous piecewise linear programming. In: Proceedings of Systems Man and Cybernetics (SMC), 2010 IEEE International Conference on, 2010. p. 1121-6.
- [28] Ma Y, Borrelli F, Hencsey B, Coffey B, Benghea S, Haves P. Model Predictive Control for the Operation of Building Cooling Systems. *IEEE Trans Control Syst Technol* 2010;20(3):796 - 803.
- [29] Ma Z, Wang S. Supervisory and Optimal Control of Central Chiller Plants using Simplified Adaptive Models and Genetic Algorithm. *Appl Energ* 2011;88(1):198-211.
- [30] Zhang Z, Li H, Turner WD, Deng S. Optimization of the Cooling Tower Condenser Water Leaving Temperature using a Component-based Model. *ASHRAE Trans* 2011;117(1):934-44.
- [31] Lee KP, Cheng TA. A Simulation–optimization Approach for Energy Efficiency of Chilled Water System. *Energ Buildings* 2012;54(2012):290-6.
- [32] Li X, Li Y, E.Seem J, Li P. Extremum Seeking Control of Cooling Tower for Self-optimizing Efficient Operation of Chilled Water System. In: Proceedings of American Control Conference (ACC), Montréal, Canada, 2012. p. 3396 - 401.
- [33] Yu FW, Chan KT. Improved Energy Management of Chiller Systems by Multivariate and Data Envelopment Analyses. *Appl Energ* 2012;92(2012):168-74.
- [34] Corbin CD, Henze GP, May-Ostendorp P. A Model Predictive Control Optimization Environment for Real-time Commercial Building Application. *J Build Perform Simu* 2013;6(3):159-74.

- [35] Quintana H, Kummert M. Potential of Model Predictive Control (MPC) Strategies for the Operation of Solar Communities. In: Proceedings of The 13th Conference of IBPSA, Chambéry, France, 2013. p. 2481-8.
- [36] Chang CC, Shieh SS, Jang SS, Wu CW, Tsou Y. Energy Conservation Improvement and ON-OFF Switch Times Reduction for An Existing VFD-fan-based Cooling Tower. *Appl Energ* 2015;154(2015):491-9.
- [37] Wetter M, Bonvini M, Nouidui TS. Equation-based Languages—A New Paradigm for Building Energy Modeling, Simulation and Optimization. *Energy Buildings* 2015.
- [38] Huang X, Xu J, Wang S. Operation Optimization for Centrifugal Chiller Plants Using Continuous Piecewise Linear Programming. In: Proceedings of IEEE International Conference on Systems, Man and Cybernetics, 2010.
- [39] Široky J, Oldewurtel F, Cigler Ji, Prívvara S. Experimental Analysis of Model Predictive Control for an Energy Efficient Building Heating System. *Appl Energ* 2011;88(2011).
- [40] Ulpiani G, Borgognoni M, Romagnoli A, Perna CD. Comparing the Performance of On/off, PID and Fuzzy Controllers Applied to the Heating System of an Energy-efficient Building. *Energy Buildings* 2011;116(2016):1-17.
- [41] Birdsall B, Buhl WF, Ellington KL, Erdem AE, Winkelmann FC. Overview of the DOE-2 Building Energy Analysis Program, Version 2. 1D. 1990.
- [42] Crawley DB, Lawrie LK, Winkelmann FC, Buhl WF, Huang YJ, Pedersen CO, et al. EnergyPlus: Creating a New-generation Building Energy Simulation Program. *Energy Buildings* 2001;33(4):319-31.

- [43] Klein SA, Duffie JA, Beckman WA. TRNSYS – A Transient Simulation Program. ASHRAE Trans 1976;82(1):623-33.
- [44] ESP-r. <<http://www.esru.strath.ac.uk/Programs/ESP-r.htm>> (accessed March 25. 2016).
- [45] Zhao J, Lam KP, Ydstie BE, Karaguzel OT. EnergyPlus Model-based Predictive Control within Design–build–operate Energy Information Modelling Infrastructure. J Build Perform Simu 2014;8(3):121-34.
- [46] Casimiro S, Ioakimidis C, Mendes J, Giestas M. Modeling in TRNSYS of a Single Effect Evaporation System Powered by a Rankine Cycle. Desalination and Water Treatment 2013;51(7-9):1405-15.
- [47] Po-ki Y, Dunn A, Yeung MR. Solar Air-Conditioning System Performance Optimization by TRNSYS Simulation Modelling. HKIE Transactions 1995;2(3):27-32.
- [48] Clarke J. Moisture flow modelling within the ESP-r integrated building performance simulation system. J Build Perform Simu 2013;6(5):385-99.
- [49] Clarke J., Kelly NJ, Tang D. A Review of ESP-r's Flexible Solution Approach and its Application to Prospective Technical Domain Developments. Advances in Building Energy Research 2007;1(1):227-47.
- [50] ASHRAE. ASHRAE Handbook HVAC Application. Atlanta: ASHRAE, Inc.; 2011.
- [51] Braun JE, Klein SA, Mitchell JW, Beckham WA. Application of optimal control to chilled water systems without storage. ASHRAE Trans 1989;95(1):663-75.

- [52] Malara ACL, Huang S, Zuo W, Sohn MD, Celik N. Optimal Control of Chiller Plants using Bayesian Network. In: Proceedings of The 14th International Conference of the IBPSA Hyderabad, 2015. p. 449-55.
- [53] Huang S, Zuo W. Optimization of the Water-cooled Chiller Plant System Operation. In: Proceedings of ASHRAE/IBPSA-USA Building Simulation Conference, Atlanta, GA, U.S.A., 2014. p. 300-7.
- [54] Lazos D, Sproul A, Ka M. Development of Hybrid Numerical and Statistical Short Term Horizon Weather Prediction Models for Building Energy Management Optimisation. Build Environ;90(2015):82-95.
- [55] Dassault Systems. Dymola. <<http://www.3ds.com/products-services/catia/capabilities/modelica-systems-simulation-info/dymola>>
- [56] Walter T, Price PN, Sohn MD. Uncertainty Estimation Improves Energy Measurement and Verification Procedures. Appl Energy 2014;130(2014):230-6.
- [57] McKinney W, PyData Development Team. Pandas: Powerful Python Data Analysis Toolkit. 2015.
- [58] Hassin R, Henig M. Dichotomous Search for Random Objects on an Interval. Math Oper Res 1984;9(2):301-8.
- [59] Eiselt HA, Sandblom. Linear Programming and its Applications. 2007 ed. Berlin: Springer-Verlag Berlin Heidelberg; 2007.
- [60] Fernandes FP, Costa MFP, Fernandes EMGP, Rocha AMAC. Multistart Hooke and Jeeves Filter Method for Mixed Variable Optimization. In: Proceedings of the 11th international conference of numerical analysis and applied mathematics Rhodes, Greece, 2013. p. 614-7.

- [61] Gyorgy A. Efficient Multi-start Strategies for Local Search Algorithms. *J Artif Intell Res* 2011;41(2011):407-44.
- [62] Kelman A, Ma Y, Borrelli F. Analysis of Local Optima in Predictive Control for Energy Efficient Buildings. *J Build Perform Simu* 2012;6(3):236–55.
- [63] Sutherland JW. Analysis of Mechanical Draught Counterflow Air/Water Cooling Towers. *J Heat Transfer* 1983;105(3):576-83.
- [64] Braun JE, Klein SA, Mitchell JW. Effectiveness Models for Cooling Towers and Cooling Coils. *ASHRAE Trans* 1989;95(2):164-74.
- [65] Schwedler M. Effect of Heat Rejection Load and Wet Bulb on Cooling Tower Performance. *ASHRAE J* 2014;56(1):16-22.
- [66] Wetter M, Zuo W, Nouidui T, Pang X. Modelica Buildings library. *J Build Perform Simu* 2014;7(4):253-70.
- [67] Otter M, Årzén K-E, Dressler I. StateGraph - a Modelica Library for Hierarchical State Machines. In: *Proceedings of the 4th International Modelica Conference, Hamburg, Germany, 2005*. p. 569-78.
- [68] Input Output Reference: the Encyclopedic Reference to EnergyPlus Input and Output.
<<http://apps1.eere.energy.gov/buildings/energyplus/pdfs/inputoutputreference.pdf>>
(accessed May 14, 2015).
- [69] Wetter M. GenOpt - a Generic Optimization Program. In: *Proceedings of the 7th IBPSA Conference, Rio de Janeiro, Brazil, 2001*. p. 601-8.

- [70] National Climatic Data Center. Quality Controlled Local Climatological Data. <<http://www.ncdc.noaa.gov/data-access/land-based-station-data/land-based-datasets/quality-controlled-local-climatological-data-qclcd>> (accessed May 14, 2015).
- [71] Honeywell. Engineering Manual of Automatic Control for Commercial Buildings. Minneapolis: Honeywell, Inc.; 1997.
- [72] Sun Y, Wang S, Xiao F. In Situ Performance Comparison and Evaluation of Three Chiller Sequencing Control Strategies in a Super High-rise Building. *Energy Buildings* 2013;61(2013):333-43.
- [73] Li Z, Huang G, Sun Y. Stochastic Chiller Sequencing Control. *Energy Buildings* 2014;84(2014):203-13.
- [74] Kent A, Williams JG. *Encyclopedia of Computer Science and Technology: Volume 25 - Supplement 10: Applications of Artificial Intelligence to Agriculture and Natural Resource Management to Transaction Machine*. New York: Marcek Dekker, Inc.; 1991.
- [75] Chang YC. A Novel Energy Conservation Method - Optimal Chiller Loading. *Electr Pow Syst Res* 2004;69(2-3):221-6.
- [76] Chang YC, Lin FA, Lin CH. Optimal Chiller Sequencing by Branch and Bound Method for Saving Energy. *Energy Convers Manage* 2005;46(13-14):2158-72.
- [77] Chang YC, Lin JK, Chuang MH. Optimal Chiller Loading by Genetic Algorithm for Reducing Energy Consumption. *Energy Buildings* 2005;37(2):147-55.
- [78] Chang YC. An Outstanding Method for Saving Energy - Optimal Chiller Operation. *IEEE Trans Energy Convers* 2006;21(2):527-32.

- [79] Chang YC. An Innovative Approach for Demand Side Management—Optimal Chiller Loading by Simulated Annealing. *Energ* 2007;31(12):1883–96.
- [80] Ardakani AJ, Ardakani FF, Hosseinian SH. A Novel Approach for Optimal Chiller Loading using Particle Swarm Optimization. *Energ Buildings* 2008;40(12):2177–87.
- [81] Chang YC, Lee CY, Chen CR, Chou CH, Chen WH, Chen WH. Evolution Strategy based Optimal Chiller Loading for Saving Energy. *Energ Convers Manage* 2009;50(1):132–9.
- [82] Lee WS, Lin LC. Optimal Chiller Loading by Particle Swarm Algorithm for Reducing Energy Consumption. *Appl Therm Eng* 2009;29(8-9):1730–4.
- [83] Fan B, Jin X, Du Z. Optimal Control Strategies for Multi-chiller System based on Probability Density Distribution of Cooling Load Ratio. *Energ Buildings* 2011;43(10):2813-21.
- [84] Geem ZW. Solution Quality Improvement in Chiller Loading Optimization. *Appl Therm Eng* 2011;31(10):1848-51.
- [85] Chen CL, Chang YC, Chan TS. Applying Smart Models for Energy Saving in Optimal Chiller Loading. *Energ Buildings* 2014;68 Part A(2014):364-71.
- [86] Coelho LdS, Mariani VC. Improved Firefly Algorithm Approach Applied to Chiller Loading for Energy Conservation. *Energ Buildings* 2013;59(2013):273–8.
- [87] Coelho LdS, Klein CE, Sabat SL, Mariani VC. Optimal Chiller Loading for Energy Conservation using a New Differential Cuckoo Search Approach. *Energ* 2014;75(2014):237-43.

- [88] Chang YC. Optimal Chiller Loading by Evolution Strategy for Saving Energy. *Energ Buildings* 2007;39(4):437–44.
- [89] Sun Y, Wang S, Huang G. Chiller Sequencing Control with Enhanced Robustness for Energy Efficient Operation. *Energ Buildings* 2009;41(11):1246-55.
- [90] Yu FW, Chan KT. Optimum Load Sharing Strategy for Multiple-chiller Systems Serving Air-conditioned Buildings. *Build Environ* 2007;42(4):1581–93.
- [91] F.W. Yu, Chan KT. Improved Energy Performance of Air Cooled Centrifugal Chillers with Variable Chilled Water Flow. *Energ Convers Manage* 2008;49(6):1595–611.
- [92] Chang YC, Chen WH, Lee CY, Huang CN. Simulated Annealing Based Optimal Chiller Loading for Saving Energy. *Energ Convers Manage* 2006;47(15-16):2044-58.
- [93] Chang YC, Chen WH. Optimal Chilled Water Temperature Calculation of Multiple Chiller Systems using Hopfield Neural Network for Saving Energy. *Energ* 2008;34(4):448-56.
- [94] Lu YY, Chen JH, Liu TC, Chien MH. Using Cooling Load Forecast as the Optimal Operation Scheme for a Large Multi-chiller System. *Int J Refrig* 2011;34(8):2050–62.
- [95] Boyd SP, Vandenberghe L. *Convex Optimization*. New York: Cambridge University Press; 2004.
- [96] Hooke R, Jeeves TA. "Direct Search" Solution of Numerical and Statistical Problems. *J ACM* 1961;8(2):212-29.
- [97] Huang S, Zuo W, Sohn MD. Amelioration of the Cooling Load based Chiller Sequencing Control. *Appl Energ* 2016;168(2016):204-15.

- [98] Eskin N, Türkmen H. Analysis of Annual Heating and Cooling Energy Requirements for Office Buildings in Different Climates in Turkey. *Energ Buildings* 2008;40(5):763–73.
- [99] Thevenard D, Haddad K. Ground Reflectivity in the Context of Building Energy Simulation. *Energ Buildings* 2006;38(8):972–80.
- [100] Ben-Nakhi AE, Mahmoud MA. Cooling Load Prediction for Buildings using General Regression Neural Networks. *Energ Convers Manage* 2004;45(2004):2127-41.
- [101] Hu C, Wei D. Prediction on Hourly Cooling Load of Buildings Based on Neural Networks. *International Journal of Smart Home* 2015;9(2):35-52.
- [102] Kwok SSK, Yuen RKK, Lee EWM. An Intelligent Approach to Assessing the Effect of Building Occupancy on Building Cooling Load Prediction. *Build Environ* 2011;46(2011):1681-90.
- [103] Sakawa M, Ushiro S, Kato K, Ohtsuka K. Cooling Load Prediction in a District Heating and Cooling System Through Simplified Robust Filter and Multi-Layered Neural Network. *Appl Artif Intell* 2001;15(7):633-43.
- [104] Guo Y, Nazarian E, Ko J, Rajurkar K. Hourly Cooling Load Forecasting using Time-indexed ARX models with Two-stage Weighted Least Squares Regression *Energ Convers Manage* 2014;80(2014):46-53.
- [105] Li Q, Meng Q, Cai J, Yoshino H, Mochida A. Applying Support Vector Machine to Predict Hourly Cooling Load in the Building. *Appl Energ* 2009;86(2009):2249-56.
- [106] Li X, Lu J, Ding L, Xu G, Li J. Building Cooling Load Forecasting Model Based on LS-SVM. *Asia-Pacific Conference on Information Processing*. Shenzhen, China, 2009.

- [107] Lin Duanmu, Wang Z, Zhai ZJ, Li X. A Simplified Method to Predict Hourly Building Cooling Load for Urban Energy Planning. *Energy Buildings* 2013;58(2013):281-91.
- [108] Sun Y, Wang S, Xiao F. Development and Validation of a Simplified Online Cooling Load Prediction Strategy for a Super High-rise Building in Hongkong. *Energy Convers Manage* 2013;68(2013):20-7.
- [109] Yao Y, Lian Z, Liu S, Hou Z. Hourly Cooling Load Prediction by a Combined Forecasting Model based on Analytic Hierachy Process. *International Joournal of Thermal Sciences* 2004;43(2004):1107-18.
- [110] Chapelle O, Vapnik V, Bousquet O, Mukherjee S. Choosing Multiple Parameters for Support Vector Machines. *Machine Learning* 2002;46(1-3):131-59.
- [111] Jensen KL, Toftum J, Friis-Hansen P. A Bayesian Network Approach to the Evaluation of Building Design and its Consequences for Employee Performance and Operational Costs. *Build Environ* 2009;44(2009):456– 62.
- [112] Toftum J, Andersen RV, Jensen KL. Occupant Performance and Building Energy Consumption with Different Philosophies of Determining Acceptable Thermal Conditions. *Build Environ* 2009;44(2009):2009-16.
- [113] O'Neill Z. Development of a Probabilistic Graphical Energy Performance Model for an Office Building. *ASHRAE Trans* 2014;120(2).
- [114] Chang CC, Lin CJ. LIBSVM: A library for support vector machines. *ACM Transactions on Intelligent Systems and Technology* 2011;2(3):27.
- [115] Groß J. *Linear Regression*. Berlin: Springer Science & Business Media; 2012.

[116] Modelica Association. <<https://www.modelica.org/>> (accessed May 22. 2015).

[117] Functional Mock-up Interface Development Group. Functional Mock-up Interface. <<https://www.fmi-standard.org/>> (accessed April 1. 2016).